

HIGH CATALYTIC PERFORMANCES OF LOW RANK COAL CHAR IN AMMONIA DECOMPOSITION AT HIGH TEMPERATURES

Yasuo Ohtsuka, Chunbao Xu, Dapeng Kong, Naoto Tsubouchi

Institute of Multidisciplinary Research for Advanced Materials,
Tohoku University
Katahira, Aoba-ku, Sendai 980-8577, Japan

Introduction

To develop a novel hot gas cleanup method to efficiently remove heteroatom compounds from coal gasification products is important to achieve high power-generation efficiency in integrated gasification combined-cycle technologies.¹⁾ The present authors have recently found that fine particles of Fe or CaO supported on chars, prepared by carbonizing brown coals with Fe or Ca ions added, promote the decomposition of 2000 ppm NH₃ diluted with He at 750 – 850°C, and the high performance of the Fe catalyst is comparable to those of Ni- and Ru-based catalysts.^{1,2)}

Since Fe and Ca ions are naturally present mainly as ion-exchanged forms in low rank coals, the present work focuses on the utilization of such cations as catalyst sources for NH₃ decomposition from a practical point of view. The inherently present, exchanged Fe ions have been reported to provide nanoscale particles of metallic Fe upon carbonization³⁾ and are thus expectable to show high catalytic activity for this reaction.

Experimental

Five kinds of low rank coals from different countries with size fraction of 150 – 250 μm were used as catalyst sources. The carbon contents were 66 – 72 wt%(daf). These coals were carbonized with a fluidized bed reactor at 900°C in a stream of He. The resulting chars had carbon contents of 88 – 92 wt%(daf) and BET surface areas of 100 – 230 m²/g.

Catalytic decomposition of 2000 ppm NH₃ diluted with high purity He was carried out mainly at 750°C with a quartz-made fixed bed reactor. To examine the effect of actual gas components, a simulated gas containing H₂, CO, and CO₂ was also used. In a typical run, the char charged into the reactor was first treated with pure H₂ at 500°C for 2 h, then heated at 15 K/min up to 750°C under flowing high purity He, which was finally replaced with feed gas, the space velocity being 45000 h⁻¹. The concentration of NH₃ or N₂ in the outlet gas was on line analyzed with a photoacoustic multi-gas monitor or a high speed micro GC, respectively. Conversion of NH₃ to N₂ was calculated by using the amount of N₂ determined.

Some chars before and after reaction were characterized with a transmission electron microscope (TEM) equipped with an energy dispersive analyzer (EDX), by the X-ray diffraction (XRD) measurement with Ni-filtered Cu-Kα radiation, and by the temperature programmed desorption (TPD) technique.

Results and Discussion

Performances of Different Coal Chars. Figure 1 shows NH₃ conversion at 750°C against time on stream. All of five chars used promoted NH₃ decomposition, though the efficiency depended strongly on kind of char. NH₃ conversion decreased with increasing time to be almost steady in most cases. When the value after 3 – 4 h reaction was compared among all of the chars, it increased in the sequence of AD < ZN ≈ SB < AB < RB and reached 80 % with RB char. It is evident that such performances of coal chars originate from the catalytic activity of Fe and Ca species naturally present in them, since Fe and Ca ions added to brown coals are active for this reaction,²⁾ as mentioned above.

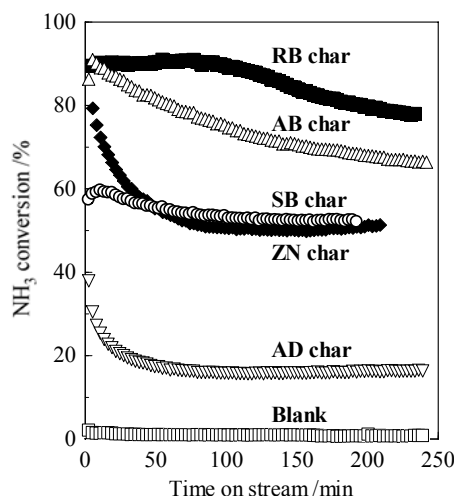


Figure 1. Catalytic performances of different coal chars in NH₃ decomposition at 750°C.

Figure 2A shows the result for the life test at 750°C of RB char with the largest performance. Although the initial conversion of about 95 % was decreased to less than 80 % after 2 – 3 h reaction, the conversion level was almost unchanged even when time on stream was further prolonged to 25 h. The activity of RB char was thus very stable under the present conditions.

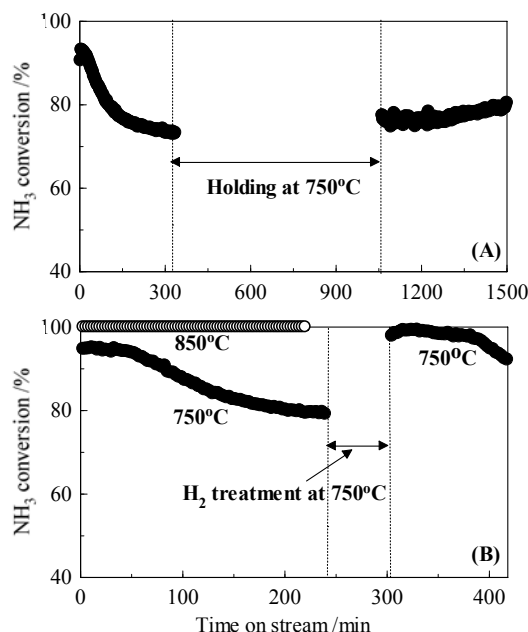


Figure 2. Catalyst life of RB char (A) and the effect of H₂ treatment of the char on NH₃ conversion (B).

To make clear the reason for the decrease of the initial activity of RB char, the char used was treated with H₂ at 750°C for 1 h. The result is shown in Figure 2B. When feed gas was first stopped after 4 h, then replaced with pure H₂, and finally passed again over the char, NH₃ conversion was restored to the initial state. A significant amount of CH₄ was formed during H₂ treatment. These observations strongly suggest that the surface of metallic Fe as the catalytically active species is partly carburized by the reaction with carbon atoms

in the char in the process of NH_3 decomposition, and H_2 treatment can restore the carbide species to the original metallic form. As is seen in Figure 2B, RB char showed no significant deactivation at 850°C . The H_2 evolved by NH_3 decomposition may prevent the iron surface from being carburized because possibly of larger reaction rate of the carbide species and H_2 at 850°C .

Catalysis by Inherent Fe and Ca in Char. Figure 3 shows a TEM picture of the fresh RB char. Fine particles with the size of 10–20 nm existed on the char. The EDX analysis of this field revealed the dominant presence of Fe and Ca elements, as is expectable. Although no significant XRD peaks of Fe species were detectable in the char, it is reasonable to see that inherent Fe ions in RB coal are reduced to the metallic form during carbonization. With Ca species, very weak diffraction lines of CaO were observed in not only RB char but other chars. The formation of nanoscale particles of metallic Fe and CaO accounts for high catalytic performance of RB char.

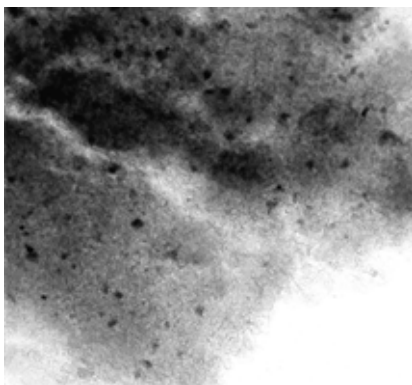


Figure 3. TEM picture of RB char before NH_3 decomposition.

To examine the relationship between NH_3 conversion and the content of Fe or Ca inherently present in char, these elements were chemically determined. The results are provided in Figure 4. The conversion at 750°C increased with increasing Fe or Ca content, and the correlation was stronger with the Fe. When Fe or Ca cations were externally added to brown coals, followed by carbonization, the Fe is much more effective for NH_3 decomposition than the Ca. It is thus likely that the inherent Fe in char plays more crucial role in this reaction than the Ca.

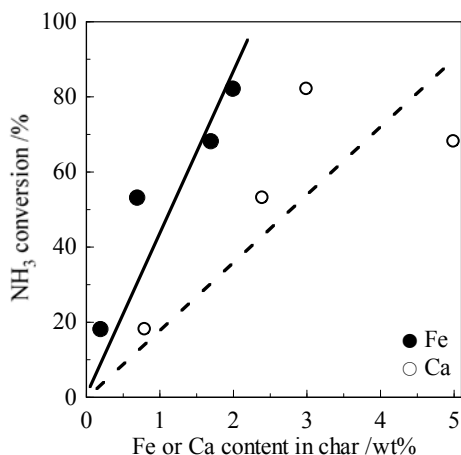
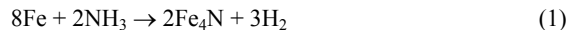


Figure 4. Relationship between the content of inherent Fe or Ca in char between NH_3 conversion at 750°C .

It has been proposed that NH_3 decomposition with Fe catalysts supported on brown coal chars proceeds through a following cycle mechanism involving $\alpha\text{-Fe}$ and the nitride species.²⁾



Thus, the inherent Fe in char can also promote NH_3 decomposition via the same mechanism as above. Although the XRD peaks of Fe_4N could not be detected in RB char after reaction, the TPD measurements revealed that, when the used char was quenched to room temperature and then heated in a stream of high purity He, the formation of N_2 started around 600°C , suggesting the decomposition of the nitride species to N_2 .

With Ca species after reaction, very weak diffraction lines of CaCN_2 appeared in RB and AB chars. This species was also observed after NH_3 decomposition with Ca catalyst added. The CaCN_2 may be formed according to the following equation:



Since the standard free energy changes are estimated to -27 kJ/mol, eq. (3) is thermodynamically favorable. The TPD measurements showed that the decomposition of CaCN_2 to N_2 occurred at higher temperatures of $> 700^\circ\text{C}$ than observed for Fe_4N . These results suggest that the Ca-catalyzed NH_3 decomposition proceeds via the mechanism involving CaCN_2 .

When a simulated gas including H_2 , CO , and CO_2 as well as 2000 ppm NH_3 was used in place of NH_3 diluted with He alone, the initial activity of RB char was low, but, in contrast to the profile observed in Figure 1, NH_3 conversion increased with increasing time on stream and was finally comparable to that in Figure 1. To make clear the catalytic effectiveness of coal chars in the coexistence of a large concentration of syngas should be the subject of future study.

Conclusions

Some chars prepared from low rank coals work efficiently as the catalysts for decomposition at 750°C of 2000 ppm NH_3 diluted with He. The presence of fine particles of metallic Fe and CaO, formed from Fe and Ca ions naturally present in low rank coals, accounts for such catalytic performances. There is a stronger correlation between NH_3 conversion to N_2 and Fe content in char. The char with the largest content of 2 wt% Fe shows the stable activity during 25 h reaction and achieves complete decomposition of NH_3 at 850°C . It is likely that the catalytic decomposition proceeds through the mechanisms involving Fe_4N and CaCN_2 as intermediate species.

Acknowledgement. The present work was supported by a Grant-in-Aid for Scientific Research on Priority Areas (B) from the Ministry of Education, Science, Sports, and Culture, Japan (No. 11218202). One of the authors (CX) gratefully acknowledges Japan Society for the Promotion of Science for the Postdoctoral Fellowship.

References

- (1) Mitchell, S.C.. In *Hot Gas Cleanup of Sulfur, Nitrogen, Minor and Trace Elements*; IEA Coal Research, London, 1998.
- (2) Ohtsuka, Y.; Xu, C.; Kong, D.; Tsubouchi, N. Prepr. Pap. - *Am. Chem. Soc., Div. Fuel Chem.*, **2001**, *46*, 152.
- (3) Wu, Z.; Ohtsuka, Y. *Energy Fuels* **1997**, *11*, 902-908.

THE INFLUENCE OF MINERAL MATTERS IN COAL ON THE REACTION OF NO-CHAR IN THE PRESENCE OF SO₂

Hui Chang, Baoqing Li, Wen Li, and Haokan Chen

State Key Laboratory of Coal Conversion, Institute of Coal Chemistry, Chinese Academy of Sciences, Taiyuan, China 030001

Introduction

The emission of NO_x from coal combustion has become one of the greatest challenges in environmental protection. It is well known that NO_x is one of the main contributors of acid rain and N₂O is the greenhouse gas and depletes the ozone layer indirectly. So great effort has been made to reduce NO economically and effectively. The reduction of NO by char *in situ* is an important reaction that determines the fuel-N converse to NO during coal combustion.

It is desirable to clarify the catalytic activities of mineral matters of coal on the reaction of NO-char. Many active components coexist in coal and their activities can be enhanced or abated each other, and the active components may have the potential synergistic activity in the reaction of NO-char. Recently, the effect of mineral matters in coal on the reaction of NO-char has been reported¹. Illan-Gomez *et al.*²⁻⁴ studied the reduction of NO by carbon materials loaded with K, Ca and Fe in inert atmosphere. The reduction of NO by coal chars loaded with Ca and Fe in various atmosphere (O₂ and CO) was also conducted⁵. Li *et al.*⁶ found the catalyst of Na-Fe has the synergistic activity in NO-char reaction.

CO, O₂ and SO₂ are inevitable in the real exhaust gases. However, the effect of mineral matters on the reaction of NO-char in the presence of SO₂ has not been addressed. The principal motive of the present work is to investigate the catalytic characteristics of mineral matters in the presence of SO₂. Furthermore, the study will also provide some valuable information about char as the reducing agent and catalyst supporter in flue gas cleaning technology.

Experimental

Chinese longkou(LK) lignite, wulong(WL) bituminous coal and yangquan(YQ) anthracite were used in the study. The characteristics of coal samples are shown in **Table 1** and **Table 2**. The deashed coals were prepared by demineralization using concentrated HF and HCl subsequently. The chars of deashed coals and raw coals were obtained in a quartz fluidized bed (i.d.50mm) at 900°C for 30min in N₂ atmosphere.

Table 1. Proximate and Ultimate Analyses of Coal Chars

Sample	Ash/w%, d	Ultimate Analysis /w%, daf				
		C	H	S	N	O*
LK	13.20	92.58	0.73	0.44	2.07	4.18
WL	13.92	94.56	0.69	0.79	1.74	2.22
YQ	11.37	96.00	0.73	0.30	1.27	1.70
LK-de	0.42	92.90	0.68	0.39	2.55	3.48
WL-de	0.89	94.73	0.70	0.51	1.69	2.37
YQ-de	1.02	95.33	0.73	0.23	1.26	2.45

* By difference

Table 2. The Analyses of Mineral Matters in Chars (w%)

Sample	SiO ₂ Na ₂ O	Al ₂ O ₃	Fe ₂ O ₃	TiO ₂	CaO	MgO	K ₂ O
LK	7.63	3.10	0.52	0.07	0.69	0.27	0.11
WL	7.66	2.52	1.92	0.12	0.51	0.10	0.24
YQ	6.77	3.29	0.20	0.14	0.12	0.08	0.23

NO-char reaction was performed in a quartz tube (i.d.20mm) fixed bed reactor with a fused quartz sieve-plate in the center as the

gas distributor and supporter of the reactant char.

Each sample was pretreated at 900°C for 30min before each experiments. Two methods were conducted in this study: (i) Temperature programmed reaction (TPR): The pretreated samples decreased to 400°C, and then Ar was switched to Ar/NO/SO₂ (NO: 560ppm, SO₂: 1000ppm). When the NO concentration reached to the stable level, TPR was performed at the heating rate of 5°C/min; and (ii) Isothermal reaction: When temperature was lowed to certain level, Ar was switched to Ar/NO/SO₂ and reacted for 20min, then switched off SO₂, and kept the same total flow rate by balance gas of Ar. After reaction for 20min, above step was repeated.

Results and Discussion

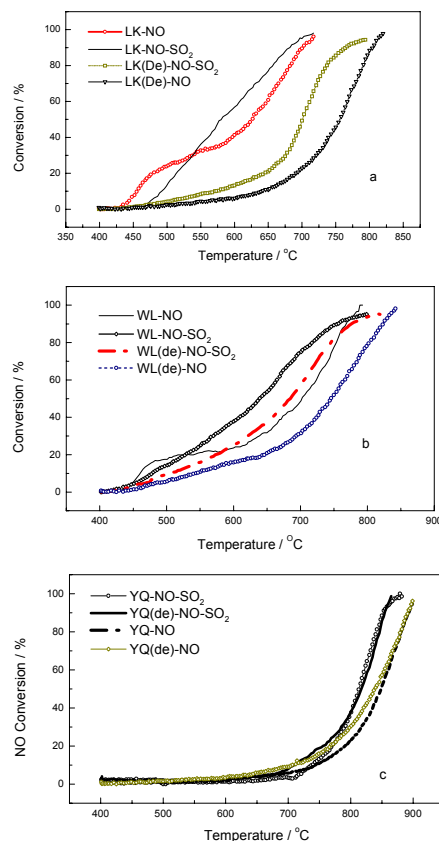
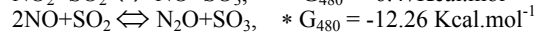
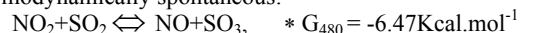


Figure 1. TPR of deashed chars and raw chars.

The effectiveness of mineral matters on the reaction of NO-char in the presence of SO₂ by TPR is presented in **Figure 1**. The result shows that the conversion of NO is enhanced with increasing temperature. The three coals have a common phenomenon, *i.e.*, the conversion of NO is higher in the SO₂-containing system at the higher temperature (>530°C for LK and WL, and >650°C for YQ) for raw char. Apart from the effect of mineral matters in char, the gas-gas reaction of NO and SO₂ become another main contributor to NO conversion, which is in agreement with Angelidis and Kruse⁷. They found that all possible nitrogen oxides can oxidize SO₂ to SO₃ at 480 °C since the respective equilibrium reactions are thermodynamically spontaneous:



We also found that at high temperature (> 600 °C) the NO-SO₂

reaction can happen easily as shown in **Figure 2**. However, SO_2 can suppress the conversion of NO at low temperature. It was known that the active components in their reduced state after the pretreatment can accept oxygen from NO and form the intermediate $\text{M}_x\text{O}_y(\text{O})^8$ during the process of NO conversion. $\text{M}_x\text{O}_y(\text{O})$ is less stable and can transfer O to active sites of the char. Sumiya *et al*⁹ found that with the addition of SO_2 the active components cannot catalyze the reduction of NO due to the formation of sulfates on the catalyst. The deashed chars have the similar phenomenon in the presence of SO_2 . The suppression of NO at low temperature is resulted from the occupation of the active sites by SO_2 .

Comparing with deashed char, LK and WL raw chars have higher activity obviously on NO reduction in the presence of SO_2 because of the catalytic effect of mineral matters in the char. As shown in **Table 2**, LK raw char contains more active components, especially sodium (Na_2O : 0.59%) and WL char more Fe (1.92%), which can catalyze the NO-char reaction effectively^{3,10}. Thus, the conversion of NO is higher for LK and WL raw chars than their deashed chars. However, YQ char shows the different phenomenon, because too much inert components exist in the char, leading to the abatement of the catalytic activities of the active components.

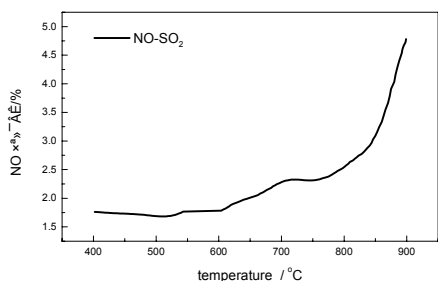


Figure 2. Gas-gas reaction of NO and SO_2 .

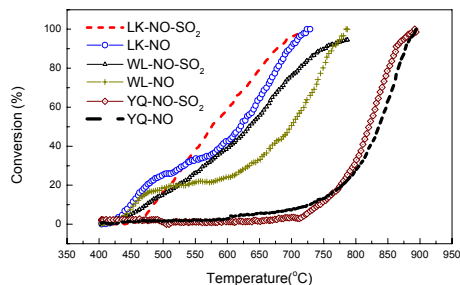


Figure 3. TPR of raw char of different coal.

NO conversion of various chars with or without presence of SO_2 is different as shown by TPR in **Figure 3**. The order of activity is LK char > WL char > YQ char. During the temperature range of NO reduction, NO conversion is mainly determined by two factors: NO- SO_2 reaction and the catalytic activities of mineral matters in char. Thus, the conversion of NO is higher for LK and WL raw chars than their deashed chars. Because of the high contents of Na and Fe in LK coal, the highest activity of LK char may imply that Na and Fe as active components have synergistic function in NO reduction.

The isothermal experiments were carried out at 700°C and 550°C for deashed chars and raw chars. The results are presented in **Figure 4**. It is proved that the effect of SO_2 on the NO-char reaction is different at different temperature. For both deashed and raw chars, SO_2 suppress the reduction of NO at low temperature, because of the occupation of SO_2 and the formation of sulfates on active sites, while at high temperature NO conversion is promoted by the NO- SO_2 reaction and the effect of active components. Furthermore, high temperature can enhance the activity of the active sites on the surface

of the chars.

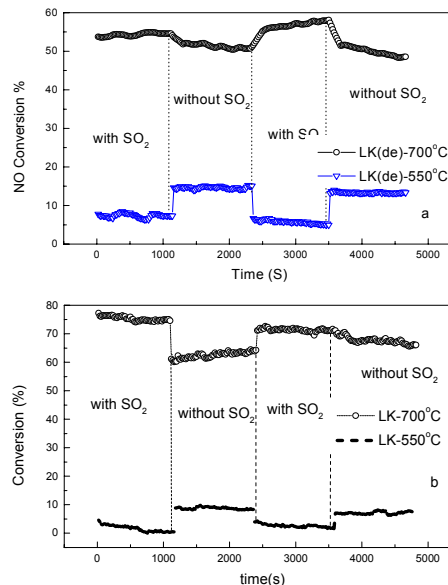


Figure 4. Effect of SO_2 on the activities of LK chars.

Conclusions

- (1) The reduction of NO is enhanced with increasing temperature during the range of 400°C-900°C;
- (2) The effect of SO_2 on the NO-char reaction is changed with temperature. At low temperature SO_2 can suppress the conversion of NO, while at high temperature NO conversion is enhanced by the reaction of NO- SO_2 ;
- (3) The effect of mineral matters is closely related to the content of active components and its dispersion. If the char contains more active components in mineral matters, it can catalyze the NO-char reaction effectively (like LK and WL chars), otherwise it will abate the NO-char reaction (like YQ char).

Acknowledgment.

The authors thanks for the financial support of Natural Science Foundation of China (29936090) and Special Funds for Major State Fundamental Research Project of China (G1999022102).

References

- 1 Zhao, Z. B., Li, W., Li, B. Q., 11th International Conference on Coal Science, U.S., 2001,9.
- 2 Illan-Gomez, M. J., Linares-Solano, A., Radovic, L. R., and Salinas-Martinez de lecea, Energy & Fuels, 1995,9,112-118.
- 3 Illan-Gomez, M. J., Linares-Solano, A., Radovic, L. R., and Salinas-Martinez de lecea, Energy & Fuels, 1995, 9,540-548.
- 4 Illan-Gomez, M. J., Linares-Solano, A., Salinas-Martinez de lecea, Energy & Fuels, 1995,9,976-983.
- 5 Zhao, Z. B., Li, W., Li, B. Q., Fuel, 2002, 81,1559-1564.
- 6 Li, B. Q., Zhao, Z. B., Li, W., Fuel Chemistry Division Preprints, 2001, 46(1), 163-166.
- 7 Angelidis, T. N., Kruse, N., Appl. Catal. B: Environ., 2001, 34(3):201-212.
- 8 Yamashita, H., Yoshida, S., Tomita, A., Energy & Fuels, 1991, 5(1), 52-57.
- 9 Sumiya, S., Saito, M., He, H., Feng, Q.-C., Takezawa, N., Yoshida, K., Catal. Lett., 1998,50-87.
- 10 Kapteijn, F., Alexander, J. C., Mierop, G. A., Moulijn, J. A., J. Chem. Soc. Chem. Commun., 1984, 1085-1086.

NUMERICAL ANALYSIS OF PULVERIZED COAL COMBUSTION CHARACTERISTICS USING ADVANCED LOW-NO_x BURNER

Ryoichi Kurose¹, Hisao Makino² and Akira Suzuki³

¹Yokosuka Research Laboratory, Central Research Institute of Electric Power Industry (CRIEPI), 2-6-1 Nagasaka, Yokosuka, Kanagawa 240-0196, Japan

²CS Promotion Office, CRIEPI, Otemachi Bldg., 1-6-1 Otemachi, Chiyoda-ku, Tokyo 100-8126, Japan

³CD-adapco JAPAN Co., LTD, Nisseki Yokohama Bldg. 16F, 1-1-8 Sakuragicho, Naka-ku, Yokohama, Kanagawa 231-0062, Japan

Introduction

Coal is an important energy resource to meet the future demands of electricity, because its reserves are more abundant than that of other fossil fuels. The major utilization method of coal in thermal power plants is pulverized coal combustion for which the reduction of environmental pollutants, especially NO_x emissions, is indispensable. In utility boilers, the most effective technology for NO_x reduction is the staged combustion method. However, this method generally causes another problem: the increase in unburned carbon.

To overcome this situation, we have investigated pulverized coal particle motion, thermal decomposition, NO_x formation and reduction and so on near the burner in a furnace, and developed an advanced low-NO_x burner called the CI- α (CRIEPI-IHI advanced Low Pollution High Ability) burner¹. The concept of the CI- α burner is that the residence time of pulverized coal particles in high temperature fields near the burner is lengthened by the recirculation flow and the thermal decomposition of coal particles is accelerated. The CI- α burner achieved a further 30% NO_x reduction compared to the conventional low-NO_x burners without any increase in the unburned carbon. However, the behaviors of the flow and coal particles in the furnace have not been sufficiently evaluated yet because of the difficulty to measure them.

The purpose of this study is, therefore, to apply a three-dimensional numerical simulation to the pulverized coal combustion field in the furnace installed with the CI- α low-NO_x burner, and to investigate the detailed combustion characteristics.

Numerical Simulation

Computational Domain and Conditions. The test furnace used was one at Yokosuka Research Laboratory of CRIEPI, in which the CI- α burner with a coal combustion capacity of about 0.1 t/h was installed. The furnace was a cylindrical furnace with a diameter of 0.85 m and a length of 8 m. The configurations of the computational domain and the CI- α burner are shown in **Figure 1**. The computational domain was half of the furnace. The combustion air was injected through the burner and through the staged combustion-air ports mounted at 3.0 m from the burner outlet. The air through the burner was divided into primary air, secondary air and tertiary air. The primary air moved in a straight motion, and the secondary and tertiary air moved in a strong swirling motion. The swirl vane angles for the secondary and tertiary air were set at 81 deg. and 72 deg. respectively, which were optimum values for bituminous coal. The pulverized coal was carried with the primary air.

The combustion conditions were the same as in our recent experiments². The value of the thermal input was 2.725×10^6 kJ/h. The air ratio was 1.24, and the excess O₂ concentration was 4.0%. The staged combustion air ratio was set at 30 %. The mass ratio of the pulverized coal (dry base) to the sum of the air and moisture in

the primary air was 1:2.2, and the mass ratio of the secondary air to the tertiary air was 1:6. The test fuel was Newlands coal (bituminous coal).

Mathematical Models and Numerical Method. The computation was performed using the STAR-CD code. The gas-phase turbulence was represented by the renormalization group (RNG) k- ϵ model^{3,4}, and the continuity and momentum equations were solved using the SIMPLE algorithm. The motion of the representative coal particles was calculated by Lagrangian formulation. The particle temperature was calculated by considering the heat transfer due to convection, radiation, heat loss due to vaporization of moisture in coal, and heat gain due to char combustion. The radiative heat transfer among the gas, particles and wall were simulated by the discrete transfer radiation method of Lockwood and Shah⁵.

The concept of pulverized coal combustion simplified for this calculation is shown in **Figure 2**. Coal devolatilisation [arrow (1)] was simulated by first-order single reaction model⁶. The gaseous combustion between the volatilized fuel and the air was calculated using the combined model of kinetics and eddy dissipation models [arrows (3)–(5)]. As a chemical mechanism, 2 global reactions, $C_aH_bO_c + 0.5O_2 \rightarrow \alpha CO + \beta H_2O$, $CO + 0.5O_2 \rightarrow CO_2$, were used. Here a , b , c , α and β were determined by the coal constituent. Regarding the kinetics, the rate of the reaction for reactants of $C_aH_bO_c$ and CO was given by Arrhenius expression⁷. Char burning [arrow (2)] was simulated using Field et al.'s model⁸.

For the NO_x formation, three different mechanisms were employed, namely Zeldovich NO_x, prompt NO_x and fuel NO_x [arrows (6)–(9)]. The Zeldovich NO was evaluated by applying a quasi-steady state approximation for N species to the extended Zeldovich mechanisms with the rate constants of Baulch et al.⁹. The prompt and fuel NO were predicted using the models of De Soete^{10,11}.

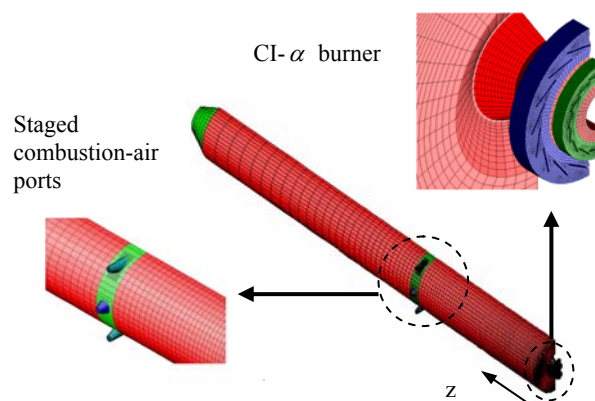


Figure 1. Computational domain and burner.

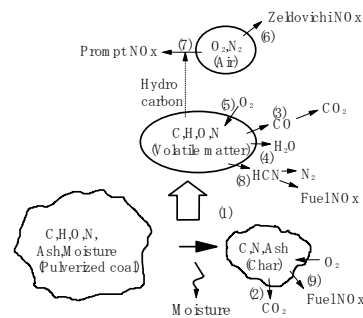


Figure 2. Concept of Pulverized coal combustion.

Results and Discussion

Gas velocity vectors and particle trajectories near the CI- α burner in the furnace are shown in **Figure 3**. As expected in the previous experiments¹, recirculation flow is generated and the residence time of coal particles is lengthened by being caught in the flow. It was also found that the residence time in this recirculation zone tends to be longer for intermediate coal particles with diameters of 20 and 40 μm than that for smaller or larger coal particles. This is attributed to the fact that the coal particles with smaller diameters instantly vanish due to devolatilisation, and those with larger diameters are not caught by the recirculation flow because of their large inertias.

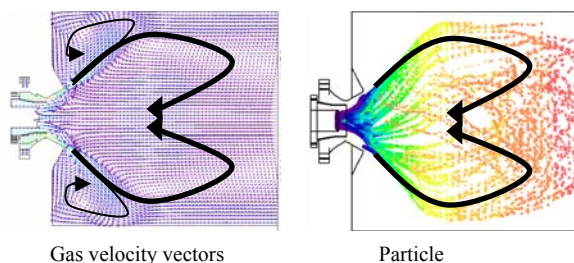


Figure 3. Gas velocity vectors and particle motions.

Figures 4 and 5 show the comparisons of axial distributions of the gas temperature and the O_2 mole fraction. The axial distribution of the gas temperature is in general agreement with the measurements², whereas that of the O_2 mole fraction indicates a greater value than the measurements² around the region where the staged combustion air is injected ($z=3.0\text{m}$). The discrepancy is considered to be due to the inlet condition of the staged combustion air and/or the limitation of the RNG $k-\epsilon$ turbulent model^{3,4}. That is, there are possibilities that the maximum velocity of the injected air is less than that of the experiments² because a non-slip condition was not set on the wall boundary of the ports, and that the numerical method using the RNG $k-\epsilon$ turbulent model^{3,4} overestimates the swirl strength, which prevents the air (O_2) from reaching the center region in the furnace. However, the specified feature that the extreme low- O_2 zone is found near the burner can be simulated well.

Figure 6 shows the comparisons of axial distribution of the NO mole fraction. Although the calculated value near the burner nearly corresponds with the experimental value², the rate of decrease with the axial distance is much less than that for the experiments². This means that the NO reduction which is observed in the experiments² does not function in the present computation. The reason for this can be explained as follows. As indicated by arrow (8) in **Figure 2**, the formation of the fuel NO from the nitrogen in volatiles are modeled under the assumption that the fuel-bond nitrogen is released as HCN and HCN transforms to NO or N_2 . However, to account for the NO reduction in the low- O_2 (fuel-rich) zone, the destruction of NO to HCN by hydrocarbon radicals ($\text{NO} \rightarrow \text{HCN}$) should be added in this model. Magel et al.¹² compared the NO emissions for staged and unstaged combustion conditions between experiment and calculation and found that the NO destruction mechanism played an important role especially for the staged combustion condition.

Conclusions

The pulverized coal combustion characteristics in a furnace installed with the CI- α burner was numerically investigated. It was observed that the recirculation flow and the extreme low- O_2 zone appeared near the burner. To improve the accuracy of the numerical

prediction for the NO_x emissions, it is necessary to account for the NO destruction mechanism in the fuel NO formation model.

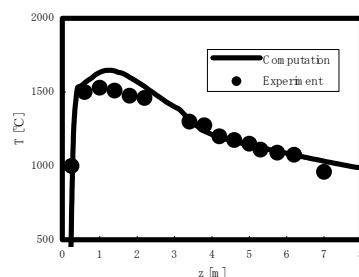


Figure 4. Axial distribution of gas temperature.

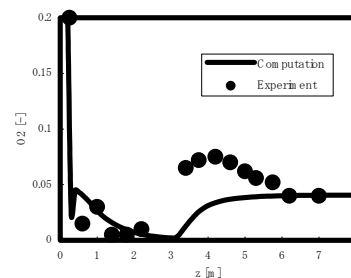


Figure 5. Axial distribution of O_2 mole fraction.

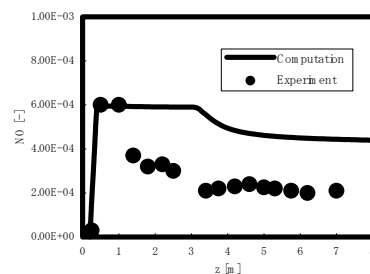


Figure 6. Axial distribution of NO mole fraction.

Acknowledgment

The authors are indebted to Mr. M. Kimoto, Dr. H. Tsuji and Mr. M. Ikeda of CRIEPI for their help in providing the experimental data. The authors also would like to thank Mr. M. Sato of CD-adapco JAPAN CO., LTD. for many helpful discussions.

References

1. Makino H et al., *EPRI-ODE-EPA Combined Utility Air Pollution Control Symp.: The MEGA Symp.*, vol.2. Atlanta, USA: EPRI, 1999. p.11.
2. Ikeda M et al., *JSME Int. J., Ser. B*, 2002;45:506.
3. Yakhot V et al., *Sci. Comp.*, 1986;1:1.
4. Yakhot V et al., *Phys. Fluids*, 1992;4:1510.
5. Lockwood FC et al., *18th Symp. (Int.) on Comb., The Combustion Institute*, 1981, p.1405.
6. Van Krevelen DW et al., *Fuel*, 1951;30:253.
7. Borman GL et al., *Comb. Engng.*: McGRAW-HILL, 1998. p.120.
8. Field MA et al., *The Combustion of Pulverised Coal*, British Coal Utilisation Research Association: Leatherhead, Surrey, 1967.
9. Baulch DL et al., *Evaluated Kinetic Data for High Temperature Reactions*: Butterworth, 1973.
10. De Soete GG, *15th Symp. (Int.) on Comb., The Combustion Institute*, 1975, p.1093.
11. De Soete GG, *23th Symp. (Int.) on Comb., The Combustion Institute*, 1990, p.1257.
12. Magel HC et al., *NOx-reduction with Staged Combustion – Comparison of Experimental and Modelling Results, Joint Meeting of the Portuguese, British, Spanish and Swedish Section of the Combustion Institute*, Maderia, 1996.

EFFECT OF IRON AND CALCIUM COMPOUNDS ON NO EMISSION DURING COAL COMBUSTION

Rengui Guan, Wen Li, Haokan Chen and Baoqing Li

State Key Lab of Coal Conversion, Institute of Coal Chemistry,
Chinese Academy of Sciences, Taiyuan, 030001, China

Introduction

Millions tons of NO_x are released into atmosphere per year by the coal-fired power stations, which causes serious environmental pollution. During coal combustion, the major proportion of NO_x is NO which can be formed by three ways: thermal NO, prompt NO and formation from fuel-bound nitrogen (Fuel-N)¹. Not all the Fuel-N thoroughly turned into NO and the conversion rate is dependent on the combustion conditions. Fuel-N partly turns into NO through two possible processes: oxidation of volatile and oxidation of char. The later was the main source of NO. The formed NO can be reduced by reductive agents such as CO, char etc. The ultimate NO emission concentration is determined by the competitive results of oxidation of fuel-N and reduction of the formed NO.

Minerals in coal affect many coal utilization processes. They also have evident influence on both formation and reduction of NO, which play an important role in NO emission². Calcium and iron, the highly active components in minerals, are paid more attention during coal combustion. Calcium-based compounds are widely used as SO₂ retention agents for their high efficiency and low cost, which are found to be responsible for higher NO emission in fluidized bed combustion. On the other hand, calcium compounds under reductive atmosphere catalytically accelerate NO reduction reactions as well. The impregnated iron is well known as an effective NO reduction catalyst, while the high content iron in mineral matters does not show high catalytic reactivity. It is important to obtain further understanding of their effects on NO emission in order to reduce the NO pollution, which is the aim of this study.

Experimental

Coal samples. Neimeng bituminous coal (abbreviated as NM) was used in this study. In order to exclude the influence of inherent minerals in coal, NM (60-100mesh) was deeply demineralized by HF and HCl. The mineral-free sample was further depyrited by newly formed CrCl₂. The treated sample was dried in vacuum and denoted as NMDM. **Table 1** was the property of NMDM. To clarify the effects of iron and calcium compounds on NO emission during coal combustion, calcium compounds including CaO, Ca(OH)₂, CaCO₃, CaSO₄ and Ca(CH₃COO)₂, and iron compounds including FeCl₂, FeCl₃, FeSO₄ and Fe₂(SO₄)₃ were introduced to NMDM by mechanic mixing. The introduced compounds are all chemical agents. The ratio of each additive was 2% wt in coal.

Table 1. Characteristics of NMDM (wt%)

Ash (ad)	0.5	N (daf)	0.95
Water (ad)	0.4	S (daf)	0.21
C (daf)	76.53	O* (daf)	17.74
H (daf)	4.57		

O*: by difference

Procedure. The combustion experiments of samples were performed in a fixed-bed quartz reactor. 0.0500g samples were combusted in Ar mixed with 5.3% O₂ at heating rate of 10K/min. The gas flow rate was 325ml/min. NO, CO and O₂ in the flue gas were determined on line by Gas Analyzer (Kane-May 9106).

Results and Discussion

Emission profiles of NO and CO. During coal combustion, carbon was firstly oxidized to form CO which was further oxidized to CO₂. The total concentration of CO and CO₂ represented the rate of coal oxidation. We did not measure the CO₂ for the limitation of the Gas Analyzer, hence the exact rate of coal combustion could not be known, but we could gain a general idea by analyzing the concentration of O₂ and CO. **Figure 1** shows the emission profiles of NO, CO and O₂. It was clearly seen that there were a major peak of O₂ reduction at nearly 600°C and a shoulder peak at about 450°C. The shoulder peak resulted from the combustion of volatile, and the main peak was due to the combustion of char. The peak temperature for CO formation is at around 500°C, which is mainly due to the oxidation of volatile matters. After that, with rising the temperature the oxidation of CO accelerated, at the same time the oxidation of char to form CO became difficult because of the bad reactivity of char compare to that of volatile matters, the CO concentration was decreased and formed a shoulder peak at about 550°C.

Very little NO was formed during volatile oxidation. After 500°C, the NO concentration increased linearly upto 650°C, then decreased sharply. The peak temperature of NO emission was nearly 50°C higher than that of O₂ consumption, which indicated that the combustion reactivity of nitrogen was lower than that of carbon as a whole. John also observed the peak temperature of NO formation is higher than that of CO₂³.

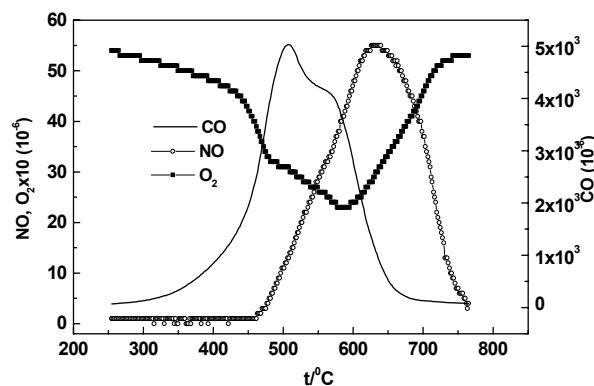


Figure 1. The emission profiles of NO, CO and O₂ during combustion of NMDM coal.

Effects of iron and calcium compounds. The iron compounds were widely used catalysts during coal gasification and combustion. They could accelerate both the formation and oxidation of CO. There are also many researches focused on their catalytic NO reduction under reduced atmosphere and catalytic NO formation under oxidation atmosphere¹. It was well known that the added iron showed high catalytic activity under CO or other reductive atmosphere, but the inherent iron in minerals of coal showed much low catalytic effect⁴, which suggested that the existing form of iron was very important for its catalytic activity.

CO emission profile during combustion of samples added with iron compounds was shown in **Figure 2**. Under our combustion conditions, the O₂ was superfluous to coal, hence the added iron compounds showed much catalytic activity of further oxidation of CO. Although the emission profile of CO was different with the different iron compounds added, especially in the second peaks, the total amount of CO emission was all decreased compared with that of

iron-free sample. It was also found that the peak temperature of CO emission of samples added with iron compounds moved to low range, which was due to catalytic effects of iron compounds on combustion of volatile and char.

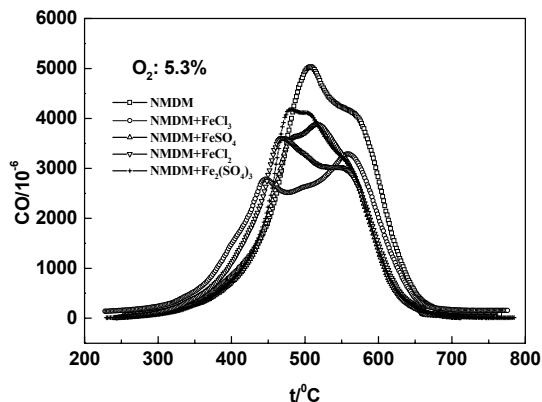


Figure 2. Emission profiles of CO during combustion of samples with and without iron compounds.

Figure 3 was the NO emission profiles during combustion of samples added with iron compounds. The added iron compounds catalyzed the combustion of carbon, and exposed the fuel-N to O₂, which resulted in decrease in both the peak temperature and the amount of NO evolution. This is believed to be due to the fact that iron compounds catalyzed the NO reduction by CO and char surface⁵. Although the iron compounds were different from each other, they showed the same catalytic tendency. This might infer that the added iron compounds turned into the same form (maybe FeO) during coal combustion.

Figure 4 compared the NO emission during combustion of different Ca-added samples. The calcium compounds showed the similar catalytic effects on both CO and NO emission with iron compounds. As a whole, the added calcium compounds decreased the NO emission⁶.

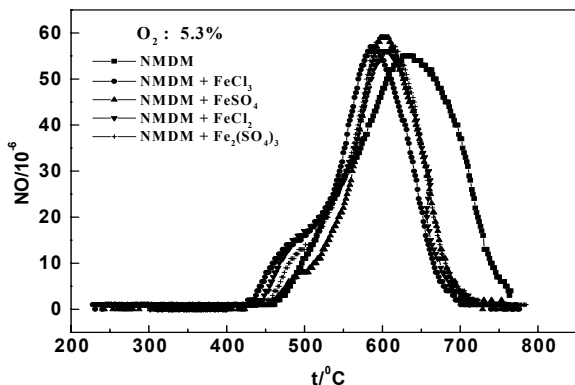


Figure 3. Emission profiles of NO during combustion of samples with and without iron compounds.

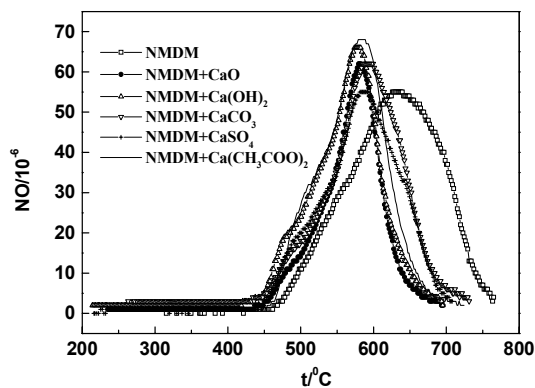


Figure 4. Comparative of NO emission during samples combustion added with calcium compounds.

Table 2 was the NO conversion during combustion of different samples under 5.3% O₂ concentration. It was found that iron compounds had higher catalytic activity in reducing NO emission than calcium compounds. This difference of catalytic reactivity between two kinds of compounds probably was due to their ability to form active intermediates and to provide active sites.

Table 2 NO Conversion for Different samples

Sample	NO conversion
NMDM	37.77
NMDM+FeCl ₃	28.23
NMDM+FeSO ₄	26.39
NMDM+FeCl ₂	28.75
NMDM+Fe ₂ (SO ₄) ₃	29.72
NMDM+CaO	33.62
NMDM+Ca(OH) ₂	30.61
NMDM+CaCO ₃	34.19
NMDM+CaSO ₄	29.86
NMDM+Ca(CH ₃ COO) ₂	32.20

Acknowledgment

This work was subsidized by the Special Funds for Major State Basic Research projects (G1999022102).

Reference:

- (1) Johnsson, J. E. *Fuel*, **1994**, 73(9), 1398.
- (2) Ralf, F. W. K.; Sven, H. *Fuel*, **1997**, 76(4), 345.
- (3) John, C. C.; Thomas, K. M.; Marsh, H. *Fuel*, **1993**, 72, 349.
- (4) Ana, I. G. A.; Thomas, K. M. *Fuel*, **1994**, 73(5), 635.
- (5) Illan-Gomez, M. J.; Linares-Solano, A.; Salinas-Martinez de Lecea, C. *Energy and Fuel*, **1995**, 9, 540.
- (6) Illan-Gomez, M. J.; Linares-Solano, A.; Salinas-Martinez de Lecea, C. *Energy and Fuel*, **1995**, 9, 976.

Simultaneous reduction of NO_x and N₂O emissions from a bubbling fluidized bed coal combustor using alternative bed material

Tadaaki Shimizu*, Jun Asazuma, Masayuki Shinkai,
Sayako Matsunaga, Kazuaki Yamagiwa, Naoki Fujiwara**

*: corresponding author, Department of Chemistry and Chemical Engineering, Niigata University, 2-8050 Ikarashi, Niigata, 950-2181, Japan

**: Idemitsu Kosan Co. Ltd

Introduction

Fluidized combustion has been developed as a coal combustion technology that can capture SO₂ by limestone feed without external wet scrubbing system. The temperature in the bed is usually maintained at approximately 1123 K so that SO₂ capture efficiency can be maximized. However, such low temperature is not advantageous for reduction of N₂O emission, which is known to be a greenhouse effect.

One approach to reduce N₂O emission is the use of catalyst as bed material to decompose N₂O. However, the use of catalysts has been reported to increase NO_x emission; red-mud (Fe-containing solid)¹, γ -alumina¹, Fe₂O₃², and MgO³ have been tested but the increase in NO_x with decreasing N₂O was reported. Limestone is also well known as a catalyst of N₂O decomposition but it also increases NO_x emission.^{2,4,5,6,7} The increase in NO_x during limestone feed is attributable to catalytic activity of limestone for NO_x formation through oxidation of NH₃ and HCN, both of which are released from coal during devolatilization.^{7,8,9} Thus the increase in NO_x with other catalytic bed materials is considered to be attributable to the oxidation of volatile-N by the catalyst.

Recently, Liu and Gibbs¹⁰ reported that a kind of alumina decreased N₂O emission without increase in NO_x during char combustion in a bench-scale BFBC. However, it is possible that their results are limited only for char combustion, where contribution of volatile-N to NO_x and N₂O emissions is less pronounced than that during coal combustion. A catalyst which reduces N₂O without increasing NO_x during coal combustion has not yet been found.

In the present study, two kinds of porous alumina particles were tested as bed materials during bubbling fluidized bed combustion of four kinds of coal. The emissions of NO_x and N₂O were compared with those during combustion in the inert sand bed.

Experimental

A bench-scale BFBC of 1.3 m in height and 5.4 cm in inner diameter was employed. The reactor was heated by electric heaters and the temperature in the bed and the freeboard was maintained at 1123 K. Primary air was fed through the distributor at the bottom of the bed. Secondary air was not injected. The superficial gas velocity was 20 cm/s at 1123 K.

Two kinds of porous alumina particles, MS-1B (Mizusawa Industrial Chemicals Ltd.) and activated bauxite (Engelhard Co. Ltd.) were used as alternative bed materials, the analysis of which is shown in Table 1. Non-porous quartz sand (QS), which is known to be inert for the reactions of NO_x and N₂O, was used as control. The minimum fluidizing velocity (U_{mf}) of each porous particle was nearly the same as that of the sand. The static bed height was 10 cm.

Four kinds of coals with different volatile matter content, from high volatile bituminous coals (HVB1 and HVB2), medium volatile bituminous coal (MVB) to semi-anthracite (SA), were employed as fuels. The analyses of the fuels are shown in Table 2. The size of the fuel was between 0.3 and 1.0 mm. The fuel was continuously fed through a vibration feeder, conveyed pneumatically in air stream, and

then injected into the bottom of the bed about 1 cm above the distributor. The feed rate of coal was controlled so that the desired O₂ concentration in the flue gas was attained.

Concentrations of O₂, total NO_x (=NO+NO₂), CO₂, and CO in the flue gas were continuously measured by a magnetic oxygen analyzer for O₂, a chemical luminescence analyzer for NO_x, and NDIR adsorption analyzers for CO₂ and CO, respectively. A portion of the dried sample gas was stored in Tedler (R) gas bags. Concentration of N₂O in the gas was measured by gas chromatography with a thermal conductivity detector.

Table 1. Composition, Size, and Surface Area of Bed Materials

Composition [wt-%]	MS-1B	Activated	Quartz sand
	(MS)	Bauxite (AB)	(QS)
	0.39mm	0.40mm	0.27 mm
Al ₂ O ₃	84.7	69.4	-
SiO ₂	2.2	7.2	100
MgO	0.0	0.0	-
CaO	0.8	0.3	-
TiO ₂	1.1	13.0	-
Fe ₂ O ₃	5.8	8.4	-
SO ₃	3.8	0.8	-
Others	1.6	0.9	-
Surface area [m ² /g]	195	124	Non-porous

Table 2 Analyses of Coals

Fuel	Ultimate analysis (daf, wt%)					Proximate analysis(dry, wt%)		
	C	H	O ^a	N	S ^b	V.M. ^c	F.C. ^d	Ash
HVB1	80.1	6.1	11.7	1.5	0.6	38.3	47.5	14.2
HVB2	78.1	6.3	13.4	1.3	1.0	41.4	43.5	15.1
MVB	85.9	4.9	7.0	1.7	0.5	27.0	57.7	15.4
SA	89.7	4.2	3.6	1.9	0.7	15.9	72.3	11.2

a: by diff.; b: combustible S; c: Volatile matter; d: Fixed carbon

Results and Discussion

Figure 1 shows the effect of bed material and flue gas oxygen concentration on emissions of NO_x and N₂O. Both alumina particles (MS and AB) employed for the present work were effective for N₂O reduction in comparison to the sand bed. This is attributable to the catalytic activity of present alumina particles to decompose N₂O.

However the role of bed material to NO_x emission was different between MS and BA; MS bed material reduced NO_x emission whereas BA increased it. At this moment, the mechanism of the difference in NO_x emission between the two bed materials is not clear. One possibility is that the selectivity of volatile-N to NO_x is different between two particles. In the following part, the results obtained by use of MS bed material will be shown since AB was not effective to the reduce NO_x.

In Figure 1, the effect of oxygen concentration on emissions of N₂O and NO_x is also shown. For the sand bed, both N₂O and NO_x emissions increased with increasing flue gas O₂ concentration. The sensitivity of N₂O and NO_x emissions to flue gas O₂ concentration was weak for the MS bed. This is advantageous not only for suppression of NO_x and N₂O emissions but also suppression of SO₂ emission. SO₂ capture by limestone is known to be inhibited by reduction of O₂/fuel ratio since the low O₂ atmosphere or reducing gases such as CO reduce SO₂ capture rate by CaO or enhance decomposition of CaSO₄ to CaO and SO₂.^{11,12} Thus operation with higher O₂/fuel ratio is preferred for SO₂ reduction but it increases NO_x and N₂O emissions for the conventional bed material. The

present bed material (MS) is considered to enable operation at higher O_2 /fuel ratio without increasing NO_x and N_2O emissions.

Figure 2 shows the effect of fuel type on conversions of fuel bound nitrogen (fuel-N) to N_2O and NO_x . For all the fuels tested, the present MS bed material reduced N_2O emission without increasing NO_x emission. But its effect was different among fuels. The reduction of N_2O by MS was more remarkable for fuels with lower fixed carbon content. On the other hand, the reduction of NO_x by MS was more effective for higher fixed carbon content fuel.

The present results were obtained using a small-scale reactor and it is necessary to discuss if the present results are applicable to large-scale FBCs. Under the present condition, the static bed height (H_s) was 10 cm and the superficial gas velocity (U_0) was 20 cm/s and the contact time, H_s/U_0 , was 0.5 s. In large-scale BFBCs, the static bed height and the superficial gas velocity are approximately 1 m and 1 m/s, respectively, and the contact time in the large BFBCs is approximately 1 s. Therefore the contact between gas and solid in the large-scale BFBCs is sufficient and the suppression of N_2O and NO_x emissions by the present MS bed material is expected to occur in the large-scale plant.

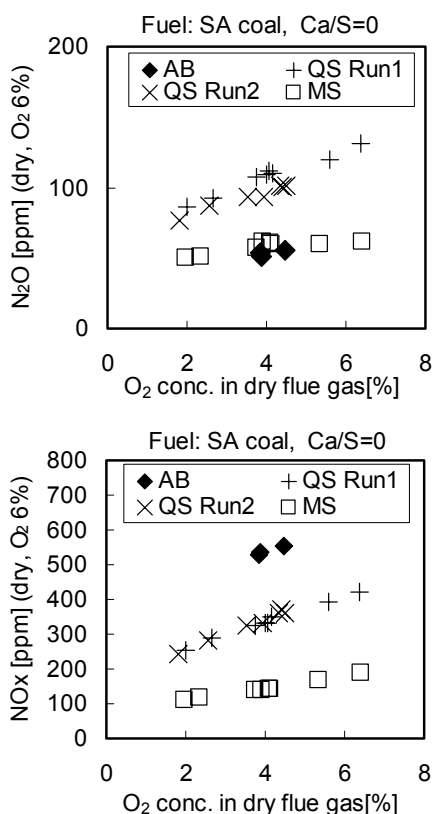


Figure 1. Effect of bed material and O_2 concentration in the flue gas on N_2O and NO_x emissions during semi-anthracite combustion.

Conclusion

The present work found one kind of porous alumina particle which was effective not only for N_2O reduction but also suppression of NO_x emission during coal combustion in a bubbling fluidized bed.

Acknowledgement. T.Shmizu express his thanks to the T. Shimizu thanks The Ministry of Education, Culture, Sports, Science and Technology for Grant-in-Aids (No.11218204).

References

- Hirama, T., Hosoda, H. Moritomi, H., Suzuki, Y., Harada, M., Shimizu, T., Naruse, I., *Nihon-Energy-Gakkai-Shi (J. Jpn. Inst. Energy)*, **1993**, 72, 252-262
- Shimizu, T., Togashi, T., Miura, M., Karahasi, E., Yamaguchi, T., Tonsyo, M., Inagaki, M., *Proc.6th Int. Workshop on N_2O Emissions (Turku, Finland, 1994)*, **1994**, 115
- Klein, M., Rotzoll, G., *Proc.6th Int. Workshop on N_2O Emissions (Turku, Finland, 1994)*, **1994**, 239
- Gavin, D.G. and Dorrington, M. A., *Proc. 1991 International Conference on Coal Science, (Newcastle, UK)*, Ed. by International Energy Agency Coal Research Ltd., Butterworth-Heinemann, Oxford, UK, **1991**, 347
- Åmand L-E., B. Leckner, S. Andersson and L. Gustavsson, *European workshop on N_2O emissions LNETI/EPA/IFP (Lisbon, Portugal)*, **1990**, 171
- Moritomi H., Y. Suzuki, N. Kido and Y. Ogisu, *Proceedings of 11th International Conference on Fluidized Bed Combustion (Montreal, Canada)*, ASME, New York, **1991**, 1005
- Shimizu, T., Tachiyama, Y., Fujita, D., Kumazawa, K., Wakayama, O., Ishizu, K., Kobayashi, S., Shikada, S., Inagaki, M., *Energy & Fuels*, **1992**, 6, 753
- Hirama, T., Kochiyama, Y., Chiba, T., Kobayashi, H. *Nenryo-Kyokai-Shi (J. Fuel Soc. Japan)*, **1982**, 61, 268
- Furusawa, T., Tsujimura, M., Yasunaga, K., Kojima, T. *Proc. 8th International Conference on Fluidized Bed Combustion (Houston, USA)*, DOE/METC-85/6021, U.S. Department of Energy, Office of Fossil Energy, Morgantown, West Virginia, U.S.A., **1985**, 1095
- Liu, H., Gibbs, B.M., *Proc. 15th Int. Conf. on Fluidized Bed Combustion (Savannah, GA, USA)*, ASME, **1999**, Paper No. FBC99-0114
- Kojima, T., Take, K., Furusawa, T. and Kunii, D. *J. Chem. Eng. Japan*, **1985**, 18, 432
- Hansen, P.F.B.; Dam-Johansen, K.; Bank, L.H.; Ostergaard, K., *Proc. 11th International Conference on Fluidized Bed Combustion (Montreal, Canada)*, ASME: New York, **1991**; 73

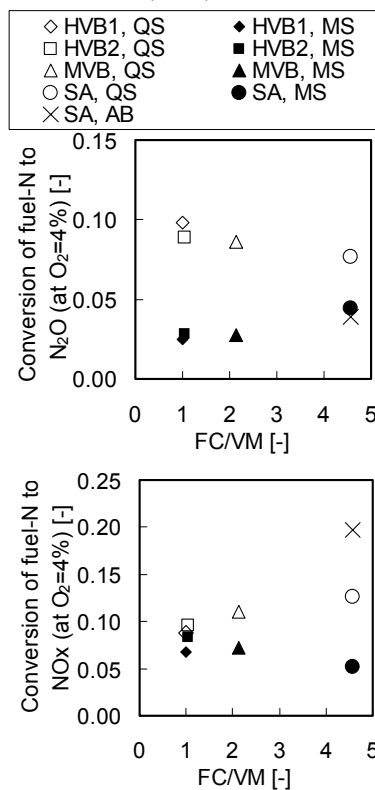


Figure 2. Effect of coal type on conversions of fuel-N to N_2O and NO_x at flue gas O_2 concentration of 4.0%

CONTINUOUS REMOVAL OF NO₂ INTO HNO₃ BY PITCH AND PAN BASED ACTIVATED CARBON FIBER

Takashi Enjoji^{a)}, Noriaki Shirahama^{a)}, Seung-Ho Yoon^{a)},
Yozo Korai^{a)}, Isao Mochida^{a)}, Akinori Yasutake^{b)},
Masaaki Yoshikawa^{c)} and Takaaki Shimohara^{d)}

a) Institute of Advanced Material Study, Kyushu University
6-1 Kasugakoen, Kasuga, Fukuoka 816-8580, JAPAN

b) Mitsubishi Heavy Industries Ltd., 5-717-1 Fukahori
Nagasaki 851-0392, JAPAN

c) Osaka Gas Co. Ltd., Torishima, Konohana
Osaka 554-0051, JAPAN

d) Fukuoka Institute of Health and Environmental
39 Mukaizano, Dazaifu, Fukuoka 818-0135, JAPAN

Introduction

SO₂ removal by wet scrubbing after NO selective reduction over V₂O/TiO₂ honeycomb has been established in the power plant to protect atmospheric environment. Nevertheless more efficient and deeper reduction of NO_x is still wanted. NO_x of very low concentration leaked to the environment causes photochemical smog and acid rain, NO_x must be removed from environmental air. Exhausted NO from automobile and boiler is oxidized in atmosphere gradually into NO₂. The most harmful species of the NO_x in atmosphere is NO₂. The 20ppm of NO_x is detected at busy cross-section. Reduction of low concentration NO₂ in atmosphere can be one of direct caution for the environmental protection.

The present authors reported that pitch based activated carbon fiber (ACF) was very effective to remove SO₂ completely at 30°C in the flue gas (1000ppm SO₂, 5vol.% O₂, 10vol.% H₂O).^{1,2)} Pitch based ACF was calcined in argon gas at 1100°C for 1hr to increase its activity for SO₂ removal. PAN-ACF showed the high activity of adsorption and oxidation of NO₂ with oxygen at ambient temperatures when the fiber was also calcined in argon gas as an inert gas at 800°C for 1hr.³⁾

In the present study, NO_x of 20ppm in air was attempted to be fixed as HNO₃, which was continuously recovered from the ACF bed. The pitch based ACF was calcined at 400~1100°C to increase activity. Influence of humidity in air was studied to simulate real atmosphere.

Experimental

Pitch-based ACF (OG20A) and polyacrylonitrile-based ACF (FE300) were manufactured and supplied by Osaka Gas Co. and Toho Tenax Co., respectively. The ACF was further heat-treated in argon gas at 400~1100°C. The oxidation and hydration of 20ppm NO₂ with O₂ were carried out in dry and wet air using a flow type glass reactor (8mm diameter). 0.1~0.5g of ACF was closely packed in the reactor. The total flow rate (F) and the contact time (W/F) were 300 ml/min and $3.3 \times 10^{-4} \sim 1.7 \times 10^{-3} \text{ g} \cdot \text{min}/\text{ml}$, respectively. NO₂ and NO concentrations were analyzed continuously at the inlet and outlet of the reactor, using a NO_x meter (ECL-77, Yanagimoto Co., Kyoto). Stationary NO₂ conversion was determined when NO₂ concentration at the outlet of the reactor became stationary. Adsorption and oxidation of NO₂ appeared to continue for several hours after the reaction started.

Results and Discussion

Effect of heat-treatment temperature of ACFs

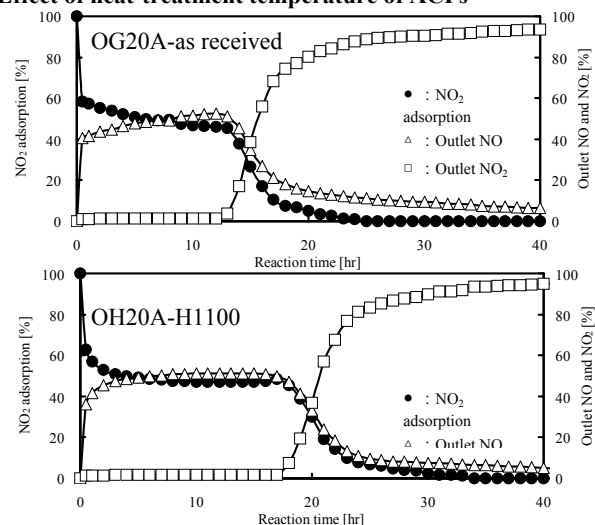


Figure 1. Profiles of NO₂ oxidation over Pitch-ACF OG20A and its heat-treatment in dry.

ACF : 0.1g, NO₂ : 20ppm, O₂ : 21%, Flow rate : 300ml/min
Relative humidity : 0%, Reaction temperature : 30°C

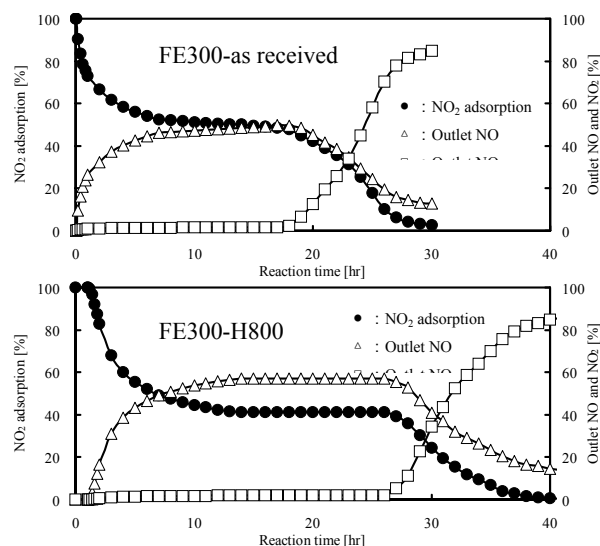


Figure 2. Profiles of NO₂ oxidation over PAN-ACF FE300 and its heat-treatment in dry.

ACF : 0.1g, NO₂ : 20ppm, O₂ : 21%, Flow rate : 300ml/min
Relative humidity : 0%, Reaction temperature : 30°C

Figure 1 illustrates reactivity of 20ppm NO₂ in dry air at 30 °C over as-received and heat-treated OG20As. NO₂ was converted to give NO in a gaseous product over OG20A series. NO₂ concentration at the outlet continued zero for 13hrs while 50% of NO₂ appeared to give NO. The some amount of NO₂ must be adsorbed on the ACF probably in form of NO₃. Hence 2 molecules of NO₂ in dry air were found to be disproportionated into NO and adsorbed NO₃ over pitch based ACF. Outlet NO concentration decreased shapes to 20% by 17hrs with an increase of outlet NO₂ concentration. After 17hrs, the outlet NO concentration decreased very slowly to be 5% by 40hrs, while no NO₂ adsorption was found.

Thus, NO_2 disproportionation continued for 23hrs. No apparent oxidation of NO_2 was observed under the condition.

Disproportionation increased with an increase of calcination temperature of ACF up to 1100°C . OG20A-H1100 continued the disproportionation for 32hrs, while the conversion of NO_2 gradually decreased to be zero, although the period of balanced NO_2 adsorption and NO outlet continued for 22hrs.

Figure 2 illustrates the reactivity of 20ppm NO_2 in dry air over as-received and heat-treated PAN-FE300 at 30°C . Over as-received FE300, outlet of NO was observed immediately when the gas started to flow. The outlet concentrations of NO and NO_2 were equivalent through disproportionation after 10hrs. The calcination of the ACF enhanced disproportionation. FE300-H800 showed the highest activity among PAN-FE300s, continuing stationary disproportionation reaction for 26hrs. The conversion of NO_2 started gradual decrease to be zero after 40hrs. Further higher calcination temperature shortened period of NO_2 adsorption and disproportionation.

Effect of humidity on NO_2 reaction in air

Figure 3 shows reactivity of 20ppm NO_2 in wet air over OG20A-H1100, varying relative humidity in the range of 0~100%. Humid air extended the period of disproportionation, its conversion to decreasing 20% by 70hrs, which appeared to continue stationary. Thus the wet air hydrates adsorbed NO_3 into aq. HNO_3 which flowed out from the bed to regenerate continuously active site of NO_3 adsorption.

Figure 4 shows reactivity of 20ppm NO_2 over PAN-FE300-H800 by varying relative humidity in the range of 0~100%. Wet air continued the removal of NO_2 at least for 60hrs while the disproportionation and oxidation reactions continued although the conversion decreased. It was found that formed HNO_3 over ACF was drained from the reactor to regenerate the active site.

Conclusions

Reactivity of 20ppm NO_2 in air was studied at 30°C over pitch based activated carbon fiber (OG20A) and polyacrylonitrile based activated carbon fiber (FE300) by varying the calcinations temperature of ACF as well as relative humidity in the reaction gas to find the continuous removal of NO_2 in atmosphere in form of HNO_3 . The calcination of ACF at a temperature up to $800\sim 1100^\circ\text{C}$ in inert atmosphere increased significantly adsorption and oxidation of NO_2 as observed for continuous removal of SO_2 into H_2SO_4 over the some ACFs. The OG20A and FE300 ACFs were calcined at 800°C and 1100°C to enhance its activity. NO_2 in dry air was found to be disproportionated into NO and adsorbed NO_3 over as-received and calcined ACF. NO_2 was oxidized and disproportionated into NO_3 to be adsorbed over the ACF, the latter reaction producing also NO . The disproportionation reaction was terminated by the saturation of NO_3 adsorption over ACF. Oxygen in air enhanced the oxidation of NO_2 into adsorbed NO_3 , reducing NO formation through the disproportionation. The same amount of adsorbed NO_3 terminated the both oxidation and disproportionation regardless of O_2 contents.

The humidity prolonged both oxidation and disproportionation reactions, before the breakthrough of NO_2 allowing stationary NO_2 removal in form of aq. HNO_3 at the release of some NO . Higher humidity increased the stationary NO_2 removal by eluting out adsorbed NO_3 in aq. HNO_3 . Higher humidity increased the NO_2 removal adsorbed NO_3 to regenerate the active site. It must be noted that the oxidation of NO_2 was limited on pitch based ACF. Large amount of PAN ACF extended the period of complete NO_2 removal and increased stationary NO_2 removal rate in air with

less NO formation. Pitch based ACF appeared to promote disproportionation more than oxidation.

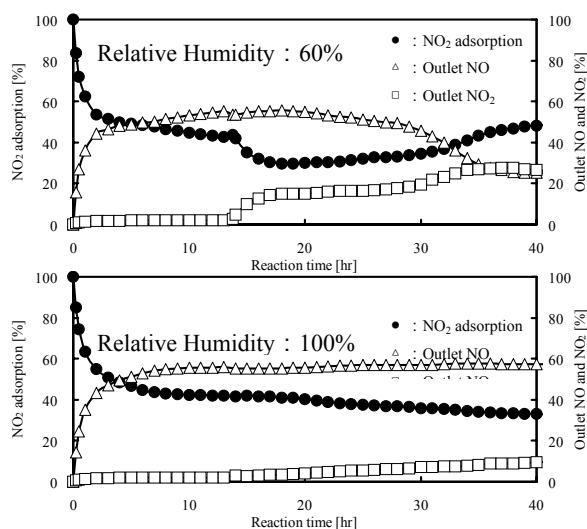


Figure 3. Reactivity of NO_2 over Pitch-ACF OG20A-H1100 at variable humidity.

ACF : 0.1g, NO_2 : 20ppm, O_2 : 21%, Flow rate : 300ml/min
Relative humidity : 60%,100%, Reaction temperature : 30°C

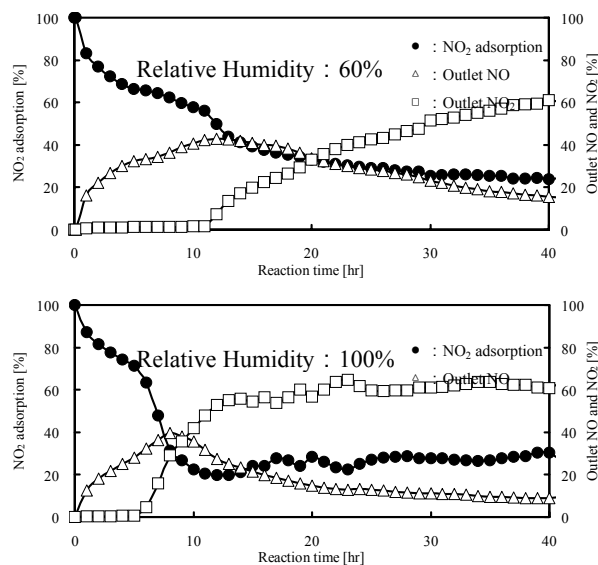


Figure 4. Reactivity of NO_2 over PAN-ACF FE300-H800 at variable humidity.

ACF : 0.1g, NO_2 : 20ppm, O_2 : 21%, Flow rate : 300ml/min
Relative humidity : 60%,100%, Reaction temperature: 30°C

References

- Mochida, I.; Kuroda, K.; Miyamoto, S.; Sotowa, C.; Korai, Y.; Kawano, S.; Sakanishi, K.; Yasutake, A.; and Yoshikawa, M. *Energy & Fuels*, **1997**, 11, 272.
- Mochida, I.; Miyamoto, S.; Kuroda, K.; Kawano, S.; Sakanishi, K.; and Korai, Y. *Energy & Fuels*, **1999**, 13, 374
- Mochida, I.; Kawano, S.; Hironaka, M.; Yatsunami, S.; Korai, Y.; Matsumura, Y.; and Yoshikawa, M. *Energy & Fuels*, **1995**, 9, 659

Reduction of NO_x by Activated Lignite Char

H. Gupta¹, S. A. Benson¹, L. -S. Fan², J.D. Laumb¹, E. S. Olson¹, C. R. Crocker¹, R. K. Sharma¹

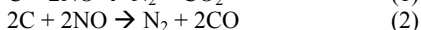
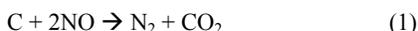
¹Energy and Environmental Research Center, 15 North 23rd Street, Grand Forks, ND 58203

²Department of Chemical Engineering, The Ohio State University, Columbus OH 43210

Introduction

Nitric oxide (NO) adsorbs physically and reversibly on graphite below ambient temperature.¹ It was observed that the extent of physisorption on a thermally pretreated activated carbon surface reduces with increasing sorption temperature in the 25-215 °C temperature range.² However, Teng and Suuberg observed that the contribution of chemisorption of NO on a thermally cleaned phenol-formaldehyde derived char increases with temperature in the 50-150 °C temperature range.³ Physisorption of NO leads to the formation of C(NO) type surface species that emit NO molecules upon thermal desorption. In contrast, chemisorption of NO occurs by the dissociation of NO molecules to form C(N), C(O), and C(O₂) type surface.⁴ Oxygen from the NO molecules form relatively stable surface complexes while nitrogen atoms from NO molecules pair up and exit the reaction system as nitrogen molecules.⁵ Saturation of the carbon surface prevents further interaction between NO molecules and carbon due to the non-availability of free carbon sites. Further increase in reaction temperature beyond 600-700 °C leads to the breakdown of surface complexes releasing CO and CO₂ from the surface and creating new carbon sites that sustain carbon-NO reaction. Desorption of chemical complexes, being a thermally activated process, increases with rising temperature. NO reduction is complete when the rate of desorption exceeds the rate of NO entering the carbon bed. This two-step mechanism has gained wide acceptance as the has been widely accepted as the mechanism of the high temperature carbon-NO reaction.⁶ The activation energy of the high temperature desorption of complexes (28-59 kcal/mol) was usually much higher than that involved in the low temperature dissociative chemisorption of NO (4.5-19 kcal/mol).⁷

When operated beyond the transition temperature (), sustained NO reduction occurs as the reaction is no longer limited by the desorption of surface complexes according to the reactions below:



However, carbon is consumed parasitically by the presence of oxygen that exists in higher concentration and has a higher oxidizing power than NO.⁸ At low concentrations of oxygen (0.1-2%), the temperature required for sustained NO reduction decreases due to gasification of carbon by oxygen leading to the creation of active surface sites that in turn react with NO and convert it to nitrogen.⁹ In this process a major fraction of carbon is consumed by oxygen and the primary challenge in commercializing this carbon based NO reduction process involves reducing the consumption of carbon by improving the selectivity of the carbon-NO reaction in the face the carbon-oxygen reaction. This study provides an insight into the efficacy of activated lignite char for its reduction of NO as measured by a global parameter for selectivity (mg NO reduced/g carbon) that can be obtained from the integral experiments conducted here.

Experimental Section

Reactor Assembly

An inlet gas mixture of preset concentrations was obtained by from mixing metered flow of helium, NO and oxygen. The gas mixture was preheated and allowed to flow through a bed consisting of 1000 mg of char housed in a stainless steel reactor. The gases exiting from the sorbent bed are analyzed for NO_x and oxygen by a host of online gas analyzers. A chemiluminescence NO_x analyzer (from The Advanced Pollution Inc., Model 200 AH) provided the on-line measurement of NO concentration. Oxygen was monitored using a Teledyne Model 3000 PA percent oxygen analyzer that generates an electric current as a function of oxygen concentration through its electrochemical galvanic micro fuel cell. Non-dispersive infrared analyzers tracked the online concentrations of CO and CO₂.

Char Synthesis

Samples of lignite coal were obtained from North Dakota, since it is well known that the lignite coal contains a large amount of sodium in it. Its combustion in air in a TGA indicated the presence of 19.8% ash, with the sodium content being about 9% as revealed by ICP-AES analysis. The initial surface area of HSLC was 16 m²/g. The role of surface area on the selectivity for carbon-NO reaction over the competing carbon-oxygen reaction was studied by conducting experiments on a series of activated lignite char differing in their structural properties. Lignite coal samples were first dried in air and then devolatilized at 750 °C in flowing helium for 2 hours. Higher surface area and porosity in HSLC was obtained by controlling the reaction time between HSLC and pure CO₂. 2 g samples of HSLC were placed in a flow through reactor and nitrogen was passed through the system till the furnace brought the bed temperature to 700 °C. Then the gas was switched to pure CO₂ and after a preset reaction time, the flow was switched back to nitrogen. The activated HSLC was allowed to cool and analyzed for conversion and morphological properties. Four samples were obtained after an exposure time of 21, 42, 60 and 90 minutes. Conversion of HSLC was obtained by taking a ratio of final and initial weight of char. **Table 1** shows the surface area and pore volumes developed in the char as a function of % burnoff in the lignite coal.

Table 1: Structural properties due to lignite char activation by CO₂.

Reaction time (min)	%burnoff	Surface Area (m ² /g)	Pore Volume (cc/g)
0	0	16	0.012
21	12	260	0.13
42	24	333	0.19
60	31	397	0.23
90	44	414	0.25

Results and Discussion

The effect of surface area on the NO reduction in the presence of 2% oxygen is quantified in **Figure 1**. The isothermal reaction data were obtained at 525 °C. It can be seen that the extent of NO reduction increases monotonically with the surface area (and its associated porosity). The presence of higher surface area allows greater contact between the gas and solid for the reaction to occur, resulting in lower NO concentration in the outlet. However, an unexpected increase in selectivity (mg NO/g HSLC) was observed

with increasing surface area as shown in **Figure 2**. The selectivity for inactivated HSLC was 81.26 mg NO/g HSLC. The selectivity increased steadily with higher surface area (93.92, 98.30, 101.52, 104.32 mg NO/g HSLC for initial surface area of 260, 332.8, 397, 414.4 m²/g.). The increase in selectivity with initial surface area can be explained on the following basis. In these experiments, the outlet oxygen concentration remains close to zero almost throughout the hour. Hence, once the oxygen is depleted, higher surface area in the remaining activated HSLC would reduce NO to a higher extent compared to an inactivated HSLC.

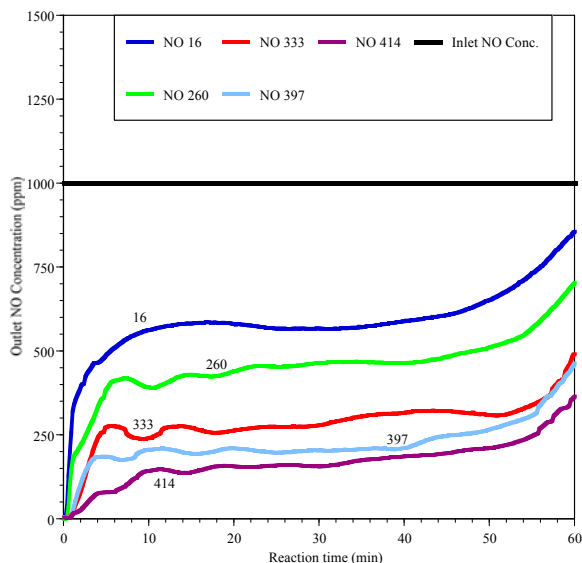


Figure 1. Effect of initial surface area of HSLC on the HSLC-NO reaction [Flow: 1000 ml/min; Inlet NO Conc.: 1000 ppm; Wt. Of Carbon: 1000 mg; Oxygen Conc.: 2.0%]

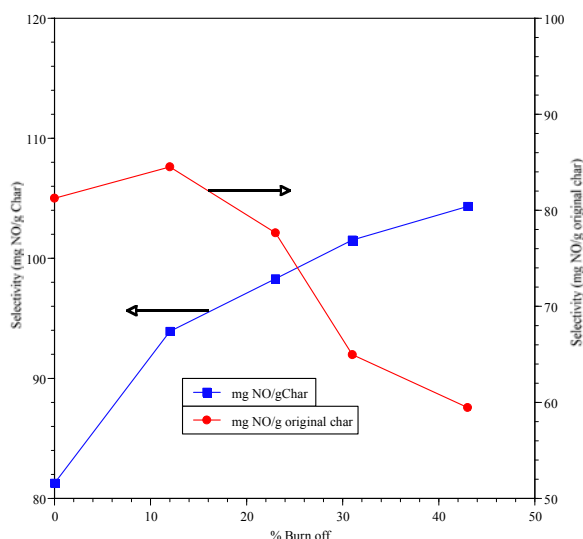


Figure 2. Effect of %burnoff on the selectivity of HSLC-NO reaction based on actual and initial char weight

Data analysis on the effect of surface area on NO reduction revealed that higher initial surface area and porosity led to higher selectivity. However, activation of char also leads to a loss in weight. Hence, the selectivity should also be compared on the basis of similar initial weight of char. Such a comparison is shown in Figure 2. From the data, we can conclude that pore volume of about 0.13 cc/g provided the optimal selectivity with respect to the original char.

Conclusions

From the experimental data we can conclude that higher sodium content leads to enhanced rate of gasification for both the carbon-NO and carbon-oxygen reactions. The lignite char provided higher degrees of activation in the form of higher pore volume and surface area compared to the sub-bituminous char. Although higher initial pore volumes lead to better NO selectivity, 0.13 cc/g pore volume provided the best selectivity among the carbons activated in this study.

Acknowledgement.

The authors acknowledge the financial support provided by the US Department of Energy and North Dakota Industrial Council for co-funding this pilot scale feasibility study.

References

- (1) Brown, C. E.; Hall, P. G. Physical Adsorption of Gases on Graphite. *Trans. Farad. Soc.* **1971**, *67*, 3558-3564.
- (2) Agnihotri, R.; Chauk, S. S.; Gupta, H.; Jadhav, R. A.; Mahuli, S. K.; Fan, L. -S. Reduction of NOx Emissions using Carbon and/or Carbon containing species. In *Proceedings of the Fifteenth Annual International Pittsburgh Coal Conference: Coal-Energy and the Environment*, Pittsburgh, PA, USA, 14-18 Sep 1998.
- (3) Teng, H.; Suuberg, E. M. Chemisorption of Nitric Oxide on Char. 2. Irreversible Carbon Oxide Formation. *Ind. Eng. Chem. Res.* **1993**, *32*, 416-423.
- (4) Smith, R. N.; Swinehar N.; Lesnini, D. The Oxidation of Carbon by Nitric Oxide. *J. Phys. Chem.* **1959**, *63*, 544-547.
- (5) Mochida, I.; Ogaki, M.; Fujitsu, H.; Komatsubara, Y.; Ida, S. Reduction of nitric oxide with activated PAN fibers. *Fuel* **1985**, *64*, 1054-1057.
- (6) Furusawa, T.; Kunii, D.; Oguma, A.; and Yamada, N. Rate of reduction of nitric oxide by char. *International Chemical Engr.* April **1980**, *20(2)*, 239-244.
- (7) Aarna, I.; Suuberg, E. A review of the kinetics of the nitric oxide-carbon reaction. *Fuel* **1997**, *76(6)*, 475-491.
- (8) Chan, L. K.; Sarofim, A. F.; Beer, J. M. Kinetics of the NO-Carbon Reaction at Fluidized Bed Combustor Conditions. *Combustion and Flame* **1983**, *52*, 37-45.
- (9) Suzuki, T.; Kyotani, T.; Tomita, A. Study of the Carbon-Nitric Oxide Reaction in the Presence of Oxygen. *Ind. Eng. Chem. Res.* **1994**, *33*, 2840-2845.

Thermal Behaviors of Dioxines Captured on a Mesophase Pitch Based Active Carbon Fiber.

Keiichi Kuroda ^{a)}, Ken-ichi Tobo ^{a)}, Nobuaki Matsuoka ^{a)},
Yuji Kawabuchi ^{b)}, Yoza Korai ^{c)}, Isao Mochida ^{c)}

a) Kyushu Environmental Evaluation Association
1-10-1 Higashikumatsukadai, Fukuoka, Fukuoka pref
813-0004, JAPAN

b) Kashima Oil Co., Ltd
4 Touwada, Kamisumachi, Kashima, Ibaraki pref
314-0102, JAPAN

c) Institute of Advanced Material Study, Kyushu University
6-1 Kasugakoen, Kasuga, Fukuoka pref 816-8580, JAPAN

Introduction

Dioxines, which are produced in the combustion of organic substances containing chlorine compounds, are now strictly regulated not to be liberated from any combustors. Complete capture at the end of the flue is one of the most reliable technologies, being applicable to any forms of dioxines for their complete removal from the flue even if the control of combustion and post-combustion is recognized effective to reduce the liberation of dioxines at its formation and decomposition. Hence it is the most feasible procedure to achieve no liberation of dioxines to install the active carbon bed in the flue. The problem is how to deal the active carbon, which has captured dioxines.

In the present paper, thermal behaviors of adsorbed dioxines were studied on a particular active carbon fiber produced for a mesophase pitch through KOH activation (MP-ACF). Its very large surface area and high hydrophobicity are recognized to show high capacity for dioxine adsorption. The adsorbed dioxines on the MP-ACF were extracted at their as-adsorbed or heated forms in an inert atmosphere up to 400°C. A series of 10 dioxine species were analyzed by a high resolution GC-MS, which told us their accurate concentrations and some of products through their thermal reactions on the MP-ACF. Such a post-treatment of used ACF allows the conversion of adsorbed dioxines into unarmful forms and its regeneration for the repeated use.

Experimental

1. Dioxines, their adsorption and heattreatment (HT)

A series of ¹³C-labeled dioxines in acetone listed in Table 1 were used as the standard samples. Their concentrations are also listed in Table 1.

2. Extraction of dioxines and their derivatives adsorbed on MP-ACF and their analysis.

Table 1. The amount of introduced ¹³C-labeled dioxines (unit:pg)

Compound	Amount of standard	Compound	Amount of standard
¹³ C-2378-TeCDD	1000	¹³ C-2378-TeCDF	1000
¹³ C-12378-PeCDD	1000	¹³ C-12378-PeCDF	1000
¹³ C-123478-HxCDD	1000	¹³ C-123478-HxCDF	1000
¹³ C-1234678-HpCDD	1000	¹³ C-1234678-HpCDF	1000
¹³ C-12346789-OCDD	2000	¹³ C-12346789-OCDF	2000

Results

1. Extraction of Adsorbed Dioxines on MP-ACF

Extracted amounts of Dioxines which have been adsorbed from acetone onto MP-ACF are listed in Table 2 where the experiments

(R1~3) were repeated three times to confirm the reproducibility. The amounts were fairly well reproduced at the pg level of analysis, 47~67% of adsorbed species being recovered. Strong adsorption of dioxines is indicated on the ACF. Among dioxines, 123478-Hexa(Hx)CDD, 1234678Hepta(Hp)CDD, and especially 12346789Octa(Oc)CDD were much less extractable, less than 50% of adsorbed species being extracted their strong adsorption being noted on the active carbon fiber. CDDs with chlorine atoms more than 6 appeared less extractable than CDF with the same numbers of chlorines. CDFs were extracted at 53~60% of adsorbed amounts, although more chlorines may increase slightly the extraction.

Table 2. Extracted amounts of Dioxines from MP-ACF without HT (unit:pg)

Compound	Amount of standard	R-1	R-2	R-3	Average
¹³ C-2378-TeCDD	1000	810	560	630	670
¹³ C-2378-TeCDF	1000	650	460	480	530
¹³ C-12378-PeCDD	1000	760	520	550	610
¹³ C-12378-PeCDF	1000	720	520	530	590
¹³ C-123478-HxCDD	1000	640	420	420	490
¹³ C-123478-HxCDF	1000	620	470	480	530
¹³ C-1234678-HpCDD	1000	510	380	530	470
¹³ C-1234678-HpCDF	1000	700	490	570	590
¹³ C-12346789-OCDD	2000	720	490	710	640
¹³ C-12346789-OCDF	2000	1300	900	1300	1200

2. Extraction of Adsorbed Dioxines on the ACF After the Heattreatment at 200~400°C for 1~2h.

Table 3 summarizes extracted amount of CDDs and CDFs adsorbed on the ACF after the heattreatment. The heattreatment was performed in the closed bottle to be cooled down to room temperature. Extraction was carried with the ACF and vessel. Hence non-volatile dioxines with chlorine more than 4 must stay in the catalyst to be extracted. Such extracted amounts after the heattreatment were compared to those without heattreatment. The heattreatment at 200°C and 300°C for 1h decreased extracted amounts of tetra-, penta-, and hexa-CDDs and CDFs whereas it did not change or even increased the amounts of hepta- and octa- CDDs and CDFs. The heattreatment at 400°C reduced significantly the extracted amounts of all CDDs and CDFs, indicating the decomposition of major adsorbed CDDs and CDFs.

Table 3. Extracted amounts of Dioxines from MP-ACF with HT (unit:pg)

Compound	Amount	200°C -1h	200°C -2h	300°C -1h	300°C -2h	400°C -1h	400°C -2h
¹³ C-2378-TeCDD	1000	500	540	480	440	6	5
¹³ C-2378-TeCDF	1000	380	410	350	320	6	5
¹³ C-12378-PeCDD	1000	460	500	410	360	8	6
¹³ C-12378-PeCDF	1000	430	450	440	360	9	7
¹³ C-123478-HxCDD	1000	360	390	320	260	5	4
¹³ C-123478-HxCDF	1000	420	430	380	320	7	3
¹³ C-1234678-HpCDD	1000	500	600	530	420	0	13
¹³ C-1234678-HpCDF	1000	590	690	690	550	8	28
¹³ C-12346789-OCDD	2000	990	1000	680	550	0	9
¹³ C-12346789-OCDF	2000	1700	1900	1200	900	0	49

The decomposition rates by the heattreatment were calculated according to a following equation to be summarized in Table 4.

$$\text{Decomposition(\%)} = \frac{\text{Extracted without HT} - \text{Extracted with HT}}{\text{Extracted without HT}} \times 100$$

According to the decomposition rates, CDD and CDF with chlorines less than 6 decomposed significantly at 200°C, the rates being 17~30%, whereas CDD and CDF with more than 7 hardly decomposed. The heattreatment at 300°C decomposed the former CDDs and CDFs at 27~36% for 1h and 23~47% for 2h, respectively while the latter CDDs and CDFs were hardly decomposed by 1h, but 7~23% by 2h. The heattreatment at 400°C decomposed all CDD and CDF almost completely, the decomposition rates being above 95% at least.

Table 4. Decomposition rates of Dioxins by the HT (unit:%)

Compound	200°C -1h	200°C -2h	300°C -1h	300°C -2h	400°C -1h	400°C -2h
¹³ C-2378-TeCDD	24.8	19.8	28.1	33.8	99.1	99.2
¹³ C-2378-TeCDF	29.4	22.6	33.8	40.1	98.9	99.1
¹³ C-12378-PeCDD	24.5	18.7	33.0	41.2	98.7	99.0
¹³ C-12378-PeCDF	26.5	23.3	26.3	39.0	98.6	98.8
¹³ C-123478-HxCDD	27.4	20.8	36.1	46.6	98.9	99.2
¹³ C-123478-HxCDF	20.9	17.3	27.0	39.4	98.7	99.4
¹³ C-1234678-HpCDD	0	0	0	11.0	100	97.3
¹³ C-1234678-HpCDF	0	0	0	6.2	98.7	95.2
¹³ C-12346789-OCDD	0	0	0	14.6	100	98.6
¹³ C-12346789-OCDF	0	0	0	22.5	100	95.8

3. Unlabeled Dioxines Found in the Extracts

Tables 5 and 6 summaries extracted amounts of unlabeled dioxine families and their particular species, respectively, after the heattreatment at 300°C for 1~2h. The heattreatment at 300°C for 1h produced large amounts of unlabeled CDDs and CDFs. Among there very large amounts of penta to octa CDFs were extracted. Such amounts of unlabeled dioxines produced by the heattreatment carried more chlorines than those of the adsorbed labeled dioxines. Chloride ions on the ACF which had remained after HCl washing must produced extra amount of dioxines.

CDFs with more chlorines tend to be produced than CDDs with the same numbers of chlorines. Some particular CDDs and CDFs appear certainly more produced. The locations of chlorines found in the standard species may stabilize the particular structure of the isomers.

Heattreatment for 2h at 300°C reduced very much the extractable unlabeled CDDs and CDFs, smaller chance of chlorine transfer from the labeled to unlabeled CDD and CDF species being suggested due to the preference of decomposition.

Table 5. Extracted amounts of unlabeled dioxine isomers (unit:pg)

Compound(isomer)	300°C-1h	300°C-2h
2378-TeCDD	4	0
2378-TeCDF	90	0
12378-PeCDD	38	0
12378-PeCDF	2000	0
23478-PeCDF	600	0
123478-HxCDD	250	0
123678-HxCDD	30	0
123789-HxCDD	120	0
123478-HxCDF	3800	0
123678-HxCDF	1300	1
234678-HxCDF	630	0
123789-HxCDF	360	5
1234678-HpCDD	220	64
1234678-HpCDF	6800	42
1234789-HpCDF	4800	14
12346789-OCDD	75	150
12346789-OCDF	5900	38

Table 6. Extracted amounts of unlabeled dioxine families

Compound(Families)	(unit:pg)	
	300°C-1h	300°C-2h
TeCDD	680	0
TeCDF	3100	0
PeCDD	1700	0
PeCDF	16000	0
HxCDD	580	5
HxCDF	13000	21
HpCDD	470	130
HpCDF	18000	77
OCDD	75	150
OCDF	5900	38
Total amount	59000 (1400pgTEQ)	430(2.6pgTEQ)

Discussion

The present study clarified the adsorption strength and reactivity for chlorine transfer ask decomposition over particular ACF of CDDs and CDFs with variable numbers of chlorines at variable locations on the their ring systems. They are stable up to 200°C but reactive to loose their chlorine atoms to other CDD and CDF rings above 300°C and very much to decompose above 400°C.

Such adsorption strength and reactivity appear to depend on the ring system and number of chlorines on the ring. Tetra to hexa and hepta to octa chlorine species behaved as two groups, respectively, in their adsorption and reactivity. The latter groups are certainly less extractable and less reactive than the former group. Nevertheless, heattreatment above 400°C decomposes all of them so far examined. The extraction level after the heattreatment stays below a few percents of introduced dioxines at 1000~2000pg levels.

At 300°C, chlorines are proved to go around among the CDD and CDF rings on the ACF. Native, not labeled, CDDs and CDFs families with variable numbers of chlorines were found in the extract after the heattreatment at 300°C. CDFs with more than five chlorines were produced more than those with four chlorines. CDFs are certainly more reactive to receive chlorines than CDDs. Native DDs and DFs at this level of concentration may be present in the ACF as the structural ring units in the carbon skeleton. Chlorination may fission their connection in the skeleton to be extractable. Chlorines feed in native DDs and DFs are definitely more than those introduced by labeled CDDs and CDFs. Chlorines present on ACF reactive to produce dioxines at 300°C. It must be noted that all of CDDs and CDFs lost their chlorines by the heattreatment at 400°C.

The adsorption, reactivity for decomposition and production of CDDs and CDFs appeared to depend on the location of chlorines on their rings. The sequence of location appears to receive more chlorines as typically indicated by the case of hexaCDFs where more amounts of 123478(3,800pg), 123678(1,300pg), 234678(630pg), and 123789(360pg) hexaCDFs were found in the extract. The most abundant native hexaCDF is noted to carry the chlorines at the same locations to those of introduced labeled hexachlorides. Although so far governing rules are not clear, stability of the product or copying reaction between mother and product dioxines may govern the distribution of product native CDFs.

Conclusions

In conclusion, dioxines are effectivity and rather strongly fixed on the ACF. Heattreatment can remove or transfer chlorines of CDD and CDF rings according to the heattreatment temperatures.

Heattreatment above 400°C decomposes almost completely all of adsorbed CDFs and CDDs. Hence ACF is an excellent material to fix the dioxines in the flue gas below 150°C and decompose them by the heattreatment at 400°C for its safe disposal or regeneration for the second use. ACF may decompose catalytically any dioxines in the exhaust at 400°C, if oxygen concentration is limited.

LEACHING BEHAVIORS OF TRACE ELEMENTS IN COAL ASH AND CHAR

Jie Wang, Akira Takaya and Akira Tomita

(Institute of Multidisciplinary Research for Advanced Materials,
Tohoku University, Katahira 2-1-1, Aoba-ku, Sendai 980-8577,
Japan)

email: tomita@tagen.tohoku.ac.jp

Introduction

Trace elements are of environmental concerns with respect to their emissions during coal combustion. Numerous studies have reported the physical and chemical fates of trace elements during coal combustion. However, there remain some important questions. For example, in what forms the trace elements exist in coal and how they are transformed with the thermal conditions are still not well known. The staged leaching method is widely used to determine the modes of occurrence of trace elements in coal.¹ We have recently proposed a determination method by leaching not only raw coal but also ashes.² In this paper, we examine the leaching behaviors of coal ash and char. This provides the further information on the modes of trace elements in coal as well as on the transformations of trace elements during coal combustion and pyrolysis.

Experimental

Coal combustion and pyrolysis were carried out in a horizontal tubular reactor. In combustion, some 1.5 g of coal sample loaded was heated in an air flow of 1 L/min at 10 °C/min, and held at the final temperature for 1 h. In pyrolysis, a nitrogen gas was used in place of air. The maximum temperature used in this experiment was 1150 °C. Quantification of the major and trace metallic elements in raw coal, char and ash was conducted on an inductively coupled plasma atomic emission spectroscope (Optima 3300XL ICP-AES instrument, Perkin-Elmer).² Coal or its resultant ash (or char) was leached in a sealed polyethylene container with 30 mL of 6% hydrochloric acid. After leaching, the solution was filtered and then used for ICP-AES analysis. Taiheyo (THY) sub-bituminous, Ermelo (EL) and Datong bituminous coals were used in this study.

Results and Discussion

Leaching of Major Metallic Elements. Figure 1 shows the leaching percentage of the major metallic elements in hydrochloric acid from ash and char, where the left figure represents the data for EL ashes and the right figure represents those for EL coal chars. For comparison, leaching results of the raw coal are also illustrated. The leaching percentage is referred to as the amount of an element leached from coal, ash, or char divided by the amount contained in the original coal. Analysis of the ashes and chars showed that the major elements were not lost by volatilization during the combustion and pyrolysis under the used experimental conditions. XRD showed that the crystalline mineral phases in EL coal were kaolinite, quartz, calcite, dolomite, pyrite, and gypsum.

Ca and Mg were highly leached out from the raw coals, 550-950 °C ashes, and 550-950 °C chars; this is because the major

Ca- or Mg-containing carbonates in coal and their decomposed species are soluble in hydrochloric acid. Mg in the 1150 °C ashes and chars was relatively stable. Fe in the 550-750 °C ashes was greatly soluble as compared with that in the raw coal, while the leaching percentage of Fe significantly decreased from the 950-1150 °C ashes. Pyrite turned to hematite upon the ashing. Hematite in the 550 °C ash was readily soluble in hydrochloric acid; however, hematite was well crystallized with increasing temperature, resulting in a low solubility. Fe in all chars was greatly soluble. This is due to the transformation of pyrite to pyrrhotite. Al in the raw coal was hardly dissolved, whereas it was fairly leached out from the 550-750 ashes and chars. This is due to the breakage of the structure of clay by the dehydration. The formed species such as meta-kailinite become partly extracted by hydrochloric acid. However, with increasing the ashing temperature to 1150 °C, the leaching percentage of Al is significantly reduced; this is because of the formation of some stable species such as mullite, examined by XRD. The leaching features of K were similar to those of Al.

Leaching of Non-vaporized Trace Elements. In a previous study, we found that Zn and Pb was vaporized,³ whereas the trace elements as shown in Figure 2 entirely remained in the ashes or chars under the used combustion and pyrolysis conditions. Figure 2 shows the leaching results of the non-vaporized elements in EL coal. The leaching percentage of Mn in the raw coal, ashes and chars was relatively high; this is because Mn exists mainly as carbonate. Mn turned to a stable phase at 1150 °C in both the combustion and pyrolysis. Be, V, Co, Cr, and Ni in the raw coal and chars were hardly soluble, whereas these elements in the 550-750 ashes were significantly soluble. These elements are postulated partly as the organic associations. When the organic matter burns out, the liberated species become soluble in hydrochloric acid. In pyrolysis, these elements are not liberated. With the exception of V, the elements including Be, Co, Cr and Ni in the ashes were hardly soluble as the temperature increased to 1150 °C. The leachability of As in the ashes was higher than that in the raw coal. Arsenic easily forms oxyanion in an oxidizing atmosphere that may be soluble in acid. In pyrolysis, Arsenic appeared to form a less-soluble species.

Leaching of Volatile Trace Elements. Figure 3 show the results of Zn and Pb in EL coal. For clarify, the volatilization loss is denoted in the figure; it is referred to as the difference in the amount of an element between the coal and the residual ash or char, divided by the amount of the element containing in the original coal. Zn and Pb significantly volatilized during the pyrolysis above 950 °C, whereas in the combustion, only Pb volatilized slightly at 1150 °C. Zn and Pb exists mainly as sulfide in coal. In pyrolysis, their oxide and sulfides are reduced by carbon; these reduction reactions lead to the vaporization of the two elements as metals.³ However, such reduction reactions can not occur in the slow-heating combustion because of the burn-out of carbon ahead of 550 °C. Leaching results showed that both Zn and Pb in the ashes became less soluble with increasing temperature. This probably implies the interaction of these trace elements with other mineral matter to form less soluble species

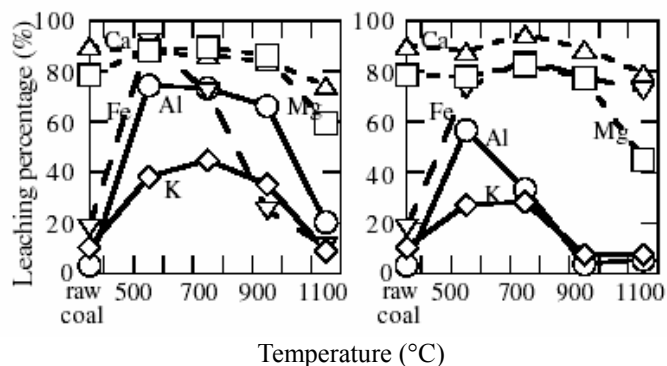


Figure 1. Leaching of major metallic elements from EL raw coal, its ashes (the left figure), and its chars (the right figure). The ashes and chars were obtained from the slow-heating combustion and pyrolysis at different temperatures.

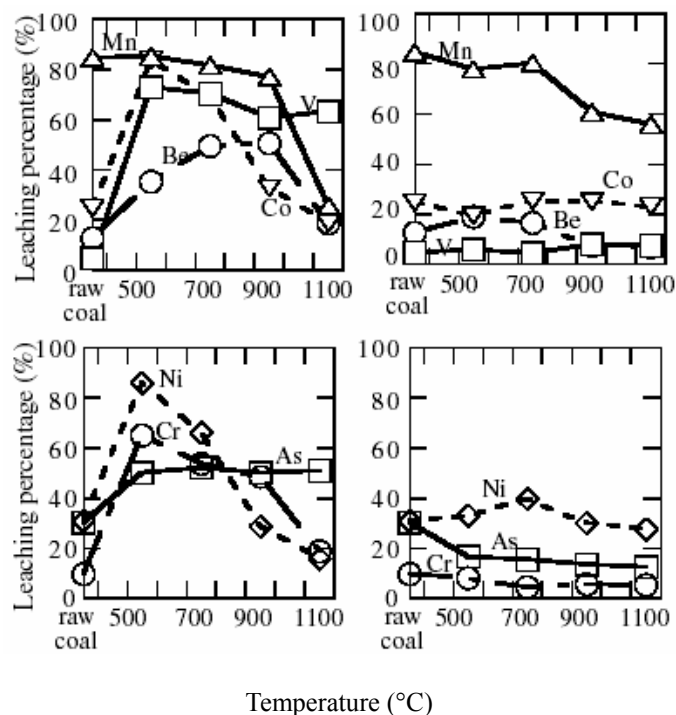


Figure 2. Leaching of non-vaporized trace elements from EL raw coal, its ashes (the left figures), and its chars (the right figures). The preparation of the ashes and chars is noted in Figure 1.

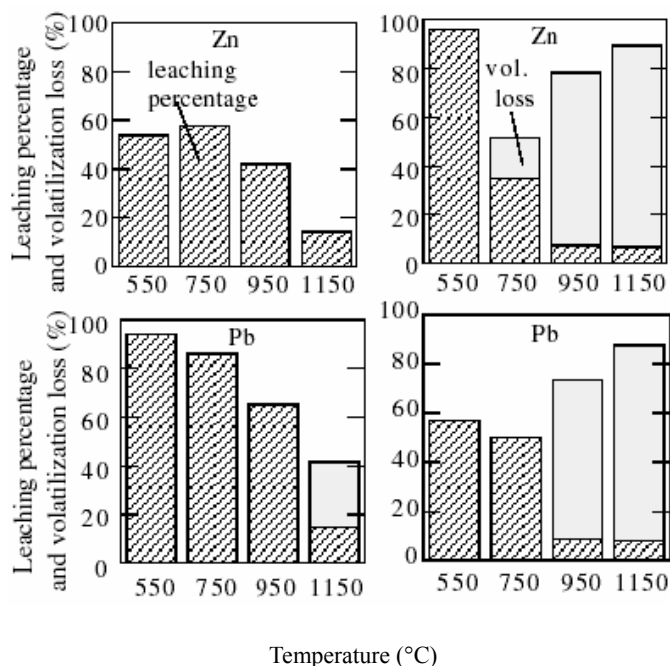


Figure 3. Leaching of volatile trace elements from EL coal ashes (the left figures) and chars (the right figures). The preparation of the ashes and chars is noted in Figure 1.

Conclusions

Leaching behaviors of the major metallic elements in the raw coal, ashes and chars are well explained by their existing form in coal and their transformations during the combustion and pyrolysis. Leaching results of trace elements showed that Mn is easily dissolved from the raw coal, ashes and chars, implying its existing form of carbonate. Be, Co, V, Cr, Ni in 550-750 ashes were more soluble than those in the raw coal and chars, suggesting their organic association. The liberated species of Be, Co, Cr and Ni in the ashes became less soluble at higher temperatures. Arsenic in the ashes is more soluble than that in the chars, implying a different transformation of As between the combustion and pyrolysis. Zn and Pb significantly volatilized during pyrolysis but little volatilized in the combustion.

Acknowledgements.

This work is partly supported by a Grand-in-Aid for the Scientific Research on Priority (No. 11218201).

References

- (1) Davidson, R. M. *Modes of Occurrence of Trace Elements in Coal*; CCC/36, IEA Coal Research: London, UK, 2000; pp1-36.
- (2) Wang, J.; Sharma, A.; Tomita, A. *Energy & Fuels* (in press,)
- (3) Wang J.; Tomita, A. *Energy & Fuels* (submitted).

TRANSFORMATION OF ARSENIC IN YIMA COAL DURING FLUIDIZED-BED PYROLYSIS

Hailiang Lu, Haokan Chen, Wen Li & Baoqing Li

State Key Laboratory of Coal Conversion, Institute of Coal Chemistry, Chinese Academy of Sciences, Taiyuan, China 030001

Introduction

Arsenic is one of the most concerned trace element in coal because of its toxicity and environmental persistence. The mode of occurrence of arsenic in coal strongly affects its transformation behaviour during coal conversion. There are many directly and indirectly methods^{1,2,3,4} for determining the mode of occurrence of elements in coal, such as X-ray absorption fine structure(XAFS) spectroscopy, scanning electron microscopy- energy dispersive X-ray (SEM-EDX) analyzer, and sequential chemical extraction. Previous work has shown that pyrite is the principal source of arsenic in coal.^{1,2} The partitioning of arsenic during coal conversion depends on many factors including coal composition, reaction conditions and the mode of occurrence of arsenic in coal. Papers^{3,5,6} show that arsenic belongs to semi-volatile elements, and most of arsenic is bound to fine particulates during coal combustion or gasification. The behaviour of arsenic is greatly influenced by its coexisting coal major and minor elements. However, there is little information about the transformation behaviour of arsenic under pyrolysis conditions. The volatilization behaviour of arsenic in Yima coal and the influence of coexisting mineral matters during pyrolysis in fluidized-bed reactor are investigated in this paper. The mode of occurrence of arsenic in Yima coal and its char were determined using three methods including density fractionation, demineralization and sequential chemical extraction.

Experimental

Coal Sample and Demineralization. The coal used in this study was a young bituminous coal. Coal sample was ground and sieved to 147 μm –246 μm . To determine arsenic affinities in Yima coal and study the effect of mineral matters on arsenic volatility during pyrolysis, demineralization was carried out. This demineralization procedure was following the method of Chen et al.⁷ Proximate and ultimate analyses for Yima raw coal (Yima) and its demineralized sample (YimaD) were given in **Table 1**.

Table 1. Proximate and Ultimate Analyses of Samples / Wt%

Sample	M _{ad}	A _d	V _{daf}	C _{daf}	N _{daf}	H _{daf}	S _{daf}
Yima	8.82	17.3	40.2	78.1	0.86	3.90	0.40
YimaD	2.92	2.73	36.6	78.2	0.85	5.20	0.40

Density Fractionation. Density fractionation had been used frequently to determine the trace element organic/inorganic affinities in coals. Most organic matters in coal occurred in <1.6g/cm³ density fractions⁸. Three density fractions including <1.3 g/cm³(YM1), 1.3 g/cm³–1.6 g/cm³(YM2) and >1.6 g/cm³(YM3) were obtained from Yima raw coal by using analytical reagent CH₂Cl₂ and CCl₄. Occurrence of arsenic in coal is obtained through coupling with other two methods, demineralization and sequential chemical extraction. Ash content of different density fractions were analyzed by using Chinese standard method (GB/T212-91).

Pyrolysis Experiment. Yima and YimaD were used for pyrolysis experiment at temperature ranging from 500°C to 900°C, respectively. The pyrolysis conditions are the same as reference 9. Chars were collected for analysis after pyrolysis.

Sequential Chemical Extraction. Sequential chemical extraction was used to determine the mode of occurrence of trace elements in coal, which represented the chemical mobility in

environment of the element. The binding forms of arsenic in Yima raw coal and its char were determined by this method. The char samples were obtained at 600°C and 900°C, and ground to <74 μm . During the sequence of extraction steps, arsenic associated with various parts of the coal or char would be extracted in the following order: (1) water soluble and ion exchangeable cations were extracted by 1M CH₃COONa; (2) primarily associated with carbonates were extracted by 1M CH₃COONH₄; (3) associated with sulfates and monosulfides were extracted by 4M HCl at 100°C; and (4) associated with disulfides were extracted by 2M HNO₃. After each step of extraction, aqueous solution was separated from the solid residue by centrifugation for 20 min. The solid was dried at 60°C for next step. Arsenic remained in extraction residue was labeled “stable forms” in this paper, which had little chemical mobility in environment. Stable forms of arsenic in coal may be present in the organic matrix, or occur in insoluble phases such as zircon, titanium dioxide, silicate and occur in crystal lattice of other insoluble mineral matters.

Determination and Calculation method. Arsenic contents in coal or its char and their extracted solutions were determined by AtomsCan16, inductively coupled plasma-atomic emission spectroscopy(ICP- AES), made in TJA company of America. The calculation method of arsenic volatility was similar to that of fluorine in reference 9.

Results and Discussion

Table 2 showed the arsenic contents in density fractions. Ash content of YM1 and YM2 were 5.06% and 6.94%, only 1/3 of that in raw coal(17.3%). The ash content of the heaviest density fraction(YM3) was 61.02%, which was much higher than that of raw coal. So most of YM3 was mineral matters, and large part of YM1 and YM2 should be organic matters. Compared with that in raw coal, arsenic contents of YM1 and YM2 were very low, while arsenic content of YM3 was very high. More than 75% of arsenic enriched in the heaviest density fraction. It indicated that most of arsenic in Yima coal was associated with mineral matters. The mass balance of arsenic is about 85%.

Table 2. Arsenic Contents in Density Fractions Obtained from Yima Coal (dry basis)

Sample	Yield/%	HTA [*] /%	As / $\mu\text{g}\cdot\text{g}^{-1}$	Fraction /%
Yima	100	17.32	33.0	100
YM1	5.91	5.06	3.8	0.68
YM2	74.38	6.94	4.0	9.02
YM3	19.61	61.02	127.6	75.81

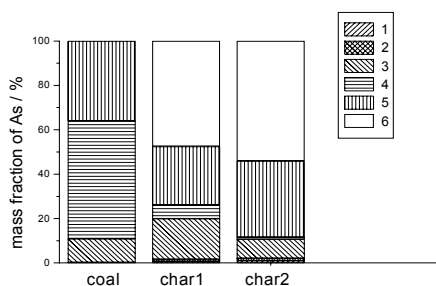
* high temperature ash (820°C)

During the demineralization process of raw coal by hydrochloric acid and hydrofluoric acid, almost all mineral matters, except pyrite, could be dissolved. **Table 3** gave the arsenic contents and sulfur forms in Yima raw coal and its demineralized coal. As shown in **Table 3**, the content of pyritic sulfur in demineralized coal was a little higher than that in raw coal, which indicated that pyrite almost all remained in demineralized coal. Arsenic content of demineralized coal was close to that of raw coal. Combined the results of density fractionations with those of demineralization, we could infer that the major arsenic in Yima coal was associated with pyrite, maybe arsenopyrite(FeAsS) or arsenical pyrite(FeAsS₂)².

Table 3. Arsenic Content and Sulfur Forms of Samples

Sample	As/ $\mu\text{g}\cdot\text{g}^{-1}$	Sulfur Forms /Wt%			
		S _{t,d}	S _{p,d}	S _{s,d}	S _{o,d} [*]
Yima	33.0	2.04	1.65	0.06	0.33
YimaD	32.1	2.14	1.72	0.03	0.39

* by difference



1–water soluble and ion exchangeable 2–associated with carbonates 3–associated with sulfates & monosulfides 4–associated with disulfides 5–stable forms 6–volatility(volatilized into gas & tar)
Figure 1. Mode of occurrence of arsenic in Yima coal and pyrolysis chars.

Figure 1 showed the results of sequential chemical extraction of Yima raw coal and its chars. The pyrolysis temperature of char1 and char2 were 600°C and 900°C, respectively. Arsenic contents occurred in water soluble, ion exchangeable and associated with carbonates were below 2% in all samples. It was difficult to compare with each other for these two kinds of forms of arsenic. It could be seen that about 65% of arsenic in raw coal was extracted, and more than 75% was extracted by HNO₃. 35.95% of arsenic in Yima coal occurred in stable forms. After pyrolysis, only a little arsenic associated with disulfides still remained in char1(6.13%) and char2(0.98%). It demonstrated that the forms of arsenic associated with pyrite were unstable during coal pyrolysis. A little increase was observed for mass fraction of arsenic associated with sulfates and monosulfides from 10.61% in raw coal to 18.25% in char1, while that in char2(8.54%) was a little decrease. Because of incomplete decomposition of pyrite at 600°C, some arsenic associated with disulfides maybe transformed into the forms associated with monosulfides. The mass fraction of stable forms of arsenic in char2 (34.26%) was higher than that in char1 (26.43%). Maybe some arsenic was transformed into stable forms before it could volatilize at high pyrolysis temperature.

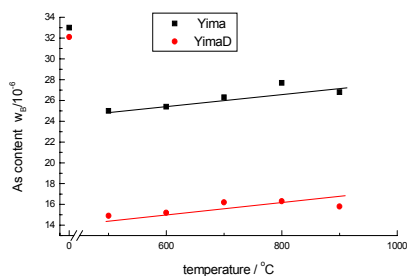


Figure 2. Effect of pyrolysis temperature on As content in char

The relationship between the arsenic content of char and the pyrolysis temperature was shown in **Figure 2**. The arsenic content in coal was indicated at 0°C. The arsenic contents of char were lower than those of coals, especially for that of YimaD. For Yima and YimaD, in the experiment temperature range, the arsenic content of char tended to slightly increase with increasing pyrolysis temperature.

The relationship between pyrolysis temperature and arsenic volatility was plotted in **Figure 3**. It could be seen that arsenic volatility was not strongly susceptible to pyrolysis temperature, which only had slightly changes in the temperature range from 500 °C

to 800 °C. But there was a great increase for arsenic volatility at 900 °C, which were about 54.0% and 72.8% for Yima and YimaD in comparison with 47.6% and 69.4% at 800 °C, respectively. It was evident that large amount arsenic already volatilized before 500 °C. Arsenic behaviour at low pyrolysis temperatures might take important role.

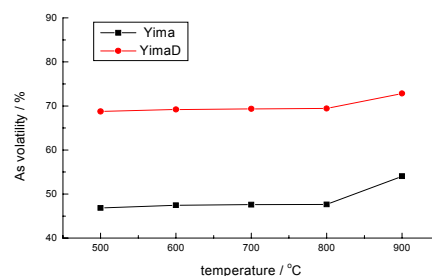


Figure 3. Effect of pyrolysis temperature on arsenic volatility

The ash composition of Yima raw coal was as following (Wt%): SiO₂: 44.17; Al₂O₃:18.88; Fe₂O₃:14.77; CaO: 10.42; MgO:2.33; TiO₂:1.15; K₂O:1.40; Na₂O:0.25; P₂O₅:0.31. From **Figure 3**, we also could see that arsenic volatility of YimaD was much higher than that for Yima during pyrolysis. From **Table 3**, it clearly showed that demineralization only had little influence on arsenic content of Yima coal. All these suggested that the vaporization of arsenic during Yima raw coal pyrolysis might be retarded by its coexisting mineral matters.

Conclusions

Arsenic in Yima coal was mainly associated with pyrite, which was unstable during coal pyrolysis. Arsenic volatility was not susceptible to pyrolysis temperature in the range studied. The vaporization of arsenic in Yima raw coal during pyrolysis might be retarded by its coexisting mineral matters. Arsenic volatility at low pyrolysis temperatures would be studied in the next stage.

Acknowledgement. Financial support for this work by the Special Funds for Major State Basic Research Project of China (Contract No. G1999022107) and Natural Science Foundation of China (29936090) are gratefully acknowledged.

References

- Koler, A.; Huggins, F. E.; Pamler, C. A.; Shah, N.; Crowley, S. S.; Huffman, G. P.; Finkelman, R. P. *Fuel Process. Technol.*, 2000, 63, p. 167-178.
- Huffman, G. P.; Huggins, F. E.; Shah, N.; Zhao, J. *Fuel Process. Technol.*, 1994, 39, p. 47-62.
- Galbreath, K. C.; Toman, D. L.; Zygarlicke C. J.; and Pavlish J. H. *Energy & Fuels.*, 2000, 14(6), p. 1265-1279.
- Querol, X.; Klika, Z.; Weiss, Z.; Finkelman, R. B.; Alastuey, A.; Juan, R.; Lopez-Soler, A.; Plana, F.; Koler, A.; Chenery, S. R. *N. Fuel.*, 2001, 80, p. 83-96.
- Richaud, R.; Lachas, H.; Healey A. E.; Reed, G. P.; Haines, J.; Jarvis, K. E.; Herod, A. A.; Dugwell, D. R.; and Kandiyoti, R. *Fuel.*, 2000, 79, p. 1077-1087.
- Yan, R.; Gauthier, D.; Flamant, G. *Fuel.*, 2001, 80, p. 2217-2226.
- Chen, H. K. Doctoral Dissertation. Chinese Academy of Sciences: Taiyuan, 1998.
- Guo, C. T. Chemical Industry Press: Beijing, 1992; pp.45-46.
- Lu, H. L.; Chen, H. K.; Li, W.; and Li, B. Q. 19th Pittsburgh Coal Conference: Pittsburgh, Sep. 23-27, 2002: CD-ROM.

REMOVAL OF MERCURY FROM COAL BY MILD PYROLYSIS AND CHELATE EXTRACTION

Akira Ohki, Akira Iwashita, Shomei Tanamachi, Tsunenori Nakajima, and Hirokazu Takanashi

Department of Bioengineering,
Faculty of Engineering, Kagoshima University,
1-21-40 Korimoto, Kagoshima 890-0065, Japan

Introduction

Coal contains many kinds of elements which include hazardous heavy metals, such as As, Hg, Pb, and Se. Among these metals, Hg is the most concerned because the element is quite volatile, so that 30-75% of Hg in coal will be released to air when coal is burned in coal-fired power plant.¹ It is reported that coal combustion is a great source for the global emission of Hg.¹ Therefore, many studies have been devoted to the problem of Hg in coal, including the occurrence of Hg in coal, its emission behavior, and the reduction of Hg emission.² There have been many studies about the removal of Hg after the combustion of coal. However, only a few studies have been done about the advanced and precombustion removal of Hg from coal. Keener et al. reported that 40-80% of Hg in coal was removed by mild pyrolysis, in which coal was heated under nitrogen flow at 300-400°C, for several American coals.^{3,4} However, the effect of varying the brand of coal upon the Hg removal and detailed mechanism have not yet been clear.

There have been several studies about the removal of heavy metals from coal fly ashes,^{5,6} incineration ashes,⁷ and contaminated soil⁸ by use of chelate extraction. However, for the heavy metals in coal, chelate extraction has not been so far applied.

In this paper, the removal of Hg from coal by mild pyrolysis as well as that by chelate extraction were examined. The dependence of the ease of Hg removal upon the brand of coal was discussed in terms of the removal efficiency for mild pyrolysis and that for the chelate extraction.

Experimental

Coals. Nine Japanese standard coals (SS coals) distributed from the Japan Coal Energy Center (JCOAL) and a certified reference material from the SA Bureau of Standards, Republic of South Africa (SARM20) were used. **Table 1** presents the analyses of these coals. The particle sizes of SS coals were under 149 μm while that of SARM20 was under 106 μm and no further pulverization was performed.

Determination of Hg in coal. Powdery coal (ca. 0.25 g) was precisely weighed and was acid-digested with HNO₃+H₂O₂ (5+3 ml) using a microwave processor (Milestone ETHOS1600). After cooling and the addition of further HNO₃+H₂O₂ (2+1 ml), microwave processing was performed again. After cooling and filtration, the filtrate was diluted to a fixed volume (25 ml) and was subjected to cold vapor atomic absorption spectrometry (CVAAS) using a Nippon Jarrel Ash AA855 with a Hg reduction system AMD-D2 for the determination of Hg concentration.

Mild pyrolysis. Powdery coal (0.5 g) was placed in a alumina board and heated by a horizontal tubular furnace at a rate of 1 °C/s to a desired temperature under N₂ flow (100 ml/min) and the temperature was kept for 1 h. Then the resulting coal was digested and analyzed for the Hg content. The value of % Hg removal was defined as [1-(Hg content in treated coal)/(Hg content in raw coal)] X 100.

Chelate extraction. An aqueous solution (20 mL) containing a chelating agent was shaken with 0.25 g of powdery coal for 24 h in a

stoppered centrifuge tube at a room temperature (24-25°C), and the filtration was performed to separate the coal. For the chelating agent, ethylenediaminetetraacetic acid (EDTA, 2Na salt), nitrilotriacetic acid (NTA), dimercaptosuccinic acid (DMSA), mercaptopropionic acid (MPA), and mercaptoethanol were used. In case of NTA and DMSA, two equivalent of NaOH was further added in the aqueous solution, while for MPA one equivalent of NaOH was added. The resulting coal was dried and analyzed for Hg content.

Results and Discussion

The nine SS coals were subjected to Hg analysis by CVAAS, and the results are recorded in **Table 1**, together with the data for SARM20. The Hg content of those ten coals varies from 0.04 to 0.25 μg/g, for which SARM20 has the highest value while SS002 has the lowest.

Table 1. Analyses of Coals

Sample coals (Producing country)	Ultimate (wt%, d.b.)			Proximate (wt%, d.b.)		Hg content (μg/g)
	C	N	S	V. M.	Ash	
SS001 (AUS)	72.7	1.4	0.4	27.0	15.4	0.08
SS002 (AUS)	69.1	1.3	0.5	38.9	14.9	0.04
SS003 (AUS)	75.6	1.7	0.3	29.3	8.8	0.10
SS004 (CHN)	74.4	1.0	0.7	29.7	10.0	0.08
SS006 (AUS)	72.2	1.6	0.5	36.3	12.2	0.10
SS020 (ZAF)	71.1	1.8	0.7	32.0	13.4	0.20
SS026 (USA)	66.2	1.2	0.3	38.7	13.9	0.06
SS027 (CHN)	71.6	0.9	0.6	29.2	10.8	0.08
SS028 (AUS)	74.0	1.7	0.3	28.2	8.4	0.05
SARM20	-	-	0.5	-	-	0.25 ¹⁾

¹⁾ Certified value

The ten coals were treated by mild pyrolysis at 300 and 400°C, and the results for % Hg removal are shown in **Figure 1**. The removal efficiency varied from 14% to 80% depending upon the brand of coal when the mild pyrolysis was carried out at 300°C. SS004 and SS020 coals provided high % Hg removal values of ca. 80%, whereas the % removal for SS006 was quite low (14%). For coals which give lower % Hg removal, greater increases in the % removal tend to be observed when the pyrolysis temperature is raised from 300°C to 400°C. When 400°C-pyrolysis was carried out, the values of % Hg removal for SS004 and SS006 were 88% and 42%, respectively. The weight loss (dry base) of coal during the mild pyrolysis varied from 0.8% to 7.5% for 300°C and from 1.9% to 20.8% for 400°C. There is no evident correlation between the weight loss values and the % Hg removal values.

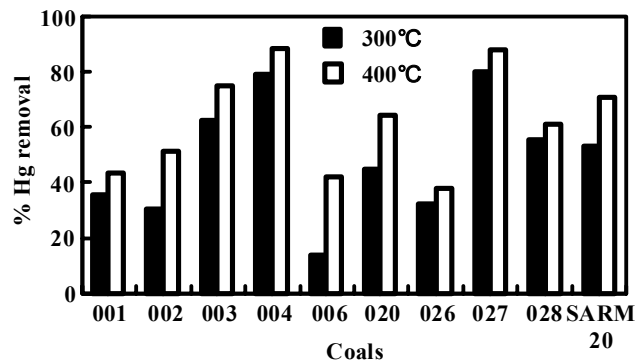


Figure 1. Removal of Hg from SS coals and SARM20 by mild pyrolysis (1 h).

When the % Hg removal values for the mild pyrolysis were plotted against the specific surface areas for those coals, almost no correlation was observed. The effect of varying the particle size of coal upon the Hg removal was assessed when SS004 was subjected to 300°C-pyrolysis (1 h). For the particle sizes of under 1000, 149, and 74 μm , the values of % Hg removal were 79, 79, and 67%, respectively. When SS001 and SS020 were examined, similar results for the effect of varying the particle size were obtained. Consequently, the Hg removal efficiency is dependent neither on the specific surface area nor on the particle size. Therefore, it is anticipated that the difference in % Hg removal for each coal is ascribed not to the difference in physical structure of coal matrix but to that in the mode of occurrence for Hg in coal.

Figure 2 shows the plot of % Hg removal against the pyrolysis temperature for SS004 and SS006. When the temperature was 200°C, both coals gave small values of % Hg removal. For SS004, the % removal rapidly increased when the temperature was raised to 300°C, and kept almost constant at higher temperatures. However, for SS006, the % removal was quite low even at 400°C, and increased to ca. 95% when the temperature was elevated to 500°C. Consequently, it is found that the Hg removal efficiency is greatly different in those two coals when the mild pyrolysis at 300-400°C is performed, although those two coals have similar Hg contents (see **Table 1**).

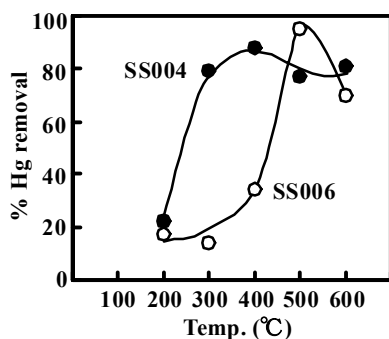


Figure 2. Dependence of Hg removal upon pyrolysis temperature.

The chelate extraction of Hg from SS004 using various chelating agents was performed, and the results of % Hg removal are summarized in **Table 2**. Ordinary chelating agents, such as EDTA and NTA, gave % Hg removals of 18 and 14%, respectively, whereas sulfur-containing chelating agents, such as DMSA and MPA, provided higher % removals of 57 and 44%, respectively. It is reasonable that the chelating agents possessing soft coordination sites give higher Hg removal because Hg ions are typical soft acids.

Table 2. Removal of Hg from SS004 by Chelate Extraction ¹⁾

Agents (50 mM)	% Hg removal
DMSA ²⁾	57
MPA	44
2-Mercaptoethanol	27
EDTA	18
NTA	14
NaOH	16
Water	0

¹⁾ L/S = 80, 24-25°C, 24h ; ²⁾ 25 mM

The ten coals shown in **Table 1** were subjected to the chelate extraction using MPA. The % Hg removal varied depending on the coal brand, and interestingly, there is an apparent correlation between the values of % Hg removal for the MPA extraction and those for the mild pyrolysis, as illustrated in **Figure 3**. Taking into account of the above result as well as that for the effects of specific surface area and particle size previously mentioned, it appears that the mode of occurrence for Hg in coal is the greatest factor which affects the ease of Hg removal both for the mild pyrolysis and for the chelate extraction.

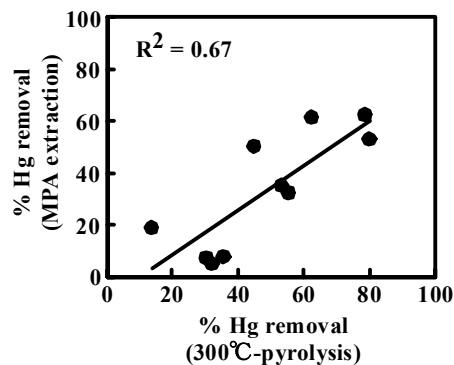


Figure 3. Correlation between Hg removal by MPA extraction and that by mild pyrolysis at 300°C.

Conclusions

The removal of Hg from coal was effectively attained by mild pyrolysis and chelate extraction. For chelate extraction, sulfur-containing agents were superior to ordinary chelating agents. The Hg removal efficiencies of the two removal methods were greatly dependent upon the coal brand, and there is an apparent correlation between those of the two methods. Detailed mechanism about this phenomenon is now under study.

Acknowledgment

This work was supported by a Grant-in-Aid for Scientific Research (No.11218209) from the Ministry of Education, Culture, Sports, Science, and Technology, Japan.

References

- (1) Clarke, L. B.; Sloss, L. L. "Trace elements-emission from coal combustion and gasification", IEA Coal Research, IEACR/49, 1992.
- (2) Sloss, L. L. "Mercury-emissions and control", IEA Coal Research, CCC/58, 2002.
- (3) Merdes, A. C.; Keener, T. C.; Khang, S.-J.; Jenkins R. G. *Fuel*, **1998**, *77*, 1783.
- (4) Wang, M; Keener, T. C.; Khang, S.-J. *Fuel Process. Technol.*, **2000**, *67*, 147.
- (5) Xu, Y.-H.; Nakajima, T.; Ohki, A. *Toxic. Environ. Chem.* **2001**, *81*, 55.
- (6) Xu, Y.-H.; Nakajima, T.; Ohki, A. *Toxic. Environ. Chem.* **2001**, *81*, 69.
- (7) Hong, K.-J.; Tokunaga, S.; Kajiuchi, T. *J. Hazard. Mater.* **2000**, *B75*, 57.
- (8) Sun, B. ; Zhao, F. J.; Lombi, E.; McGrath, S. P. *Environ. Pollut.*, **2001**, *113*, 111.

TRACE ELEMENTS IN COAL AND RELEASE OF TRACE ELEMENTS DURING PYROLYSIS

Ruixia Guo, Jianli Yang, Dongyan Liu, Zhenyu Liu

State Key Laboratory of Coal Conversion, Institute of Coal Chemistry, Chinese Academy of Sciences, P.O. Box 165, Taiyuan, Shanxi 030001, P.R. China

Introduction

Environmental problem resulted from the release of hazardous trace elements during coal processing have attracted attention of many researchers. Their studies have been focused on the physico-chemical form of trace elements in coal, the toxicity and partitioning behavior in the combustion/ environmental control system [1-4]. It has been shown that the emission behavior of trace elements during coal process varies with element and coal type, chemical form presented in coal and process conditions significantly. Pyrolysis is the most important stage of coal utilization processing such as gasification, combustion, or liquefaction [5]. It is thus of great important to understand the behavior of trace elements during pyrolysis to guide for the effective control of the emission of the toxic trace elements during coal processing.

The attempt was made in this paper is to understand the release behavior of As, Pb, Cd, Cr and Mn at different pyrolysis temperature, atmosphere and holding time. Their chemical forms transformation during pyrolysis was also investigated.

Experimental

2.1 Coal sample and pyrolysis prededure. A Chinese bituminous coal, named Datong coal, was crushed and sieved to 0.16~0.27mm, and dried under vacuum at 110°C with a nitrogen purge. The characteristics of Datong coal are shown in Table 1.

Table 1. Analysis of Datong coal, wt%

Proximate analysis			Ultimate analysis, daf				
V _{ad}	A _{ad}	M _{ad}	C	H	N	S	O ^a
26.91	10.00	0.26	88.18	5.17	1.05	1.64	3.96

A schematic representation of experimental apparatus was shown in Fig.1. It consisted mainly of a rotary furnace and a pyrolysis reactor. Prior to a reaction, about 2.5g of coal sample was placed at the top of the reactor. Then it was sealed and filled with the desired gas to certain pressure. The furnace with the reactor was in the horizontal position first. The fast heating experiment was obtained by quickly rotating the furnace with the reactor to the vertical position. After desired holding time, the reactor was pulled out from the furnace and quenched in the cold water. Gases were released slowly. Char was collected from the bottom of the reactor. Amount of gases produced was determined by the weight difference of the reactor with the samples before and after reaction. Amount of tar produced was calculated by subtraction of char and gas produced from weight of original coal

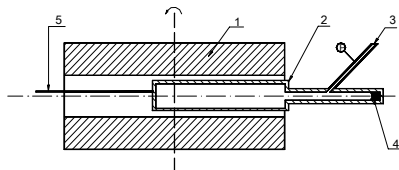


Fig.1. The diagram of high pressure closed fast pyrolysis apparatus

2.2 Analysis of the elements. The elements (As, Pb, Cr, Cd and Mn) in raw coal and chars were separated into five chemical forms by a sequential chemical extraction procedure. Through the sequence leaching steps, elements associated with various parts of the coal were removed in the following order: (1) Ion exchangeable element (named form 1), including water soluble or cations associated with ion exchange sites in organic and inorganic matter, and being removed by 1N NaOAc (PH~8.2) at room temperature for 1h; (2) Element bound to carbonates (named form 2), including cations primarily associated with carbonates, and being removed by 1N NaOAc (PH~5.0) at room temperature for 5h; (3) Element bound to iron and manganese oxides (named form 3), including Fe-Mn oxide associated, well-crystallized sulfides or organosulfur compounds, and being removed by 0.04 N NH₂OH·HCl in 25%(v/v) HOAc; (4) Element bound to organic matter (named form 4), consisting of paraffin-like material and resistant structural (nonhumified) organic matter residues, and being removed by HNO₃/H₂O₂ (PH~2) and NH₄OAc; (5) Element remaining in the residual after the four preceding extractions (named form 5), consisting essentially of detrital silicate minerals, resistant sulfides, and a small quantity of refractory organic material, and being dissolved into solution by using HF-HClO₄ mixture after ashing. The sequential extraction procedure used in this study was described elsewhere in detail [6-7]. Elements content of the raw coal, the corresponding chars after pyrolysis, and the samples from leaching processing were measured by inductively coupled plasma-atomic spectroscopy (ICP-AES).

Bleeding ratio (Br) used to evaluate the release extent of trace element in coal during pyrolysis defined as:

$$Br(\%) = \frac{\text{concentration in coal} - \text{concentration in char} \times \text{char yield}}{\text{concentration in coal}} \times 100\%$$

Results and Discussion

3.1 Effect of pyrolysis temperature on release of trace elements. Fig.2 shows the bleeding ratios of trace elements at various pyrolysis temperatures for Datong coal. It was found that the bleeding ratio of trace elements increased with the increasing of pyrolysis temperature, especially for As, Pb and Cd at 700~1000°C. However, the emission of As reached to a higher level at relative lower temperature. More than 67% of releasable As was released at the temperature of 300 °C. The significant release of Pb and Cd did not occur until 700°C. Cr and Mn released from coal only slightly in the temperature range of 300~1000°C. It can be concluded that the release ability of As, Cd and Pb is higher than that of Cr and Mn. This may be related to the properties of the element itself and their chemical form transformation during pyrolysis.

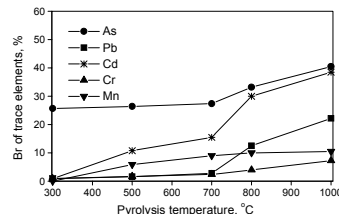


Fig.2. Effect of pyrolysis temperature on bleeding ratio of trace elements under N₂ pressure of 0.1MPa with the holding time of 20s

3.2 Effect of atmosphere and holding time on release of trace elements. Fig.3 illustrates the bleeding ratios of trace elements at different atmospheres and holding times. H₂ atmosphere resulted in the higher bleeding ratio of trace elements than N₂ atmosphere. The

difference in bleeding ratio of the elements between both atmospheres increased with the increasing of the holding time. Among the five elements, the relative volatile elements (As, Pb and Cd) were greatly influenced by atmosphere and holding time. Fig. 4 gives the corresponding volatiles yield at different atmospheres and holding times. H₂ atmosphere and longer holding time led to more volatiles release from coal. In one hand, the release of more volatiles can assist the transportation of the elements from the pore of coal and decrease the possibility of the element retention in the char. In the other hand, as the higher heating rate used in this study, coal may not be heated sufficiently at relatively short holding time. This resulted in incomplete release of the elements from coal. As further increasing the holding time, enough energy was obtained to break strong affinity of the elements to coal matrix structure. Both effects resulted in the more trace elements emitted from coal.

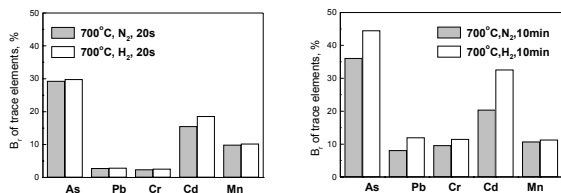


Fig.3 Effect of atmospheres and holding time on release of trace elements at 700°C under 0.1MPa

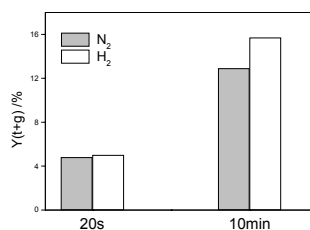
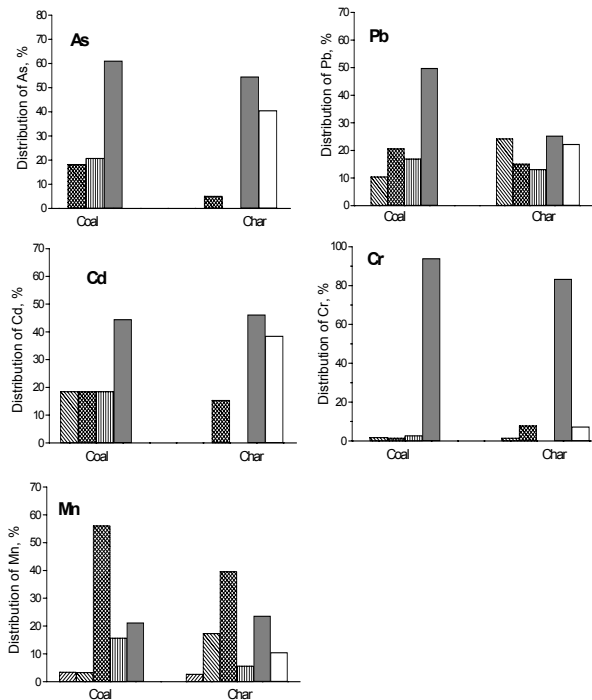


Fig.4 Effect of atmospheres and holding time on volatile (tar+gas) yield at 700°C under 0.1MPa

3.2 Chemical forms transformation of trace elements upon heating. Fig.5 presents the chemical form distribution of As, Pb, Cd, Cr and Mn in Datong coal and char. Char was obtained by pyrolyzed at 1000°C under N₂ pressure of 0.1MPa with the holding time of 20s. It can be seen that As, Pb, Cd and Cr in the raw coal are mainly presented as form 5 with the small amount of forms 2 to 4 but Mn as form 3. Form 1 represents ion exchangeable element. It was only observed for Mn in the raw coal and showed the same value after pyrolysis. Form 2 represents the element bound to carbonates. It was found in raw coal less than 5% for Cr and Mn, and about 10-18% for Pb and Cd. It disappeared for Cd, almost unchanged for Pb and Cr, and increased for Mn after 1000°C heat treatment. There was no observation of As in both raw coal and char. Form 3 represents the element bound to Fe-Mn oxides. This form was observed for all the elements tested in the raw coal (15-20% for As, Pb and Cd, less than 2% for Cr and more than 55% for Mn). It decreased generally after the heat treatment except for the case of Cr. Form 4 represents the element bound to organic matter. Although it was not the major form, it was found for all the elements tested. The element in this form disappeared or decreased after 1000°C pyrolysis. For form 5, residual elements, contained 60% of As, around 50% of Pb and Cd, more than 90% of Cr and 21% of Mn originally. It decreased for As, Pb and Cr after pyrolysis, and slightly increased for Cd and Mn. Form 6 represent the elements went to the volatile phase. Comparing to the less than 10% of Cr and Mn released into volatile phase, As, Pb and Cd have higher volatility and are considered as the primary toxic

trace elements in coal. Clearly, trace elements in coal not only emitted into volatile phase but also transformed from one form to another in solid phase significantly during pyrolysis.



Form 1: Ion exchangeable ; Form 2: Bound to carbonates;
Form 3: Bound to Fe-Mn oxides; Form 4: Bound to organic matter;
Form 5: Residual element; Form 6: Element went into volatile phase.

Fig.5 The distribution of trace elements in coal and char (1000°C, N₂)

Conclusions

The effects of temperature, atmosphere and holding time on trace elements release behavior in a closed fast pyrolysis reactor were investigated. The bleeding ratio of trace elements increased with increasing temperature and holding time. H₂ atmosphere promotes the release of trace elements. During pyrolysis, As, Pb and Cd show the higher emission ability than Cr and Mn. Form 1 element was only found for Mn in the raw coal and was not affected by heat treatment. Change of forms 2 and 5 was dependent on the type of the elements. Elements in form 3 and 4 decreased generally after pyrolysis.

Acknowledgement. The authors gratefully acknowledge the financial support from the Special Funds for Major State Basic Research Project (G19990221), the Chinese Academy of Sciences, and the Natural Science Foundation of China (20076049).

References

- Helble, J.J.; Mojtahedi, W.; Lyyräinen, J.; and Jokiniemi, J. *Fuel*, **1996**, 75(8), 931.
- Dismukes, E.B. *Fuel Processing Technology*, **1994**, 39, 403.
- Yan, R.; Gauthier, D.; and Flamant, G. *Fuel*, **2001**, 80, 2217
- Querol, X.; Fernández-Turiel, J.L.; and López-Soler, A. *Fuel*, **1995**, 74 (3), 331.
- Gryglewicz, G. *Fuel Processing Technology*, **1996**, 46, 217.
- Zhao, F.H. Ph. D. Thesis, in *Chinese with English abstract*. Beijing graduate School, China University of Mining and Technology, **1997**, p.63.
- Tessler, A.; Campbell, P.G.C.; and Bisson, M. *Analytical Chemistry*, **1979**, 51(7), 844.

THE BEHAVIOR OF TRACE ELEMENTS FROM HIGH TEMPERATURE COAL COMBUSTION PROCESS

Yasushi SEKINE, Tomohiro KAWABATA, Kuniyoshi SAKAJIRI,
Eiichi KIKUCHI, Masahiko MATSUKATA

Department of Applied Chemistry
Faculty of Science and Engineering
WASEDA University
3-4-1 Ohkubo, Shinjyuku,
Tokyo, Japan 169-8555

Introduction

Coal has great advantage that deposits are abundant as compared with other fossil fuels. On the other hand, coal includes much kind of trace elements with several 10 ppm concentrations. They volatilize at the combustion and gasification of coal, and are released into the atmosphere. Moreover, on the occasion of the reclamation by coal ashes, they elute into drainage, and become the cause of environmental pollution. Especially it worries about the bad influence to a human body, so it is important to elucidate the releasing behavior of the trace elements in coal. In this study, how the combustion temperature and existence of the steam in combustion atmosphere influence the releasing behavior of the trace elements from coal was investigated.

Experimental

In this study, we employed Wallarah coal as the sample first. It was crushed into particle and sieved under 150 μm before the combustion experiment. The combustion experiment was conducted under the temperature range of 573~1573 K, and the contents of the trace elements in the coal in each temperature was measured. The schematic diagram of experimental apparatus is shown in Fig. 1. The proximate analysis and ultimate analysis of Wallarah coal is shown in Table 1. About 0.1 g of coal sample was put into the platinum basket, and it inserted into the reactor which was preset at 573~1573 K beforehand. The alumina tube (i.d. 42 mm and length 1 m) was used for the reactor. Combustion atmosphere was air; 5.6 l min^{-1} and 0 or 10 % of steam was supplied together. The coal or ashes which remained in the platinum basket after 10 min combustion were collected carefully, and it was dissolved into acid media using microwave sample pretreatment equipment (Ethos Plus, by Milestone General; solvent; HNO_3 7 ml, HF 1.5 ml in the first step, and HNO_3 2 ml, HF 0.5 ml, and HClO_4 3 ml in the second step was added). Raw coal was also dissolved by just the same method. The contents of the trace elements (Be, V, Cr, Mn, Co, Ni, Zn, As, Se, Cd, Sb, Hg, Pb) in the solution was determined by ICP-AES (CIROS). About Hg, Se, Sb, and As, their amount was measured by the hydride generation method.

Results and discussion

The residual ratio of the trace elements in the coal or ash which remained in the platinum basket after 10 min combustion (573~1573 K, air atmosphere) was defined as follows.

$$\text{Residual ratio } [\%] = \frac{\text{Contents in ash } [\mu\text{g} \cdot \text{g}^{-1} \text{ coal}^{-1}]}{\text{Contents in raw coal } [\mu\text{g} \cdot \text{g}^{-1} \text{ coal}^{-1}]} \times 100$$

Table 1 Proximate and ultimate analysis of Wallarah coal

Proximate analysis	Water Content	3.0
	Ash Content	13.7
	Volatile Matter	29.4
	Fixed Carbon	53.9
Ultimate analysis	Carbon	71.9
	Hydrogen	4.2
	Nitrogen	1.4
	Sulfur	0.3
	Oxygen	8.1

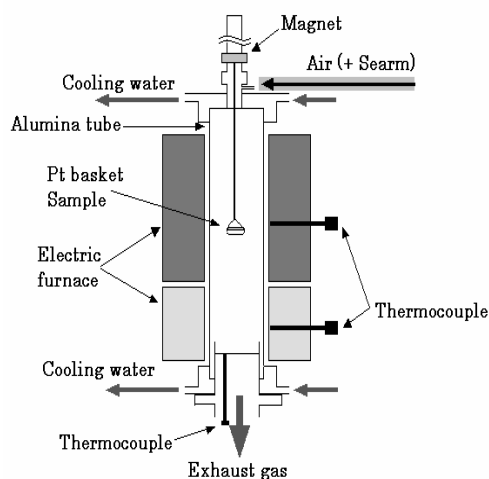


Fig. 1 Schematic diagram of experimental apparatus.

As for Zn, Se, Sb, Hg, and Pb, residual ratios in coal changed with the rise of temperature. A change of residual ratio was not observed about other elements. The relation between the residual ratios of Zn and Pb and temperature (573~1573 K) is shown in Fig. 2, and the relation between the residual ratios of Se, Sb, and Hg and temperature is also shown in Fig. 3. In Figs. 2~3, the vapor pressure curves of the compounds containing Zn, Pb, Se, Sb, and Hg were also shown together. Residual ratios of Zn and Pb decreased at 1173 K or more, irrespective of existence of steam. Considering that boiling point of metal-Zn is 1181 K, it is thought that Zn compounds in coal decomposed and released from coal as a metal-Zn form. Moreover, considering that boiling point of PbCl_2 is 1223 K, it is thought that Pb compounds in coal released as PbCl_2 . Even if it was in the presence of steam, residual ratios of Zn and Pb were same as the case where it was in the absence of steam. On the other

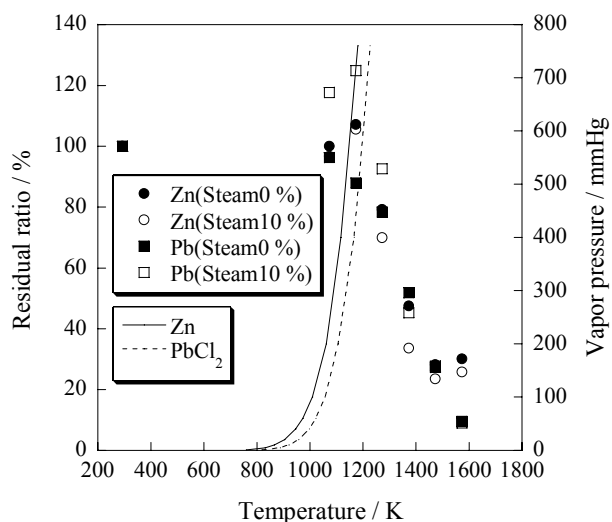


Fig. 2 Relation between temperature and the residual ratios of Zn and Pb in comparison with vapor pressure.

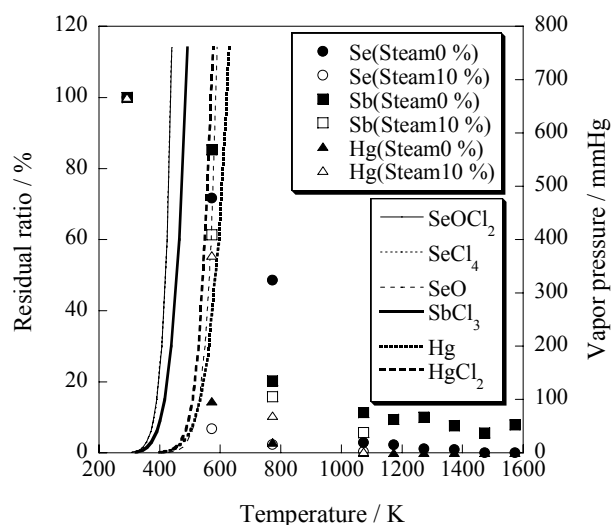


Fig. 3 Relation between temperature and the residual ratios of Se, Sb and Hg in comparison with vapor pressure.

hand, as for Se, Sb, and Hg, the residual ratios in coal decreased greatly at low temperature (573~773 K). It is thought that Se released as SeOCl_2 , SeCl_4 , and SeO , Sb released SbCl_3 , Hg released as metal-Hg and/or HgCl_2 .

The residual ratios of Se, Sb, and Hg in coal changed in the presence of steam unlike Zn and Pb. As for Se and Sb, residual ratios decreased in the presence of steam. This is considered because it released from coal via a hydroxide form under low temperature region. However, residual ratios of Hg increased in the presence of steam conversely. Considering that boiling point of Hg is 630 K, boiling point of HgCl_2 is 577 K, Hg released from coal as metal-Hg and/or HgCl_2 under low temperature region in the absence of steam. On the other hand, under steam existing condition, it will be converted into

Hg(OH)_2 at low temperature, then decomposed to HgO at high temperature. HgO is decomposed into Hg and O_2 at 773 K. Therefore, release of Hg depressed in the presence of steam.

Conclusion

Zn and Pb were released from coal at high temperature (1173 K~), and were not influenced by steam. Se, Sb, and Hg were released from coal at low temperature (573~773 K), steam influenced the releasing behavior of these elements. Whereas Se and Sb enhanced, that of Hg depressed in the presence of steam. They are considered that their existence form has correlation.

Acknowledgement

This work was partly supported by the fund of National Department of Science and Technology Japan (its group leader; Prof. K.Miura from Kyoto Univ.).

EMISSION OF ALKALI AND TRACE ELEMENTS IN CO-COMBUSTION OF COAL WITH SEWAGE SLUDGE

Y. Ninomiya*, L. Zhang, M. Ito and A. Sato

Department of Applied Chemistry, College of Engineering,
Chubu University, Matsumoto-cho, 1200, Kasugai, Aichi, Japan
Tel: +81-568-51-9178, Fax: +81-568-51-3833

*: Corresponding author, Email: ninomiya@isc.chubu.ac.jp

Introduction

Co-combustion of coal with sewage sludge has the potential to overcome the drawbacks of firing pure coals. The most attractive advantage of it is to significantly reduce the net CO₂ emissions^{1,2}. Besides of it, the use of sewage sludge can diversify the power plant's fuel portfolio by adding a potentially less expensive non-fossil fuel². Furthermore, it had been reported that cofiring can also reduce the SO_x and NO_x emissions since in one hand, the biomass fuels including sewage sludge generally contain less sulfur than coal. On the other hand, the alkali and calcium in biomass fuels can react with gaseous sulfur to form deposition on the slag³. In addition, the biomass fuels contain high volatile matter contents than coal that tend to form less NO_x in low-NO_x burners.

Co-combustion is generally carried out by cofiring coal with biofuel in the existing pulverized coal boiler. Experience showed that co-combustion could significantly impact on the pulveriser performance. The major subjects of concern are related to the problems of ash and particulate matters in co-combustion⁴. Since the mineralogical of biomass fuels including sludge has the distinct compositions and association compared to coals, co-combustion inevitably incurs the new ash-related problems. Emission of alkali and trace elements played important roles in the process^{2,4}.

The purpose of this paper is to investigate the fate of alkali and trace elements in co-combustion of coal with sewage sludge in laboratory-scaled drop tube furnace. The reaction temperature was kept at 1200°C; three coals were used to study the influence of coal type. The combustion residues including char and fly ash were collected by cyclones to probe the existence of alkali and trace elements within them. In addition, the particulate matters (PM) were collected by using low-pressure impactor for concerning on the volatilized elements.

Experimental

Properties of coals and sludge

Three coals and one sludge were used in this study, they are pulverized to <125 μm and dried before use. Their proximate and ultimate properties were shown in **Table 1**. Compared to coals, sludge is lean in fixed carbon, but rich in moisture and ash. The oxide composition in ashes shown in **Table 2** indicated a distinct ash composition in sludge. CaO, MgO and P₂O₅ are of most prevalence in the ash of sludge, whilst SiO₂ and Al₂O₃ are the main compounds in the ash of coals. In addition, as to the alkali elements, they have relatively high contents in coals. The trace elements are more abundant in sludge than in coals. Zn, Cu, and Ti are the most prevalent in the former fuel⁵.

Experimental procedure

Combustion of fuel alone and co-combustion were carried out in drop tube furnace (DTF), the combustion procedure and conditions are similar to used previously⁶. The weight ratio of coal to sludge was kept as 50:50 in co-combustion. O₂ 10% and N₂ being the balance was used as the atmosphere, reaction temperature was selected at

1200°C, while reaction time varied from 0.6 to 2.4 seconds. The combustion residues having micron-ordered size were collected by a water-cooled, rapid N₂ quenching probe and cyclones, which roughly have the particle cut-off size of 1.0 μm. On the other hand, the PM, existing in the exiting gas, was collected by low-pressure impactor (LPI), which is composed of 11 stages having the aerodynamic cut-off diameters ranging from 0.06 to 12.1 μm.

Table 1. Proximate and ultimate analysis on three coals and sludge

	Sludge	THY	DT	YZHS
<i>Proximate analysis, dry, wt%</i>				
Moisture	21.8	0	7.8	2.5
VM	37.0	45.7	24.7	38.8
Ash	15.8	12.6	12.8	9.7
FC	25.4	41.7	54.7	49
<i>Ultimate analysis, daf, wt%</i>				
C	34.4	78.7	78.6	76.4
H	5.5	6.2	4.9	5.6
N	7.5	1.2	0.8	1.4
S	0.8	0.1	1.7	5.7
O	51.8	18.3	14.2	11

Table 2. Ash compositions in three coals and sludge

	Sludge	THY	DT	YZHS
SiO ₂	26.91	50.3	45.1	48.2
Al ₂ O ₃	13.04	23.5	15.3	10.7
Fe ₂ O ₃	8.89	6.2	8.9	17.4
CaO	15.81	9.6	1.5	9.8
MgO	1.98	2	0.5	0.4
Na ₂ O	0.37	1.3	0.3	0.4
K ₂ O	0.53	1.1	1.2	0.6
SO ₃	9.92	4.0	13.3	11.6
P ₂ O ₅	24.85	-	0.33	0.02

Characterization methods

The combustion residues, collected by both probe and cyclones, were analyzed by several methods including ICP, XRD, SEM-EDX and CCSEM. The size-segregated PM was digested with filter together in a 15HNO₃: 2HF: 5HClO₄: 28H₂O solution. The filtered solution was analyzed by ICP for the elemental composition. Furthermore, PM was also observed by SEM-EDX for probing the chemical formations within it.

The novel CCSEM categories were developed for alkali elements and zinc in the combustion residues, which were listed in **Table 3**. For the Na-based compounds, they were defined as Na(Ca/Fe)PO₄, Na/al-si, Na(Ca,Fe)/al-si and Na(Ca,Fe)PO₄/al-si. The first one refers to sodium phosphate containing calcium/iron or not; similarly, the third one refers to sodium aluminosilicate containing calcium/iron together, and the fourth being the molten sodium phosphate/aluminosilicate containing calcium/iron or not. The same definition was used for potassium-based compounds. For the zinc-based compounds, they include Zn(Ca,Fe)PO₄, Zn/al-si, Zn(Ca,Fe)/al-si and Zn(Ca,Fe)PO₄/al-si. The first definition was used considering of the alloys formed in residues, whilst the second refers to the reaction of Zinc with aluminosilicate, and the third and fourth ones were defined for the possible capturing of Zn in slag.

Table 3. CCSEM categories for alkali elements and Zinc

	Category	Wt%
Na- based or K- based	Na(Fe)PO ₄	Na>1, P>5, Si<10, Ca<5
	Na(Ca)PO ₄	Na>1, P>5, Si<10, Fe<5
	Na/al-si	Na>1, Ca<5, Fe<5, Si>10, P<5
	Na(Ca, Fe)/al-si	Na>1, Ca(Fe)>5, Si>10, P<5
Zn- based	Na(Ca, Fe)PO ₄ /al-si	Na>1, Ca(Fe)>5, Si>10, P>5
	Zn(Ca, Fe)PO ₄	Zn>0.1, Ca(Fe)>5, P>5, Si<10
	Zn/al-si	Zn>0.1, Si>10, Ca<5, Fe<5
	Zn(Ca, Fe)/al-si	Zn>0.1, Ca(Fe)>5, Si>10, P<5
	Zn(Ca, Fe)PO ₄ /al-si	Zn>0.1, Ca(Fe)>5, Si>10, P>5

Results and discussion

Retention of alkali and trace elements in combustion residues

In combustion, the alkali and trace elements would undergo partitioning, a portion of which would be kept in the residues whilst the other would vaporize, suspending in the gas atmosphere and becoming into PM. The retention of alkali and trace elements during co-combustion in 2.4 s (more than 98% of carbon burnt out) was illustrated in **figure 1**, which was expressed as the comparison of the experimental to calculated values. The calculated value was the arithmetic average of data obtained in combustion of coal or sludge alone. Clearly, the retention of alkali and trace elements varied with coal type. Cofiring YZHS and sludge led to more of these elements kept in the residues than calculated, whilst cofiring DT with sludge resulted in less of these elements kept in residues. On the other hand, cofiring THY had little effect on retention of these elements.

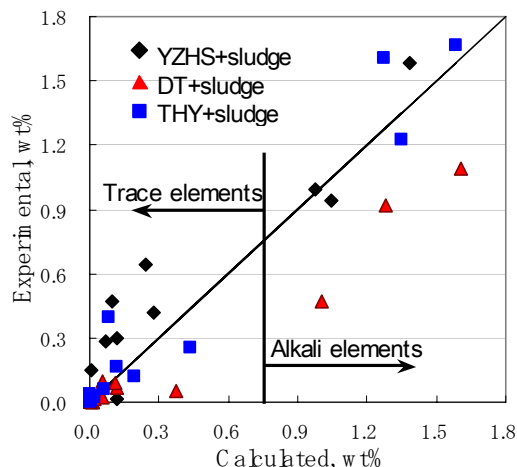


Figure 1. Retention of alkali and trace elements in residues

The distributions of alkali and Zinc were shown in **figure 2** for co-combustion of YZHS with sludge at 2.4s. For alkali based compounds, almost all them were reduced in co-combustion, especially for Na/K(Fe)PO₄ and Na/K(Ca,Fe)PO₄/al-si. Conversely, the Zinc-based compounds in residues were enhanced obviously. The above results implied the strong interaction of coal with sludge in co-combustion. The reduction of alkali elements in residues was caused by deterioration of the wall of chars. Cofiring YZHS (being rich in excluded minerals) in one hand changed the ash layer around sludge particle; a more porous char was formed as a result. Furthermore, reaction of CaO/Fe₂O₃, aluminosilicate with P₂O₅ in sludge resulted in formation of more apatite and molten (Ca,Fe)PO₄/al-si, both of them are capable of capturing trace elements^{5,7}.

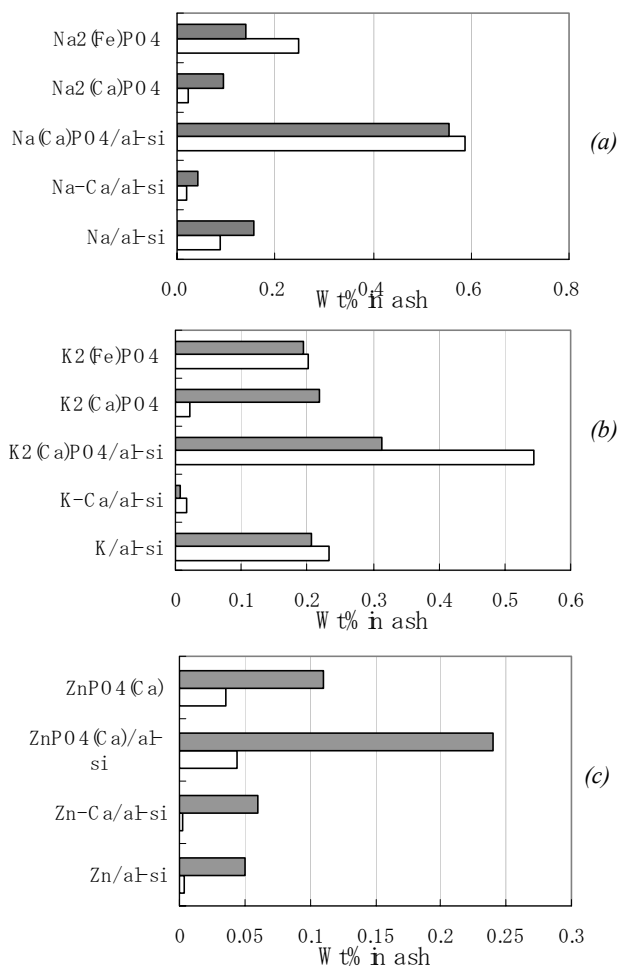


Figure 2. Distribution of alkali and Zinc in residues after co-combustion of YZHS with sludge in 2.4s

Vaporization of alkali and trace elements

The vaporized alkali and trace elements in PM were illustrated in **Figure 3**. It substantiated the conclusions in above section. For both trace elements including Boron and Zinc, the fine particles having size of ca. 0.3 μm disappeared due to condensation of them on molten phases. On the other hand, for the alkali elements in PM, both particles having mean size of 0.3 and 2.0 μm were enhanced. The former one was caused by formation of alkali sulfate/chlorium/phosphate in PM, whilst the latter one mainly contains alkali with other refractory elements; it functioned as the nuclei for the growth of aerosols by heterogeneous nucleation.

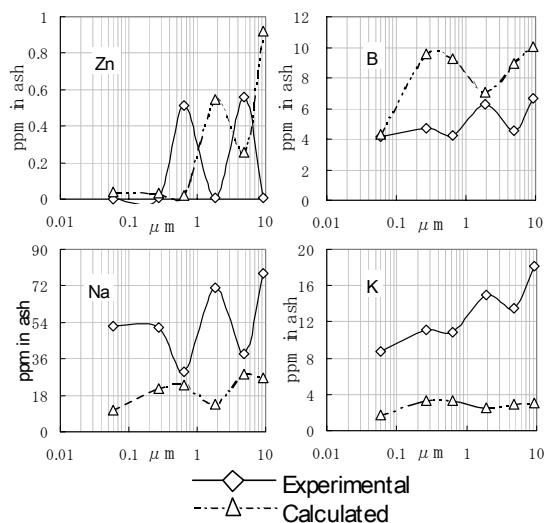


Figure 3. Vaporized alkali and trace elements in PM

Acknowledgements

The authors would like to thank Grant-in-aid for Scientific Research on Priority Areas (B), 11218211, the Ministry of Education, Culture, Sports, Science and Technology of Japan for the financial support. The special appreciation is also given to Mr. M. Masui, Actree cooperation in Ishikawa prefecture, Japan for supplying the sewage sludge.

References

1. Smith I.M., and Rousaki K., IEA Coal Research, UK, May 2002.
2. Fernando Rohan, IEA Coal Research, UK, Oct. 2002.
3. Robinson A. L., Junker H., and Baxter L.L., *Energy & Fuels* 2002, 16, 343-355.
4. Hein K.R.G., Wolski N., and Hocquel M., Trace element workshop 2002, 141-154. Japan.
5. Zhang L., Ito M., Sato A., and Ninomiya Y., proceedings of the 39th coal science symposium, 2002, 10.29-30, Japan.
6. Zhang L., Sato A., and Ninomiya Y., *Fuel*, 2002, 81, 1499.
7. Yoshiie R., Nishimura M., and Moritomi H., *Fuel*, 81(2002), 1335-1340.

CO-PYROLYSIS OF COAL AND WOODY BIOMASS

Behdad Moghtaderi, Chatphol Meesri, and Terry F Wall

Co-operative Research Center for Coal in Sustainable Development
Discipline of Chemical Engineering, School of Engineering
Faculty of Engineering & Built Environment
The University of Newcastle
Callaghan, NSW 2308
Australia

Introduction

Fears of climate change and increasing concern over the global warming have prompted a search for new, cleaner methods of electrical power generation. Co-firing of biomass fuels (e.g. wood chips, straw, bagasse, peat and municipal solid waste) and coal is presently being considered as an effective means of reducing the global CO₂ emissions¹. Demonstrations have been performed in a number of utility installations across the world, including Australia, Europe and the United States. All types of combustion technologies have been used but a particular attention has been given to pulverised fuel (PF) boilers, as they constitute the bulk of power generation hardware in many countries. Despite the simplicity of the co-firing concept, its application in PF boilers is associated with many technical issues including combustion related problems such as fuel ignition, flame stability, temperature, and geometry as well as char burnout. There is still no fundamental understanding of the underlying mechanisms that cause such technical problems. In particular, Studies on fundamental issues such as pyrolytic behaviour of biomass/coal blends or biomass char reactivity are scarce¹.

Previous investigations on co-pyrolysis of biomass/coal mixtures have mostly concentrated on the mechanism of production of the gas phase species. There has also been a handful of studies²⁻³ on the impact of synergistic effects (i.e. chemical interaction between the two fuels) on the yield of major pyrolysis products, in particular, volatile matter. However, much less attention has been given to the influence of synergistic effects on the composition of the pyrolysis products. In addition, most previous studies focused on examining the impact of various controlling parameters (e.g. heating rate, temperature, blending ratio, etc) in isolation.

The objective of this study was to address these shortcomings through a comprehensive investigation of the pyrolytic behaviour of woody biomass/coal blends over a wide range of heating rates and temperatures relevant to PF boilers. The fundamental knowledge gained from this project is essential for the proper understanding of co-firing in practical PF based systems. For example, the knowledge of the low heating rate pyrolysis of biomass/coal mixtures may help to prevent the accidental fires, which sometimes occur in fuel handling units (e.g. mills or pulverisers) of typical PF boilers during co-firing exercises⁴. Similarly, the knowledge of the high heating rate pyrolysis of biomass/coal blends, may help to understand and predict the impact of co-firing on the combustion related phenomena in PF boilers.

Experimental

Equipment. Two sets of experiments were carried out to investigate the pyrolytic behaviour of biomass/coal blends under the low and high heating rate conditions. The low heating rate experiments were conducted to understand the pyrolytic characteristics of coal, woody biomass, and their mixtures under conditions pertinent to the pulveriser units (i.e. mills) of typical PF boilers. That is a heating rate between 10-50°C/min and a temperature between 200-400°C. The high heating rate experiments,

on the other hand, were performed to study the pyrolytic behaviour of the individual solid fuels and their blends at heating rates often observed in pulverised fuel combustors (10⁴ °C/s ≤). The low heating rate experiments were carried out in a horizontal tubular reactor consisting of a horizontal alumina tube (reactor), a carbolite horizontal tube furnace, a mass flow controller, a pressure regulating valve, a pressure transducer, a data acquisition system, several thermocouples and controllers.

The high heating rate experiments were conducted at atmospheric pressure in a 330 mm by 50mm ID electrically heated drop tube furnace (Astro Model 1000A graphite vertical furnace) equipped with a Honeywell temperature controller/programmer (Model DCP 7700). The set-up included the tubular furnace, furnace controllers, a solid fuel delivery system, and a char collection device consisting of a cyclone and a water-cooled probe.

A gas analysis train was employed in conjunction with both low and high heating rate set-ups for on-line measurements of the gaseous pyrolysis products. The train comprised of a gas manifold, a fast response micro gas chromatograph (VARIAN, model CP-2003) equipped with a thermal conductivity detector, a cold trap for removing tar compounds, and a data acquisition system.

Materials. Experiments were conducted on blends of Radiata pine sawdust and Drayton coal, which were prepared by manual mixing of the two fuels. To eliminate the effect of moisture content, prior to each test sufficient amounts of fuel samples were oven dried at 105 °C for several hours and then stored in a desiccator. Particle size measurements indicated a range of particle sizes between 0.045-0.063 mm for coal and 0.09-0.125 mm for pine sawdust. These size ranges are consistent with those produced in practical milling systems used in pulveriser units of PF boilers¹. While blending ratios (weight of biomass to that of coal/biomass mixture) of 5%, 10%, 25%, 50%, and 75% (w/w) were used in the low heating rate experiments, for the high heating rate investigation, only two blending ratios of 5% and 10% w/w were employed. The details characteristics of both fuels (eg ultimate and proximate analysis) were given in one of our earlier works².

Methods and Techniques. The high heating rate experiments were conducted in the temperature range of 900-1400°C. High purity nitrogen (99.5% purity) was used as a carrier gas. Before commencing the experiment, the system was purged with nitrogen for 15 min, after which the concentration of oxygen within the system was continuously monitored by the Micro GC. Once the oxygen concentration approached zero, a 2 L/min flow rate of the carrier gas (primary N₂, 0.5 L/min and secondary N₂, 1.5 L/min) was introduced into the reactor. This provided a residence time of approximately 1 (s) for the individual pulverised fuel particles. The fuel particles were next fed at a uniform rate, depending on the type of material. For the coal and blend samples, the feed rates were about 2-3 g/h whereas for the sawdust samples a feed rate of 0.5 g/h was employed to avoid the blockage of the fuel feeding system. The above-mentioned flow rates were controlled by mass flow controllers and uniformly maintained by a suction pump equipped with a flow regulator. The flow of the gas inside the furnace was maintained at a uniform rate by replacing a filter membrane at 20 minute intervals.

The char was collected in the sample receiver of the cyclone and weighed at the end of the experiment. The ultimate volatile yields % (w/w, daf) of the coal and the blended materials were determined by employing the ash-tracer techniques (ASTM D 1102). For sawdust, the extent of mass loss during devolatilisation was ascertained by determining the content of inorganic metals⁵ (average of SiO₂, TiO₂, and Al₂O₃) of the collected char assuming that the mass of these metals is conserved. This was done using the X-ray fluorescence (XRF) technique to minimise the inaccuracy that

would have occurred due to the vaporisation of alkali and alkali earth components of the biomass ash had the ash tracer method been used.

The details of the low heating rate experimental procedures and techniques have been given elsewhere² and are not repeated here.

Results and Discussion

Figure 1(a) illustrates the yield of volatiles of coal and sawdust as a function of furnace temperature under the low heating rate condition of 10°C/min. The devolatilisation processes of both coal and sawdust follow a similar trend under these conditions. In the temperature range of 300<T< 600°C the cellulose content of the woody biomass, which accounts for 40% of its weight, undergoes thermal decomposition and transforms primarily into levoglucosan. While almost 80% (w/w) of the woody biomass is converted in the second stage, coal exhibits only 35% (w/w) conversion at this stage and yields much less volatiles. The striking distinction is attributed to the difference in the strength of the molecular structure of the two fuels².

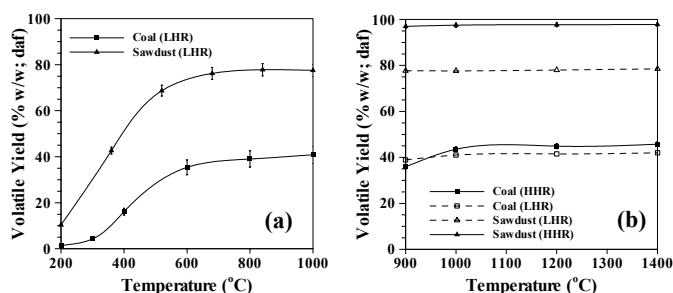


Figure 1: Yield of volatiles as a function of temperature under (a) low heating rate, 10 °C/min, and (b) high heating rate conditions.

Figure 1(b) depicts the yield of volatiles from coal and sawdust over a temperature range of 900 to 1400°C under the high heating rate regime. For comparison, the results extrapolated from the low heating rate experiments (for T > 1000°C) are also shown in the same figure. Both coal and sawdust show similar behaviours and produce higher yields of volatiles compared to those produced under low heating rate conditions. The difference between the two fuels, however, can be seen in the quantity of the volatile yields and the temperature range at which the bulk of devolatilisation takes place. The pulverised woody biomass generates much higher volatile yields (about 98% w/w, daf) compared to that of the coal under the same conditions. This can be attributed to the stronger effects of the temperature and heating rate on the depolymerisation reaction, which leads to the rapid evolution of volatile content of the woody biomass. The yield of volatiles for coal under the high heating rates, however, is not much higher than those of the low heating rate regime. This is most likely due to the stronger molecular structure of coal.

To investigate the behaviour of blends, the yields of pyrolysis products (gas, tar, and char) were plotted against the blending ratio for both low and high

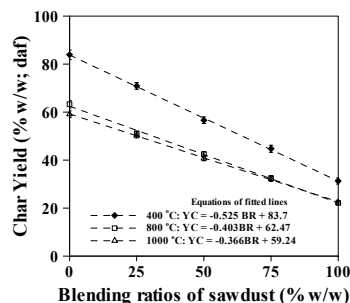


Figure 2: Yield of char as a function of blending ratio under a low heating rate of 10 °C/min.

heating rate regimes. The amounts of pyrolysis products from a particular blend appeared to be linear functions of the blending ratio (e.g. see **Figure 2** for char). This implies, for instance, that the yield of char at any given blending ratio (Y_{char}) is equal to the algebraic sum of the normalised char yields of the parent fuels. That is:

$$Y_{char} = \frac{k}{100} \times [Y_{Biomass, char}] + \frac{(1-k)}{100} \times [Y_{Coal, char}] \quad (1)$$

where k is the blending ratio in percentage, $Y_{Biomass, char}$ is the yield of biomass char (correspond to $k = 0\%$), and $Y_{Coal, char}$ is the yield of coal char (correspond to $k = 100\%$). Similar linear relationships can be applied to tar and gaseous products. This even applies to the individual constituents of the gas phase (eg CH₄, CO₂, CO, etc), as shown in **Figure 3**.

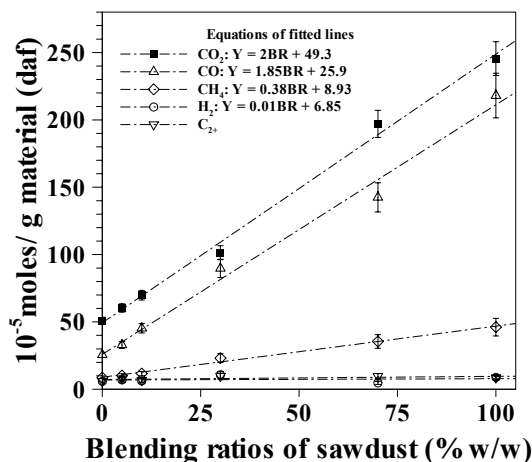


Figure 3: Composition of the gaseous products at a temperature of 400°C and a low heating rate of 10 °C/min.

Similar to the low heating rate results, the blended materials followed the same trend as the parent fuels in the high heating rate regime. More importantly, the yield of the volatiles of the blends seemed to be proportional to the blending ratios of the parent materials. In addition, much like the low heating rate regime, the composition of the gaseous products generated from the blended materials under the high heating rate and the high temperature (900-1400°C) conditions were linearly proportional to the composition of the parent materials (not shown here).

Acknowledgment

The authors wish to acknowledge the financial support provided by the Co-operative Research Centre for Coal in Sustainable Development, which is funded in part by the Co-operative Research Centres Program of the Commonwealth Government of Australia.

References

1. Sami, M., Annamalai, K., and Wooldridge, M., *Progress in Energy and Combustion Science*, **2001**, 27, 171-214.
2. Meesri, C., and Moghtaderi, B., *Biomass & Bioenergy*, **2002**, 23(1), 55-66.
3. Pan, Y.G., Velo, G., Puigjaner, L., *Fuel*, **1996**, 75(4), 421-418.
4. Moghtaderi, B., *Journal of Loss Prevention in Process Industries*, **2001**, 14(3), 161-165.
5. Mitchell, R.E., Hurt, R.H., Baxter, L.L., Hardesty, D.R., Milestone Report SAND92-8208., Sandia National Laboratories, California, USA, **1992**.

FUNDAMENTALS ON CO-COMBUSTION CHARACTERISTICS OF LOW-GRADE COAL WITH BIOMASS

Ichiro Naruse, Kunihiro Nishikawa and Keiju Morishita

Department of Ecological Engineering
Toyohashi University of Technology
Tempaku-cho, Toyohashi 441-8580, Japan

Introduction

In some developing countries, low-grade coals, which contain high fixed carbon, sulfur, nitrogen and/or ash contents, are necessitated to be utilized as fuels due to its cost and so forth. However, it is hard for the low-grade coals to be burnt completely in current combustors. Additionally, emission control devices for de-NO_x and de-SO_x are not placed sufficiently in those countries. On the other hand, biomass resources have become more attractive even in developed countries. This is because the biomass is one of carbon-neutral fuels, which do not increase CO₂ emission in the atmosphere. Although inventory of biomass resources, energy consumption for collection and conveyance of biomass and so forth are still unknown, the biomass must be one of candidates to make up for energy produced by fossil fuels.

From this viewpoint, co-combustion technology of coal with biomass has been applied in several practical coal boilers in order to reduce CO₂ emission, fuel cost and so forth. Furthermore, the biomass may be able to enhance the combustion performance and to control NO_x emission since the biomass contains much volatile matter and evolves NH₃ as volatile-N species¹. However, fundamental combustion and NO_x emission characteristics for biomass alone and mixture of coal with biomass have not been elucidated precisely yet. In this study, the fundamental pyrolysis and combustion characteristics for several kinds of biomass were discussed first, using a thermobalance. Second, the combustion behaviors of biomass alone, coal alone and biomass-coal mixture were tested, using an electrically heated drop tube furnace. In the combustion test, the ignition behavior, combustion efficiency and NO_x (NO and N₂O) emission behavior were focused, based on the results of gas compositions along the furnace axis. Furthermore, effect of co-combustion on the size of ash particles at the exit was also discussed, sampling the particles and observing them by a scanning electron microscope (SEM).

Experimental

Fundamental tests on pyrolysis and combustion for several kinds of biomass were carried out, using a thermobalance. Experimental conditions in the thermobalance test are summarized in Table 1. The pyrolysis and combustion experiments are operated in the N₂ and air atmosphere, respectively. Five kinds of biomass, which are derived from agricultural or lumbering wastes, were used as a sample. Properties of the biomass employed are shown in Table 2. From the table all of the biomass contain high amount of volatile matter content and little amount of ash content.

The co-combustion test was performed, using an electrically heated drop tube furnace. The furnace mainly consists of a feeder, a process tube made of quartz, electrical heaters and a sampling line. The experimental conditions in the co-combustion test are shown in Table 3. From the table the furnace temperature and combustion stoichiometry are kept constant in all experiments. The mixture ratio of coal to biomass is set at 1 to 1 as mass basis. The input heating value are controlled to keep constant by changing the total feed rate even when varying the coal type. The coal tested in the co-combustion experiments are also shown in Table 2. Three types of

coal were burned as a sample. In three types of coal SH coal is classified as a low-rank coal since the content ratio of fixed carbon to volatile matter is the highest of the three as shown in Table 2. NL and TH coals were chosen as a reference to elucidate the effect of volatile matter content on the ignition and combustion behaviors. The biomass tested in the co-combustion is Hinoki sawdust. Mean particle size of coal is about 80 μm, which corresponds to pulverized coal. For the biomass, on the other hand, the particles shifted less than 1000 μm were used.

Table 1. Experimental conditions in thermobalance experiments

		Conditions
Sample		Hinoki, Rice straw, Rice husks, Larch bark, Corn stalk
Temperature increasing rate		20 K/min
Sample weight		7mg
Gas flow rate		120ml/min
Thermal decomposition	Gas	N ₂
	Final holding temp.	900°C
Combustion	Gas	Air
	Final holding temp.	815°C

Table 2. Properties of coal and biomass tested

Sample	Coal			Biomass						
	SH	NL	TH	Sawdust Hinoki	Larch bark	Rice straw	Rice husks	com stalk		
Low heating value	MJ/kg	air dry	29.16	26.82	25.75	18.02	12.03	11.75	13.54	9.20
Proximate analysis	Moisture	wt %	1.7	1.8	5.2	11.0	9.4	5.8	7.2	7.4
	Ash	wt %	13.8	17.0	11.8	1.2	3.4	19.2	19.3	1.9
	VM	wt %	11.2	27.0	45.4	86.6	87.2	75.0	73.4	82.1
	FC	wt %	73.3	54.2	37.6	1.2	≈ 0	≈ 0	≈ 0	8.5
Fuel ratio	-	-	6.54	2.01	0.83	0.01	0.00	0.00	0.00	0.10
Total S	wt %	dry	0.40	0.35	0.22	0.00	0.02	0.05	0.02	0.00
Ultimate analysis	C	wt %	90.12	84.57	77.84	55.87	47.07	47.50	52	40.10
	H	wt %	3.95	4.91	6.17	7.06	5.5	6.49	6.89	5.20
	N	wt %	1.16	1.79	1.13	0.24	0.23	1.21	0.29	2.10
	S	wt %	0.47	0.25	0.06	0.00	0	0.02	0.01	0.00
	O	wt %	4.30	8.47	14.91	39.83	47.20	44.79	40.84	52.90
H/C (mole ratio)	-	-	0.53	0.70	0.95	1.52	1.40	1.84	1.58	1.56

Table 3. Experimental conditions in co-combustion

Sample	Conditions						
	SH	NL	TH	BM	SH+BM	NL+BM	TH+BM
Furnace temperature [°C]	800						
O ₂ concentration [vol%]	21						
Lower heating value [kW]	0.225	0.218	0.215	0.224	0.362	0.194	0.224
Sample feed rate [g/min]	0.46	0.49	0.5	0.75	0.92	0.52	0.62
Air ratio	1.2						

BM :Biomass (Sawdust)
Mixing ratio= 50 :50 (wt%)

Results and Discussion

Fundamental pyrolysis and combustion characteristics of biomass. Figures 1 show the decrease curves of unburnt fraction for two kinds of biomass and lignin and cellulose under pyrolysis conditions. From the figure, the pyrolysis begins at about 200 degree C for all samples. After about 500 degree C, however, pyrolysis behavior for bark differs from that for rice husks. This phenomenon is caused by the composition difference in the biomass. In order to elucidate the effect of chemical composition on the pyrolysis behavior, pyrolysis experiments for cellulose and lignin were done under the same experimental conditions. For the cellulose the mass rapidly decreases at about 200 degree C, and almost mass is evolved as volatile matter. For the lignin, while, the mass gradually decreases, and the residual matter remains even at 900 degree C. This result suggests that the lignin has the content of fixed carbon. Comparing the results for the cellulose and lignin with those for two types of biomass, Bark may contain more lignin component than Rice husks. Consequently, lignin content in the biomass may affect the combustion characteristics.

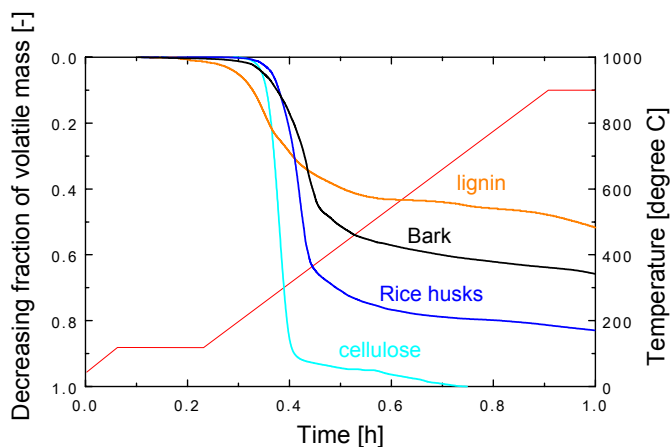


Figure 1. Decreasing profiles of volatile mass for cellulose and lignin, compared with two kinds of biomass

Co-combustion characteristics of coal with biomass. In the co-combustion experiments the reaction gas was sampled along the furnace axis, and the reacting particles were sampled at only the exit of furnace. In order to evaluate the co-combustion characteristics, both biomass alone and coal alone were also burnt under the same experimental condition. O_2 and CO_2 profiles and CO profile along the furnace axis for SH coal, which is categorized as a low-grade coal, are shown in Fig. 2. Comparing the results for biomass and SH coal co-combustion with those for SH coal alone, the ignition point, where O_2 concentration rapidly decreases and CO_2 produces approaches the burner and O_2 is also consumed more during the combustion. Those phenomena suggest the effect biomass addition. For CO profile, biomass produces high concentration of CO during the initial stage of combustion. For SH coal the position of the maximum CO concentration comes near to the burner due to the co-combustion with biomass.

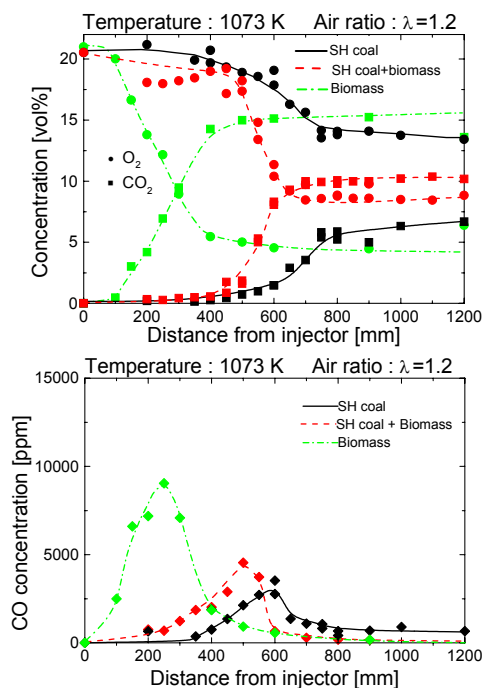
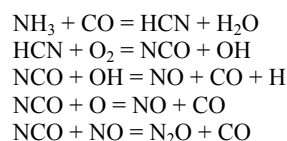


Figure 2. CO_2 and O_2 profiles and CO profile along the furnace axis for biomass alone, coal alone and co-combustion for SH coal

Some reports² have presented that biomass addition played a role for NO_x reduction since biomass tends to evolve NH_3 as volatile nitrogen species. However, the effect of NO_x reduction depends on combustion conditions, furnace type, fuel type and so forth¹. From this viewpoint, NO_x and N_2O were also measured along the furnace axis during the combustion in this study. Figure 3 shows NO and N_2O profiles along the furnace axis for biomass alone, coal alone and co-combustion for SH coal. Both NO and N_2O under the co-combustion condition are not intermediate between those under coal-alone and biomass-alone condition, but are similar to those under coal-alone combustion. Fuel-N input for the co-combustion is half as much as that for the coal-alone. Thereafter, both NO and N_2O emissions for the co-combustion are biased to those for the coal-alone. At the initial combustion stage under the co-combustion N_2O concentration is a little larger than that under the coal-alone combustion condition. Based on those experimental results obtained, the following reaction scheme may be dominant to produce NO and N_2O under the co-combustion condition.



The reason why the scheme above was proposed is caused by production of high CO concentration at the initial stage during biomass combustion. It is necessary to confirm the scheme by means of chemical kinetic theory since the first reaction of $NH_3 + CO = HCN + H_2O$ is not generally adopted in elementary reaction group relating to NO and N_2O .

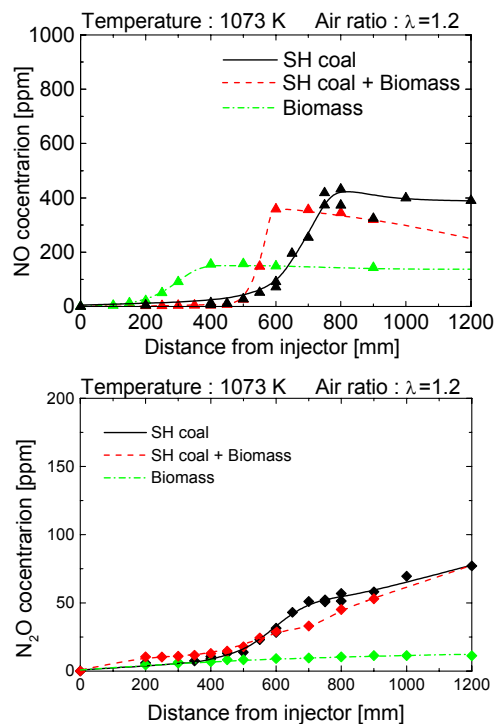


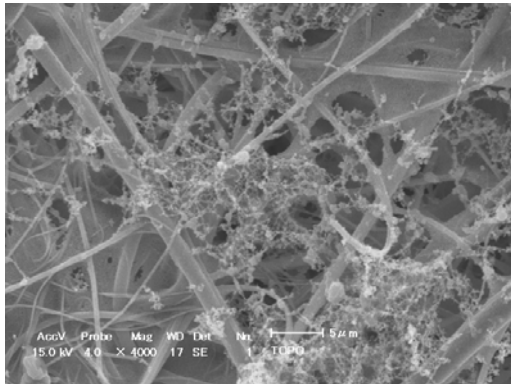
Figure 3. NO and N_2O profiles along the furnace axis for biomass alone, coal alone and co-combustion for SH coal

Recently, fine particulates exhausted from combustion processes, so-called PM_{2.5}, have been focused in terms of health effect. Biomass, especially for agricultural biomass, usually contains a small amount of ash content, as shown in Table 2. Therefore, when biomass is burnt out, fine particulates may be produced during the combustion. Figure 4 shows SEM photos of ash collected by a filter for (a) biomass alone and (b) co-combustion of NL coal with biomass. In (a), fibers of the filter are also observed. When the biomass is burnt out, only fine particulates are captured in the filter. Mean particle diameter of those fine particulates was about 1.3 μm. Under the co-combustion condition, on the other hand, co-combustion of coal with biomass contributes to have those fine particulates adhered during the combustion.

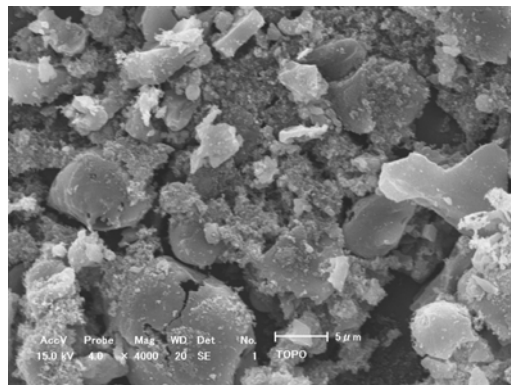
Acknowledgement This study has been partly supported, as Priority Areas Research of Grants-in-Aid for Scientific Researches and COE project, by Monbu Kagaku-sho.

References

- (1) Davidson, R. M. (1999) *IEA Coal Research*, Feb.
- (2) Morgan, D. J. and van de Kamp, W. L. (1995) "Combined combustion of biomass/sewage sludge and coals", Bemtgen, J. M. *et al.* (eds.), 35.



(a) Biomass alone



(b) Co-combustion

Figure 4. SEM photos of ash collected by a filter for biomass alone and co-combustion of NL coal with biomass

EFFECT OF INORGANIC MATTER ON REACTIVITY AND KINETICS OF COAL PYROLYSIS

Quanrun Liu^a, Haoquan Hu^{a*}, Qiang Zhou^a, Shengwei Zhu^a
Guohua Chen^b

^aInstitute of Coal Chemical Engineering, Dalian University of Technology, 129 Street, Dalian 116012, China

^bDepartment of Chemical Engineering, The Hong Kong University of Science & Technology, Clear Water Bay, Kowloon, Hong Kong SAR

*hhu@chem.dlut.edu.cn

Introduction

Coal pyrolysis is one of the most important aspect of coal behavior for its occurring in all major coal conversion processes, such as combustion, gasification, carbonization and liquefaction etc. Many works have examined the relationship between inorganic components in coals and their reactivity. Because of the differences in composition and properties for different coal, there were many discrepancies in the results obtained by different researchers for different coal samples^[1]. Moreover, there is little on the relationship between inorganic matter and the kinetics of coal pyrolysis has been reported.

In this work, two Chinese coals, Shenfu bituminous coal (SF) and Huolingel lignite (HLGL), were used as samples. The coal was demineralized, then several inorganic matters were added to the demineralized coals. The raw, demineralized and inorganic matters added coals were pyrolysed by using thermogravimetry to investigate the effects of mineral matter on the reactivity and kinetics of coal pyrolysis.

Experimental

Coal Samples Coal sample, with particle size of -120mesh, was demineralized by HCl/HF. The procedure of demineralization followed the method used by Oztas^[2]. After the acid treatment, the content of ash in coals are below 1wt%. Three inorganic matters, including Al₂O₃, the main constituents of kaolinite and illite; CaO, the production of calcium carbonate during coal pyrolysis; K₂CO₃, the famous catalyzer for gasification, were ground to 120 mesh and baked at 800°C for 2h, then added to the demineralized coals by co-slurrying with water in concentrated suspension for 24h and dried in vacuum oven. The content of the inorganic matters additive in coal is 10wt%.

Pyrolysis Pyrolysis was carried out with a thermogravimetry (SDTA851e). About 20mg raw, demineralized or inorganic matter added samples were placed with an aluminum crucible and pyrolysed under N₂ flow at the heating rate of 10K/min from 110°C to 800°C.

Results and Discussion

Effect on reactivity The effects of inherent mineral and the mineral additive on the weight loss during coals pyrolysis as a function of temperature are shown in **Figure 1**. From the results it can be seen that the conversion of organic matters in the demineralized coal is almost the same as raw coal. This indicates that the inherent mineral matter has no effect on the reactivity of coal pyrolysis. Upon 550°C, the weight loss of raw HLGL is a little higher than that of its demineralized coal, which might be due to the mineral itself decomposition^[3].

When Al₂O₃, CaO or K₂CO₃ was added into the demineralized coal, the weight loss curve changed greatly, which indicated the effect of this mineral matter on coal pyrolysis. The trend of effect of Al₂O₃ and CaO is more evident than that of K₂CO₃ with temperature increasing, but upon 450°C, they have same trend with little change.

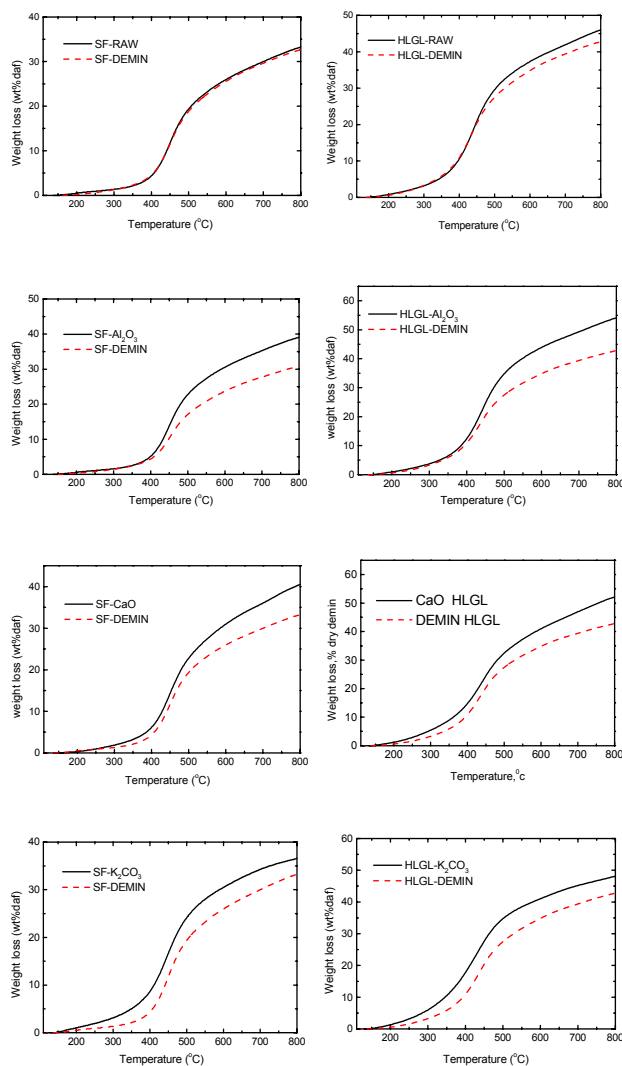


Figure 1 Weight loss of coal samples as a function of temperature

CaO and K₂CO₃ affect the reactions as soon as the beginning of coal pyrolysis, while the effect of Al₂O₃ only occurs upon the temperature of 450°C. These phenomena make out that different inorganic matter has different catalytic nature. The mechanism of the effect of inorganic matters on coal pyrolysis is not very clear, but it may be explained from the nature of these mineral matters. Clay, which exists in coal, affects the coal gasification and catalyzes hydrogen transfer to coal^[4], therefore, it is not surprising that Al₂O₃, the main active component of clay, has catalytic effect on coal pyrolysis. CaO is active in effect on cracking oxygen functional groups in coal^[4]. A large portion of oxygen in bituminous coal exists in acidic functional groups such as phenol carboxylic acids. CaO might react with these groups. The interaction of K₂CO₃ with -COOH and -OH functional groups possibly resulted in the formation of K-oxygen surface groups or clusters. These surface functional groups have been considered as the active sites on the coal surface^[2].

Effect on the kinetics The kinetic parameters, activation energy (E) and pre-exponential factor (A), of coal pyrolysis were determined by Coats-Redfern method^[5]. As shown in **Figure 2**, the reaction of coal pyrolysis can be described by multi-step first order reaction.

During processing the data, the relative conversion, x , was defined as: $x=(w_0-w)/(w_0-w_f)$, where w_0 is the sample weight at the beginning of pyrolysis; w is the weight of the instantaneous residue; w_f is the weight of the residue at the end of coal pyrolysis.

Figure 3 is the typical TG and DTG curves of coal pyrolysis. In the figure some characteristic temperature of pyrolysis has been lined out. The beginning temperature of coal pyrolysis T_0 is defined as temperature at $x=5\%$; T_p is the temperature at maximum weight loss rate and the end temperature T_F is that at $x=85\%$.

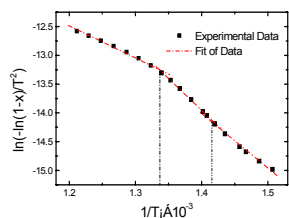


Figure 2 Plot of $\ln[-\ln(1-x)/T^2]$ vs $1/T$ of coal pyrolysis

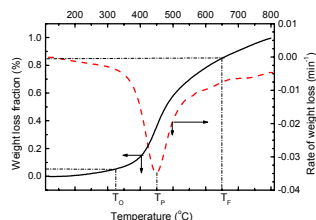


Figure 3 The characteristic temperature of coal pyrolysis

Table 1 Kinetic parameters and characteristic temperatures of coal pyrolysis

Sample	Temp (°C)	T_p (°C)	E (KJ/mol)	A (min^{-1})	-R*
SF-DEMINE	326-406	446	61.2	1.39E+3	0.999
	406-478		97.2	1.28E+6	0.999
	478-549		45.1	1.40E+2	0.998
SF-CaO	307-380	450	26.5	1.16E+0	0.999
	380-467		54.4	2.85E+3	0.999
	467-592		20.9	8.90E-1	0.997
SF-K ₂ CO ₃	250-369	444	18.4	2.90E-1	0.999
	369-467		50.2	2.90E+2	0.996
	467-540		24.8	2.50E+0	0.998
SF-Al ₂ O ₃	324-369	450	56.3	8.40E-1	0.997
	369-467		54.2	1.51E+4	0.999
	467-580		16.9	1.25E+0	0.997
HLGL-DEMINE	270-406	440	41.3	5.04E+1	0.998
	406-479		73.3	2.73E+4	0.999
	479-530		42.9	1.23E+2	0.999
HLGL-CaO	224-371	438	22.7	1.06E+0	0.999
	371-467		38.4	3.29E+1	0.998
	467-574		14.6	2.70E-1	0.998
HLGL-K ₂ CO ₃	234-369	438	17.4	4.20E+0	0.998
	369-467		37.3	3.64E+1	0.999
	467-535		17.4	6.70E-1	0.997
HLGL-Al ₂ O ₃	270-371	436	38.5	9.10E-1	0.999
	371-467		36.7	6.18E+2	0.999
	467-555		12.4	8.90E-1	0.998

*correlation coefficient

Table 1 shows the kinetics parameters and the characteristic temperature of coal pyrolysis. The kinetics parameters are calculated in the range from $x=5\%$ to $x=85\%$. The experimental and calculating results indicated that the raw and its demineralized coal has almost

same kinetic parameters and characteristic temperature, so the results of raw coal aren't listed in the table. The good correlation coefficient indicated that Coats-Redfern model fit the experimental data very well.

From **Table 1**, it can be seen that addition of inorganic matters, the characteristic temperature, activation energy and pre-exponential factor are different from those of raw and demineralized coals. This makes out that addition inorganic matters alter the course and mechanism of coal pyrolysis. Moreover, the influences are different by different coals.

T_p is related to coal structure^[6]. Usually, the same structure of coals have same T_p . **Table 1** shows that addition of inorganic matters has little effect on T_p during coal pyrolysis, which indicate that the procedure of demineralization and addition of inorganic matters didn't change the coal structure very much. T_0 and T_F are related to the difficulty of chemical reaction. For the two demineralized coal samples, addition of CaO gives rise to T_0 decrease about 20 to 30°C and T_F increase about 40 to 50°C. For demineralized SF coal, addition of K₂CO₃ leads to T_0 descend for 70°C and 40°C for demineralized HLGL coal. This indicates that the influence of K₂CO₃ is very different from different coals. But K₂CO₃ has little effect on T_F of coal pyrolysis for both coals. Addition of Al₂O₃ has no effect on the T_0 , but make T_F increase about 20 to 30°C.

Reaction with high activation energy needs high temperature or long reaction time^[7]. For coal pyrolysis, high activation energy means that the reaction needs more energy offered by exterior. As shown in **Table 1**, there is highest activation energy in the middle temperature range for all samples. Compared to raw and demineralized coal samples, addition of CaO, K₂CO₃ or Al₂O₃ results in the decrease of activation energy at the corresponding temperature range. At low temperature, activation energy of inorganic matter added coals follows the order K₂CO₃ < CaO < Al₂O₃ indicates that K₂CO₃ has the highest catalytic effect on coal pyrolysis; At the middle temperature, the activation energy of the three inorganic matters is similar order, which indicate that they have similar catalytic nature at this temperature range; At high temperature, the activation energy of Al₂O₃ added coal is the least. The change of activation energy shows that different inorganic matter has different catalytic nature at different temperature.

Conclusion

In the conditions studied, the inherent mineral in coal has no effect on the reactivity and kinetics of coal pyrolysis. When some inorganic matters, such as CaO, K₂CO₃ and Al₂O₃, were added into the demineralized coal, they showed the positive effect on reactivity of coal pyrolysis. The pyrolysis process of all samples studies can be described by multi-step first order model. Addition of inorganic matters makes the activation energy decreased and the characteristic temperature of coal changed.

Acknowledgment The work was supported by fund of the National Key Fundamental Research and Development Project of China (G1999022101)

References

- [1] Lemaignen, L.; Zhuo, Y.; Reed, G.; Dugwell, D. R.; Kandiyoti, R., Fuel, 2002, 81, 315-326.
- [2] Oztas, N.A.; Yurum, Y., Fuel, 2000, 79, 1221-1227.
- [3] Coats, A. W.; Redfern, J. F., Nature, 1964, 68, 201.
- [4] Crpres, R.; and Furfari, S., Fuel, 1982, 61, 76.
- [5] Slaghuis, J. H.; Ferreira, L.C.; and Judd, M. R., Fuel, 1991, 70, 471.
- [6] Xu, Y., Coal Chem. Ind., 1995, 72, 62-65.
- [7] Lazaro, M.J.; Moliner, R.; and Suelves, I., J. of Analytical and Applied Pyrolysis, 1998, 47, 111-125.

An Overview of the U.S. Department of Energy's Gasification Technologies Program

Gary J. Stiegel

National Energy Technology Laboratory
U.S. Department of Energy
P.O. Box 10940
Pittsburgh, PA 15236

Massood Ramezan

Science Applications International Corporation
P.O. Box 18689
Pittsburgh, PA 15236

Introduction

Coal gasification is a well-proven technology that started with the production of coal gas for urban areas, progressed to the production of fuels, chemicals, and most recently to large-scale power generation. More than 160 commercial gasification plants (equivalent to nearly 61,000 MW_{th} syngas capacity) are currently in operation, under construction, or in planning and design stages in 28 countries worldwide.

Gasification-based technologies can be used to convert coal or other carbon-containing resources into a clean gas with high value as a fuel for combined cycle power generation or as a feedstock for the production of liquid fuels and chemicals. Moreover, these systems have the advantage of being capable of co-generating electricity and fuel/chemical efficiently, economically, and in an environmentally acceptable manner. Environmental performance of these systems can be tailored to any specific requirements. In addition, due to the high efficiency nature of these plants, the emissions of CO₂ are inherently low. The DOE Gasification Technologies Program has a history of success in technology development and demonstration. The R&D portfolio of today's program will enable deployment of the clean and affordable energy systems required for growing energy markets.

Program Drivers and Goals

The nation's energy mix is dependent primarily on fossil energy. According to the public- and private-sector forecasts, the nation's electricity and transportation fuels will continue to be fossil-fuel based for the next 20 years — and well beyond. This continued use, however, must be matched by combining energy availability at reasonable prices with increasingly clean environmental performance throughout the energy life cycle of production, conversion, and end-use. In the foreseeable future, the cornerstone of our energy will remain fossil-fuel based, but it will be cleaner and sustainable.

Goals for Growing Markets

To capture the opportunity for broad public benefits — and to enable market development for gasification technologies — the program focuses on process efficiency, environmental performance, and plant economics. The program goals are:

- near-zero emissions
- feedstock flexibility
- multiple, high-value products
- efficiency greater than 60% by 2015
- cost competitive

Related technical objectives such as modularity and standardization of plant design, improved plant availability and the capability for CO₂ capture will help make gasification the choice for a range of

markets. Achieving these goals can provide the clean, secure, and affordable energy the nation requires.

The Gasification Process

Gasification utilizes virtually any carbon-containing material to produce a gaseous product "syngas". This syngas (made up primarily of H₂ and CO) can be used in many ways, including the production of electricity, chemicals, fuels, hydrogen, and as a source of substitute natural gas. Possible feedstocks include coal, petroleum coke and other residue from petroleum processes, biomass, and municipal and industrial waste. The feedstock enters the gasifier, where it encounters steam and oxygen at high temperatures and pressures. These conditions cause the feedstock to be broken down into syngas and a solid ash/slag product. The ash/slag is removed from the bottom of the gasifier while the syngas enters a purification system. Gas cleaning removes impurities including sulfur, particulates, and related products, the majority of which are saleable by-products. Additional separation units can recover H₂ and remove CO₂. While gasification systems are not new, most applications have focused on single products, generally electric power or chemicals. For a new generation of gasification systems, the program strategy is to enhance the flexibility of gasification in meeting new and growing markets. Achieving a combination of improvements in process efficiency, economics, and environmental performance will enable gasification to be the preferred technology in a wide range of markets. Figure 1 depicts a simplified flow chart illustrating gasification-based energy conversion options.

Program Technology Areas

The program implements strategic, time-phased R&D such as: lower-cost, lower-risk technologies to improve the economic environmental performance of existing systems by 2005, advanced technologies for a new generation of gasification systems by 2010, and advanced integrated energy plants by 2015. The program is currently structured in five technology areas:

- 1) **advanced gasification** – To further develop fuel flexibility, higher efficiency and reliability, and improved economic and environmental performance. Advances in the gasifier itself to enhance efficiency, reliability and feedstock flexibility and economics are crucial for gasification system improvements. Research is being conducted on advanced gasifiers, such as the transport gasifier, so higher performance goals can be reached and the variety of possible feedstocks can be further expanded. Advanced refractory materials and new process instrumentation are being developed to improve system reliability and availability, operational control, and overall system performance. Studies of alternative feedstocks (biomass and waste from refineries, industries, and municipalities) will improve gasifier flexibility and utility. Data from fluid dynamic models are being used to develop and improve advanced gasifiers. Promising developments will be tested and evaluated in large demonstration and/or commercial-scale gasifiers.
- 2) **gas cleaning and conditioning** – To evaluate novel concepts to meet rigid syngas quality specifications for fuel cells and catalytic conversion processes. In the gas cleaning and conditioning area, the goal is to achieve near-zero emissions while simultaneously reducing capital and operating costs. Novel gas cleaning and conditioning technologies are undergoing development to reach this goal. Processes that operate at mild to high temperatures and incorporate multi-contaminant control to parts-per-billion levels are being explored. These include process for trace metals, H₂S, HCl, and particulates removal; membrane processes for control of H₂S and CO₂; and sorbents for NH₃ control. Both ceramic and

metallic filters are being assessed for particulate control. Promising technologies will be scaled-up and integrated into existing demonstration facilities. Furthermore, investigation of technologies for mercury removal is currently underway.

- 3) **advanced gas separation** – To investigate alternatives to energy intensive separation methods, such as cryogenic separation. Advanced gas separation research offers the potential for substantial improvement in environmental and cost performance. These technologies will also enhance process efficiency. A major program objective is the development of cost-effective air-separation membranes. These can provide substantial cost reduction for oxygen production compared to conventional cryogenic methods. Improved hydrogen recovery and CO₂ removal are also important. Currently, the program is developing high-temperature ceramic membranes for hydrogen recovery from gas streams, as well as low-temperature approaches to recovery and removal. Other novel approaches for H₂, CO₂, and O₂ separation will be investigated under different operating conditions.
- 4) **product and by-product utilization** – To enhance project revenues and eliminate waste streams. The economics of gasification can be improved by fully utilizing all outlet streams of the process. Sale of value-added by-products from waste streams and minimization of waste disposal can substantially improve the economics of gasification processes. By-products include pressurized CO₂ ash/slag, sulfur and/or sulfuric acid, and ammonia. Program activity seeks to expand market options, such as improving the quality of slags and improving the use of sulfur. The program is developing a bench-scale demonstration of a direct sulfur-reduction process. The development of advanced concepts for warm-gas desulfurization technology are targeted as well as a one-step process for elemental sulfur. Methodology is also being developed to produce a lightweight aggregate from gasification ash.
- 5) **Systems Analysis/Technology Integration** - To achieve improvements in plant economics. The Systems Analysis/Technology Integration area targets integration of all relevant gasification technologies, regardless of the end products. Economic analyses, performance assessments, and market studies provide guidance for future R&D and deployment opportunities. Barriers to deployment are identified and system performance targets are developed. Studies are conducted on topics such as novel warm gas cleaning, membrane-based separation, and co-feeding applications. Also, product outreach activity focuses on the public benefits of gasification today and in the future. Stakeholders include the public, industry officials, environmental groups, and local, state, and Federal legislators and regulators. Efforts are underway through industry stakeholders to identify technology and environmental issues, and to facilitate commercialization.

The Clean Coal Projects

First-generation Integrated Gasification Combined Cycle (IGCC) plants have demonstrated the efficiency and environmental performance benefits. Working with a broad range of industrial, university, and national laboratory stakeholders, the program will establish the technology capability to expand the success to a new generation of technology that will serve broader markets - power, chemicals, hydrogen, and steam - with improved economics.

- **The Wabash River Coal Gasification Repowering Project** located in Vigo County, Indiana was the first full-size commercial gasification combined cycle plant built in the U.S. that repowered an existing pulverized coal plant. It is one of the

world's largest single train gasification combined cycle plants operating commercially.

- **The Tampa Electric Polk Station Project** located in Polk County, Florida is the Nation's first "Greenfield" commercial gasification combined cycle power station. The power plant is one of the world's cleanest. The plant's gas cleaning technology removes more than 98% of the sulfur in coal, converting it to a commercial product. Nitrogen oxide emissions are reduced by more than 90%.
- **The Kentucky Pioneer Energy IGCC Demonstration Project** located in Clark County, Kentucky is currently in design phase with construction start up scheduled for 2003. This plant will demonstrate and assess the reliability, availability, and maintainability of utility-scale IGCC systems. It will use a high-sulfur bituminous coal and municipal solid waste blend in an oxygen-blown, slagging gasifier.
- **The Air Products' Liquid Phase Methanol Project** located in Sullivan County, Tennessee has successfully demonstrated the production of methanol from coal gas at commercial scale. The methanol can be used directly as a fuel product or as an intermediary for a wide range of petrochemical products.

Technical Successes

The program builds on this history of success by producing results that will enable clean, affordable energy systems. Improvements in gasifier design and efficiency, in gas-stream cleanup and by-product quality, and in systems integration will provide both enhanced environmental performance and process economics. Recent successes in the R&D program point to the future deployment of new technologies for both current and new markets.

- **Air Separation Membranes** Recent process analyses on a variety of gasification-based processes continue to show significant cost and efficiency advantages with the application of high-temperature membranes for oxygen production compared to conventional cryogenic technology.
- **Hydrogen Production From Coal Gasification** New technology using ceramic membranes are being developed that have increased the hydrogen permeation rates of dense ceramic membranes at high temperature by over an order of magnitude.
- **Coal-Based Hydrogen Production and CO₂ Capture Technology** The feasibility of separating CO₂ and hydrogen from coal-derived shifted synthesis gas has been confirmed in laboratory testing of the CO₂ hydrate process.
- **Gasification Design Optimization** The application of value engineering to the design of gasification-based processes resulted in the identification ideas that had potential for significant capital and O&M cost savings. Furthermore, significant strides have been made toward successful demonstration in of oxygen-blown gasification using the transport gasifier at the Power Systems Development Facility in Wilsonville, Alabama.
- **Advanced Materials to Enhance Gasifier Reliability** A new slag resistant refractory material has been developed that has potential for increasing the lifetime by five to ten times that of current refractories.
- **Advanced Gas Cleaning Technology** A novel gas cleaning technology developed to achieve ultra-low levels of emissions. The technology has shown potential to achieve sulfur levels of <1 ppm in the fuel gas to the gas turbine at capital costs of much below than that of existing commercial technologies.
- **Co-Production of Electricity and Fuels** Industrial teams are currently assessing the technical and economic feasibility of co-producing electricity and fuels from coal. A low heating value

coal-derived gas, representative of the fuel gas expected to be produced in a co-production process, has been successfully combusted in a GE 6FA turbine.

Clean, Affordable Energy Options for the Future

New markets are emerging that will benefit significantly from the flexibility, environmental improvements, economic successes, and efficiency of gasification. Two examples of emerging markets are repowering, and multi-production.

- **Repowering of existing coal plants** As demand for power production increases, the nation’s coal plants — the heart of stable and affordable electric power in the United States — face the need for ever-cleaner power production. Repowering of these plants with gasification can offer major benefits: improved environmental performance, reduced capital investment, feedstock flexibility, and capacity increases due to improved process efficiency. Also, gasification can be used to repower existing gas-fired facilities. A gasifier placed upstream of existing natural-gas-fired turbines can provide an alternative to natural gas with long-term price stability.
- **Multi-production facilities for industry** Feedstock and product options will become increasingly important as the nation continues to make the difficult transition from a regulated environment to one having market-based energy options. Gasification offers the most flexible route to using variable feedstocks and producing electric power, fuels, hydrogen, chemicals, or steam. Feedstock flexibility, with feedstocks that include coal, biomass, petroleum “bottoms” (coke and residuum), and waste materials, will ensure that stable, low-cost

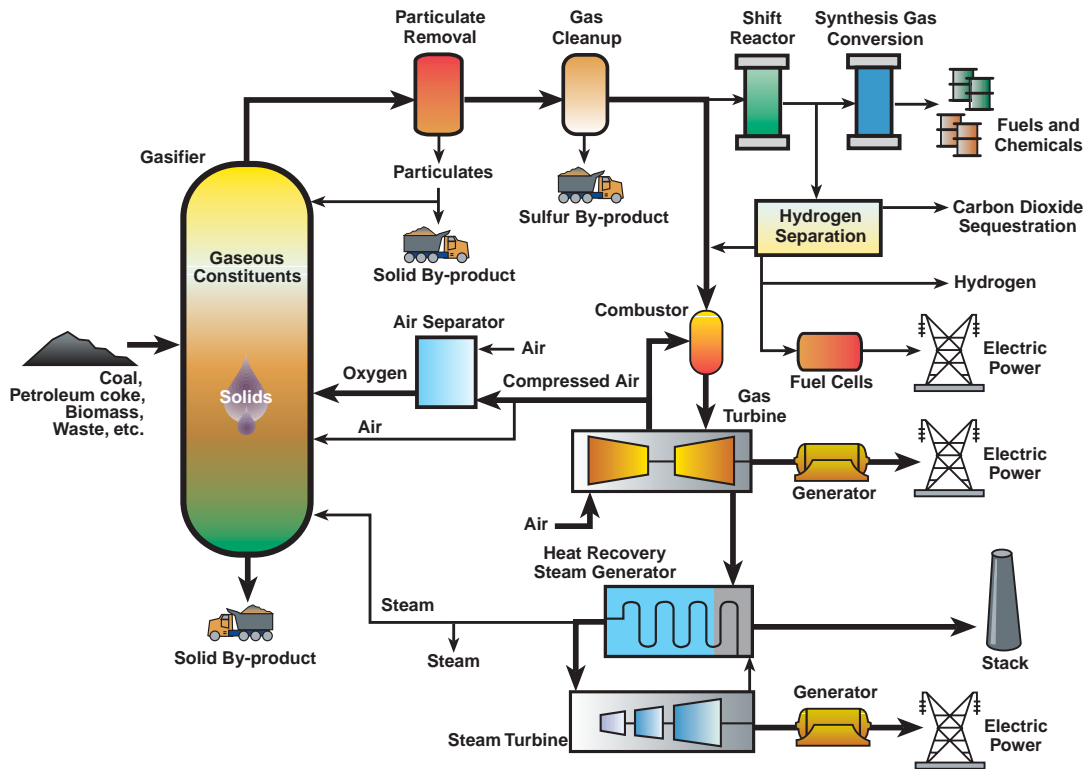
fuel sources are available. The ability to vary the product slate will both improve plant economics *and* support market stability.

Gasification: Technology of Choice for Markets Today and Tomorrow

Markets and market drivers are changing at a rapid pace. Environmental performance is a greater factor as emission standards tighten and market growth occurs in areas where total allowable emissions are capped. Also, reduction of carbon dioxide emissions is one of the challenges in response to global climate change. Industries have expressed a need for more environmentally sound processes, more efficient and reliable systems, and an ever-present demand for higher profitability. They need a technology that can match these requirements — a means to remain flexible, reduce risk, decrease emissions, increase stockholder return on investment, and consume fewer resources. Gasification is the technology that can meet these requirements. Today, the majority of existing applications have been geared toward the production of a single product or a constant ratio of two or more products per facility. Tomorrow, the potential of gasification in expanding markets is in its use of low-cost and blended feedstocks and its multiproduct flexibility. With deregulation, rapidly changing market demands, fluctuation in natural-gas prices, and increased environmental concerns, gasification will become the cornerstone technology for market flexibility.

For more information visit <http://www.netl.doe.gov/coalpower/gasification/>

Figure 1. GASIFICATION-BASED ENERGY CONVERSION SYSTEM CONCEPTS



Role of Water Vapor in Oxidative Decomposition of Calcium Sulfide

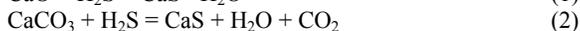
Shengji Wu, Md.A.Uddin, Shinsuke Nagamine and Eiji Sasaoka

Faculty of Environmental Science and Technology
Okayama University
3-1-1Tsusima-naka Okayam
700-8530 Japan

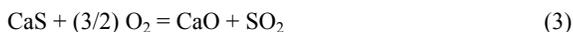
Introduction

Limestone is very important material as a high-temperature desulfurization sorbent: limestone is used in coal gasifiers for the in-bed removal of H₂S.

In gasifiers of coal, decomposition of limestone into CaO and CO₂ depend on the concentration and /or pressure of CO₂ and the temperature. Therefore, two sulfation reactions have to be considered:



The products CaS has to be converted to CaSO₄ before disposal because H₂S is released from the reaction between CaS and Water.¹ The conversion of CaS to CaSO₄ is expressed as follows:



The molar volume ratio of CaS to CaSO₄ in eqs 3 and 4 is ca.1.6/1. This large volume change induces the plugging of the intraparticle pore of CaS if the pore size is not sufficiently large. If a layer of CaSO₄ covers the outside of the CaS particle, then CaS is not converted to CaSO₄ until the CaSO₄ decomposes into CaO, SO₂ and O₂ at a high-temperature.

We have found a method with acetic acid for the preparation for a highly active macroporous lime. The macroporous CaS formed from the macroporous lime was easily converted to CaSO₄ and CaO. However, the CaS formed from natural lime to CaSO₄ was partially converted to CaSO₄ and CaO because only small amount of pore were present in the CaS sample.^{2,3}

To find out a method for perfect conversion of CaS formed from a natural lime to CaSO₄, the basic characters of the oxidative decomposition of CaS were examined using reagent grade CaS. The decompositions of CaS were examined in the presence of H₂O because hot combustion gas containing moisture is usually used for the decomposition of CaS. The main purpose of this study is to clarify the role of H₂O in the oxidative decomposition of CaS.

Experimental

CaS Samples. Pure CaS powder (average diameter: < 325 micro meter, purity: >99 %) was obtained from Soekawa Chemicals. Cylindrical pellets were formed from the CaS powder by pressing using a cylindrical die. The pellets were crushed and sieved to the two size sample particles (average diameter: 2.0mm and 0.2mm). The pore size distribution of the sample measured by mercury penetration porosimeter showed that the main pore size was around 1micro meter

Apparatus and Procedure. The oxidative decomposition of CaS were carried out using a flow-type thermogravimetric apparatus under atmospheric pressure. About 60mg sample particles (2.0mm dia.) was set in a net sample holder. The reaction temperatures examined were 800, 900 and 1000°C. The reaction commenced when

a mixture of (0-10%)O₂, (0-52.8%) H₂O, and N₂ (balance gas) was fed into the reactor at 500cm³STP/min. Weight gain of the sample during the reaction was measured by the balance and also the amount of SO₂ evolved during the reaction was measured by a wet-type absorption method (Arsenazo III). The composition of the oxidized sample was calculated from the weight gain and the amount of the evolved SO₂.

Experiments Using Tracer H₂¹⁸O. To clarify the role of H₂O in the oxidative decomposition of CaS with O₂, H₂¹⁸O (purity: ca.95%) was used instead of H₂¹⁶O. The experiments using the H₂¹⁸O were carried out using a micro-reactor system equipped with a small U tube reactor. The concentrations of S¹⁶O₂, S¹⁶O¹⁸O and S¹⁸O₂ in the outlet gas from the sample (0.2mm dia.) were continuously monitored by a quadrupole mass spectrometer.

Results and Discussion

Effect of H₂O on the Rate of the Decomposition of CaS.

Figure 1 shows typical weight gains of the samples both in the absence and presence of H₂O at 900°C. Figure 2 shows the compositions of the samples after the oxidation in Figure 1. it is evident that the presence of H₂O drastically accelerates the decomposition of CaS with O₂. A similar results were obtained in the experiment at 800°C. However, at 1000°C, the acceleration by H₂O was not clearly observed.

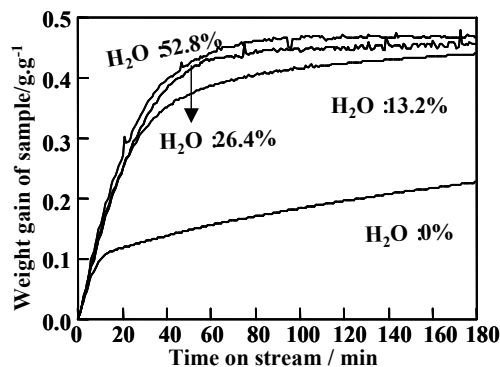


Figure 1. Effects of the concentration of H₂O on the oxidative decomposition of CaS. Temp.900°C; O₂: 1%.

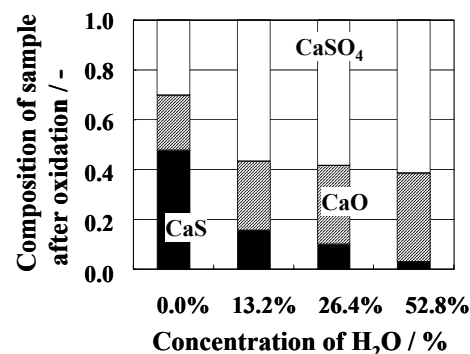
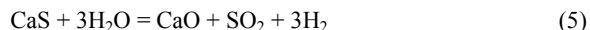


Figure 2. Composition of the samples after the oxidation

Reaction between CaS and H₂O. The reactivity of CaS with H₂O was examined in the temperature range from 800 to 1000°C in the absence of oxygen. From this experiments, it was confirmed that CaS directly reacted with H₂O and formed CaO, SO₂ and H₂ according to the following reaction.



In order to know the temperature zone in which the reactions of eq 5 and 3 occur, the temperature programmed reaction (TPR) spectra were measured in 3 systems: system (a): 10% H_2O -He; system (b): 1% O_2 -He; system (c): 10% H_2O -1% O_2 -He. **Figure 3** shows the evolution of SO_2 during the TPRs. The reaction of eq 5 occurred almost at the same temperature zone. The evolution of SO_2 in the system (c) indicated that there is a synergistic effect of H_2O and O_2 on the oxidative decomposition of CaS.

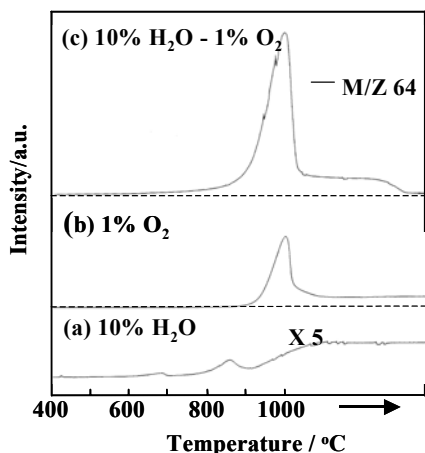


Figure 3. Evolution of sulfur dioxide during the TPR

Role of H_2O in the Oxidative Decomposition of CaS. To clarify the role of H_2O in the oxidative decomposition of CaS with O_2 , H_2^{18}O was used instead of H_2^{16}O . **Figure 4** shows the evolution of S^{18}O_2 , $\text{S}^{16}\text{O}^{18}\text{O}$, and S^{16}O_2 , during the constant-temperature-decomposition of CaS in the 1000°C in system (c). In this system, S^{18}O_2 , $\text{S}^{18}\text{O}^{16}\text{O}$, S^{16}O_2 evolved from the sample. As the amount of the evolved S^{18}O_2 was highest in the three species, it was confirmed that the following reactions mainly occurred.

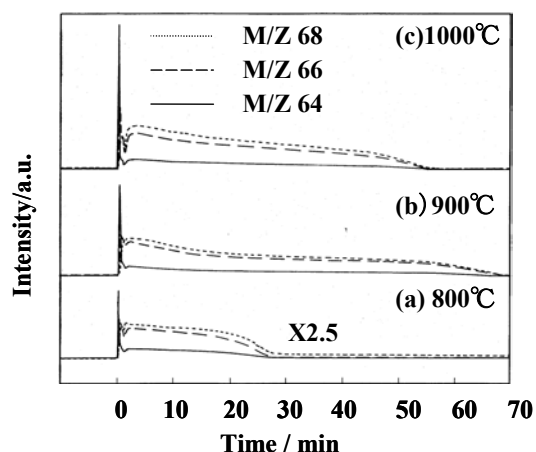
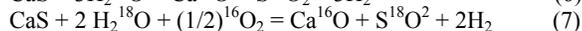
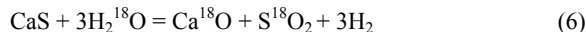
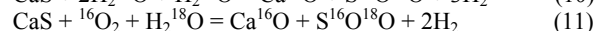
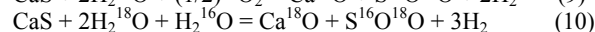
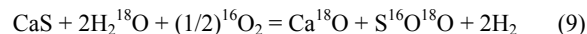


Figure 4. Evolution of sulfur dioxide from CaS in the presence of both $^{16}\text{O}_2$ (1%) and H_2^{18}O (10%).

As these reactions are thermo-dynamically unfavorable, the following reaction followed the reactions of eqs 6 and 7.



$\text{S}^{18}\text{O}^{16}\text{O}$ might be formed via the following reactions:



The following reaction was not main reaction in the system (c)



Furthermore, reaction of eq 8 might radically occur because the temperature was high enough for the radical reaction in that case OH radical might play an important role in the reactions.

The reaction mechanism seems to be complex. However, the formation of $\text{S}^{18}\text{O}^{16}\text{O}$ clearly indicates that the oxidation of CaS occurs stepwise. Unfortunately, the amount of the evolved $\text{S}^x\text{O}^y\text{O}$ could not be quantitatively analyzed by our mass spectrometer. The ratio of $[\text{S}^x\text{O}^y\text{O}]$ to Total $[\text{S}^x\text{O}^y\text{O}]$ (where $\text{S}^x\text{O}^y\text{O}$ is either S^{18}O_2 or $\text{S}^{16}\text{O}^{18}\text{O}$ or S^{16}O_2 species and Total $[\text{S}^x\text{O}^y\text{O}] = \text{S}^{18}\text{O}_2 + \text{S}^{16}\text{O}^{18}\text{O} + \text{S}^{16}\text{O}_2$) was calculated from the data of the $\text{S}^x\text{O}^y\text{O}$ evolution peak areas shown in Figure 4. As shown in **Figure 5**, the three molar ratios of the $\text{S}^x\text{O}^y\text{O}$ were almost constant in the temperature range from 800 to 1000°C . This result suggested that the reaction mechanism did not change in the temperature range in the system (c). When the concentration of O_2 was increased in the presence of 10% H_2O at 1000°C , the ratios changed except the ratio of the $\text{S}^{16}\text{O}^{18}\text{O}$. This result suggests that the direct contribution of $^{16}\text{O}_2$ might be high. However, the ratio of the $\text{S}^{16}\text{O}^{18}\text{O}$ to total $\text{S}^x\text{O}^y\text{O}$ was almost constant suggesting that H_2O play an important role even if the O_2 concentration is high.

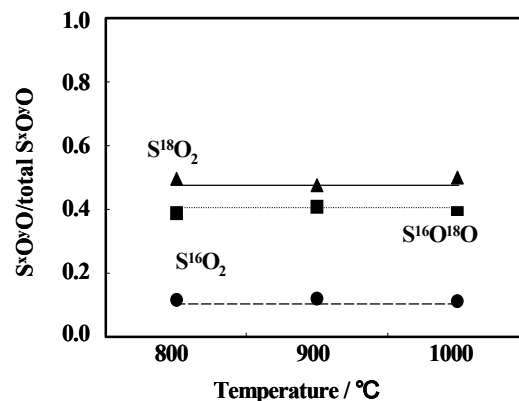


Figure 5. Effect of temperature on $\text{S}^x\text{O}^y\text{O}/\text{total } \text{S}^x\text{O}^y\text{O}$

Acknowledgment. This work was supported by the Ministry of Education, Science, Sport and Culture of Japan through the Grant-in-Aid on Priority-Area Research(Region No.737, Grant No.11218207)

Literature Cited

- Ninomiya, y.; Sato, A.; Watkinson, A., Int. Conf. Fluidized Bed Combustion, 13th 1995,1027-33.
- Sasaoka, E.; Uddin, M, A.; Nojima, S., Ind. Eng. Chem. Res., 1997, 36, 3639-46.
- Sasaoka, E.; Sada, N.; Uddin, M, A, Ind. Eng. Chem. Res., 1998, 37, 3943-49.

Dynamic behavior of sulfur evolved in the gas phase from pyrolysis of seven Chinese coals

Long Xu, Jianli Yang, Yunmei Li, Zhenyu Liu

State Key Laboratory of Coal Conversion,
Institute of Coal Chemistry, Chinese Academy of Sciences,
Taiyuan 030001 P. R. China (zyl@public.ty.sx.cn)

Abstract

Sulfur compounds evolved in the gas phase from pyrolysis of seven Chinese coals are studied using TPD-FPD method in the temperature range of up to 800°C under N₂ and H₂. The effect of H₂ is complex, which promotes certain peak and suppresses other peaks. Interactions between volatile sulfur-containing compounds and the coal matrix are attributed to be the main factor determining the dynamic behavior.

Introduction

More than 70% of the primary energy in China is coal. Sulfur emitted from burning of coal has caused severe environmental pollution. Studies on sulfur emission behavior during thermal processing of coal is very important for development of desulfurization technique prior to combustion, as well as for understanding of sulfur species distributed in coal.

The sulfur compounds in the gases emitted from pyrolysis of coal are generally H₂S, SO₂, COS, CH₃SH and CS₂, with H₂S as the dominant species [1]. The extent of sulfur emission during pyrolysis varies greatly, owing to the variations in coal rank, content of sulfur forms, nature of mineral matters, and the influence of pyrolysis conditions such as reactor design, the temperature, the nature of the atmosphere and the pressure [2].

In this paper, dynamic behavior of the total sulfur emission from pyrolysis of seven Chinese coals, using a TPD-FPD method under both nitrogen and hydrogen atmospheres, is presented. The results are useful in understanding of thermal selectivity in cleavage of C-S and C-C bonds and sulfur emission from different organic matrix.

Experimental

Seven Chinese coals were used. All the samples were ground to less than 0.25mm before use. Ultimate and sulfur-form analyses of the coals are shown in Table 1.

Table 1. Ultimate and Sulfur-form analyses of sample coals

Samples	Ultimate (wt%, daf)					Sulfur-form (wt%, total)		
	C	H	O (diff.)	N	S	pyritic	sulfate	organic
YM	80.18	4.32	12.29	0.86	2.35	77.72	0.00	22.28
PSH	81.32	5.40	11.00	1.57	0.71	76.79	0.00	23.21
YZ	81.35	5.19	8.30	1.21	3.95	65.70	2.03	32.27
DT	82.76	5.07	8.93	0.82	2.42	64.18	2.99	32.83
SHH	78.60	4.95	14.61	1.13	0.71	6.15	0.00	93.85
QJ	62.19	5.67	30.25	1.47	0.42	0.00	5.56	94.44
HLH	76.57	4.59	16.60	1.51	0.73	3.70	0.00	96.30

Temperature programmed decomposition with on line FPD analysis for gaseous sulfur, TPD-FPD, was used. Detailed setup was shown elsewhere [3]. About 5 mg coal sample was heated from 25 to 800°C at a rate of 5°C/min. Hydrogen or nitrogen was used as the

carrier gas at a flow rate of 120ml/min to constitute different atmosphere. The FPD was operated at 150°C, and the combustion gases were made up of 60ml/min H₂ and 50ml/min air.

Results and Discussion

According to the sulfur-form distributions in the coal samples listed in Table 1, the coals are categorized into three groups. The first group contains YM and PSH coals, in which the pyritic sulfur contents are dominant (more than 75%) and the sulfate sulfur content is zero. The second group includes YZ and DT coals which contain a less pyritic sulfur than that of the first group (about 65%). The third group, SHH, QJ and HLH coals, has low sulfur content and the sulfur are mainly in organic states (more than 90%).

Figure 1 shows dynamic evolution profiles of total gaseous sulfur from the first group of the coals during pyrolysis in H₂ and N₂. Although YM coal and PSH coal have similar sulfur-form distributions, the sulfur evolution profiles are very different from each other. YM coal (a) shows three evolution peaks at around 410, 510, and 550°C, and H₂ significantly enhances all the three peaks. PSH coal in N₂ (b) shows only one sharp peak at around 520°C, and possibly a weak peak at around 430°C. H₂ significantly suppresses the peak at 520°C, but slightly promotes the peak at 430°C, and possibly generates a flat peak at temperatures greater than 550°C.

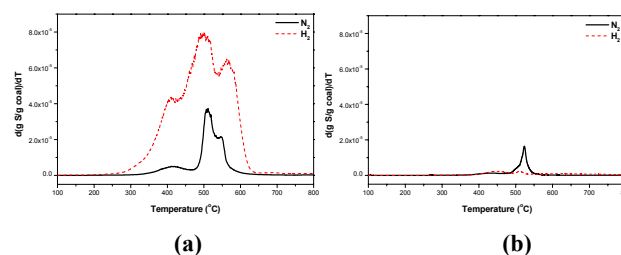


Figure 1. Dynamic gaseous sulfur evolution profiles from the first group of the coals during pyrolysis: (a) YM coal, (b) PSH coal.

The profiles of sulfur evolution from the second group of the coals are shown in Figure 2. YZ coal (a) shows three sulfur evolution peaks at around 400, 530 and 580°C in N₂, and H₂ significantly depresses the sulfur release at above 500°C. DT coal shows one prominent peak at around 505°C in N₂, but only a number of weak peaks in H₂, indicating strong suppression effect on sulfur release at 500°C and promotive effect at around 460°C and at temperatures greater than 600°C by H₂. Overall, H₂ shows negative effect on gaseous sulfur evolution for these two coals.

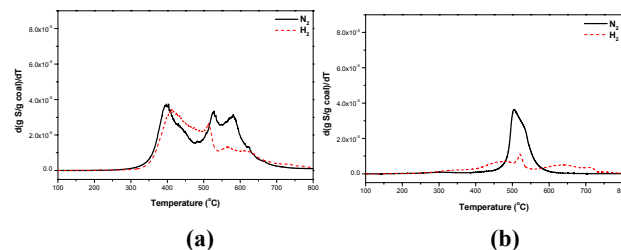


Figure 2. Dynamic gaseous sulfur evolution profiles from the second group of the coals during pyrolysis: (a) YZ coal; (b) DT coal.

Figure 3 shows dynamic evolutions profiles of gaseous sulfur from the third group of the coals in pyrolysis. The peaks in this figure are all small due to small sulfur contents in these coals. SHH coal (a) shows one obvious peak at around 520°C in N₂. H₂ depresses the

520°C peak, but yields small new peaks at lower and higher temperatures, 450°C and 650°C, which is similar to that of DT coal and PSH coal. Both HLH and QJ coals show one main peak in N₂, at 405°C and 350 °C, respectively, and H₂ promotes these peak and yields new peaks at the high temperature ends, 505 and 570°C for HLH, and 475 and 525°C for QJ. In these cases, H₂ has a little negative effect on gaseous sulfur release on SHH coal and positive effect on HLH and QJ coals.

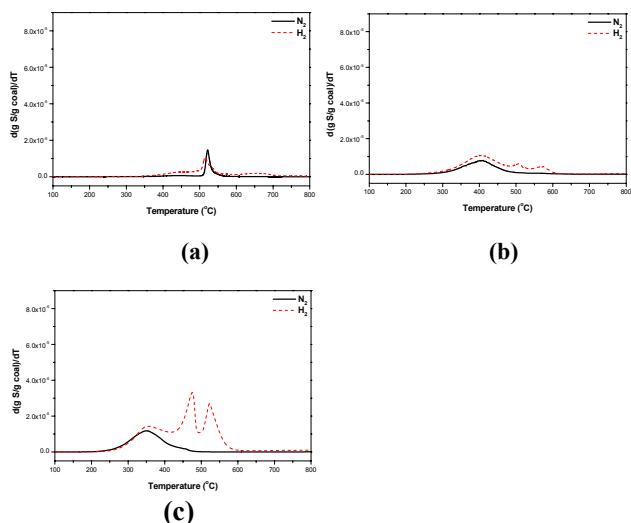


Figure 3. Dynamic gaseous sulfur evolution from the third group of the coals during pyrolysis: (a) SHH coal; (b) HLH coal; (c) QJ coal.

Clearly, H₂ has very different effects on gaseous sulfur evolution in pyrolysis from the coals, promoting certain kinds of sulfur release and suppressing other kinds of sulfur release. This phenomenon is different from the general belief that H₂ always promotes sulfur release from the coal compared to N₂. It is very likely that these H₂ effects are related to the physical and chemical states of sulfur in the coals, as well as to the interactions of sulfur with the components of the coals, in their original forms or as intermediate products migrating in the coal matrix during pyrolysis.

It is generally accepted that sulfur in coal stays in organic and inorganic forms, and pyrite is often the dominant form of inorganic sulfur. H₂ accelerates the decomposition of pure pyrite resulting in increased H₂S release. The decomposition of pyrite in coal are different from and more complex than that of pure pyrite. The pyrite in coal generally begins to decompose at about 500°C during pyrolysis [2]. For the coals in the first and the second groups, more than 64% of the sulfur are pyritic, the peaks between 500-550°C are most probably resulted from decomposition of pyrite, although the contribution of organic sulfur decomposition may be overlapped. The peaks at temperatures below 500°C and higher than 550°C are probably mainly from the decomposition of organic sulfurs. However, H₂ promotes the sulfur release for YM coal, but suppresses the sulfur release for PSH, YZ and DT coals, especially at temperatures between 500-550°C. Clearly, these phenomena can not be explained solely by the decomposition of pyrite, and may be related to the interactions of pyritic sulfur or H₂S, generated from decomposition of pyrite, with other components of coal. It was reported [4] that pyrite finely distributed in coals as tiny particles, or entrapped in coal matrix structure, or specially bonded with coal matrix, would result in significant secondary reactions in pyrolysis, which would reduce H₂S release and generate sulfur-containing structures of higher thermal

stability[5, 6]. But further increase in temperature may decompose the newly formed sulfur-containing structures and release the sulfur into the gas phase. H₂ may promote the formation of both H₂S and the sulfur-containing structures in pyrolysis. The information presented in Figures 1(b) and 2 seems to suggest that the H₂ promotion on the formation of sulfur-containing structure is much stronger than that on H₂S formation due to suppressed sulfur release from pyrolysis of pyrite, at least in the cases studied. It is important to note, however, that the overall peak areas in H₂ in Figures 1(b) and 2 are much smaller than that in N₂. This may suggest that the newly formed sulfur-containing structures in the secondary reaction are mainly in the form of tar, which leave the reactor as the volatile phase and do not have a chance to experience higher temperatures. This hypothesis needs to be verified by tar and char analysis for sulfur content.

The coals in the third group, SHH, HLH and QJ, all have very high organic sulfur contents, greater than 93%. Therefore, most of the peaks in Figure 3 are resulted from the decomposition of organic sulfur. The promotive effect of H₂ may suggest increased cleavage of S-C bonds in H₂, especially in the high temperature range.

It is well accepted that pyrolysis of coal follows the radical mechanism. The coal undergo thermal cracking at elevated temperatures to generate radicals of different sizes, small and large. The large radicals tend to further crack. All the radicals are reactive and tend to recombine to form relatively stable compounds. The effect of H₂ on the gaseous sulfur evolution may also follow the radical mechanism. Stabilizing small sulfur-containing radicals by H₂ may result in increased gaseous sulfur evolution. Stabilizing large sulfur-containing radicals by H₂, on the other hand, may result in increased sulfur-containing tars and/or increased sulfur-containing chars. The formed sulfur-containing chars may undergo further pyrolysis at higher temperatures to evolve volatile sulfur-containing compounds.

Conclusions

Dynamic behavior of total gaseous sulfur evolution from pyrolysis of seven Chinese coals show complex H₂ effects, promotion of some peaks, suppression of other peaks, generation of new peaks especially at higher temperatures. These behavior can be explained by promotive effect of H₂ on pyrite decomposition, by secondary reactions between the products of pyrite decomposition and the matrix structures of coal, and by the radical mechanism. The negative effect of H₂ on gaseous sulfur release may correspond to increased sulfur in tars. H₂ promotes the formation of gaseous sulfur from organic sulfur in the coals during pyrolysis.

Acknowledgement. The project is subsidised by the Special Funds for Major State Basic Research Project (G19990221), the Chinese Academy of Sciences, and the Natural Science Foundation of China (29725614, 20076050, and 20076049) and the State Key Laboratory of Coal Conversion.

References

- (1) Andrzej Czaplicki; Wojciech Smolka. *J. Fuel Processing Technology*, **1998**, 55, 1-11.
- (2) Amir Attar. *J. Fuel*, **1978**, 57(4), 201-212.
- (3) Xu Long; Li Yunmei; Yang Jianli and Liu Zhenyu. *M. 7th Chinese-Japanese Coal Chemistry and C₁ Chemistry*, Hainan, China, **2001**; pp 259.
- (4) Baruah, M. K.; Gogoi, P. C. *J. Fuel*, **1998**, 77(9/10), 979-985.
- (5) Chen Hao-kan; Li Bao-qing; Yang Ji-li. *J. Fuel*, **1998**, 77(6), 487-493.
- (6) Jose, V. I.; Jose, M. P.; Rafael, M. and Ana, J. B. *J. Fuel*, **1994**, 73(7), 1046-1050.

DESULFURIZATION OF COAL WITH PYROLYSIS IN DIFFERENT ATMOSPHERE

Haoquan Hu*, Xiaodan Wu, Shengwei Zhu

Institute of Coal Chemical Engineering, Dalian University of Technology, 129 street, Dalian 116012, P.R. China
*hhu@chem.dlut.edu.cn

Introduction

The release of sulfur during the utilization of coal, especially the pollution caused by coal burning has attracted more and more attention. Therefore, how to remove the sulfur from coal economically and efficiently becomes more and more important and necessary for coal utilization. So far, there have been many physical, chemical and microbial desulfurization methods studied^[1], among those coal pyrolysis desulfurization is one of relatively simple and effective one, especially hydrolysis^[2] which has made a high sulfur removal. However, since many complicated second reactions would occur during coal pyrolysis, especially the formation of some steady thiophenic sulfur^[4] such as the reaction of pyrite and hydrocarbon compound, the organic matters in coal and hydrogen sulfide which produced during pyrolysis, and the sulfur retained by mineral in coal etc.; all those would lead to an undesirable sulfur removal and constitute a main problem in coal pyrolysis desulfurization as a result.

A new and effective way is to add some trapping materials which can react with hydrogen sulfide to form metastable sulfur compound and consequently avoid its reacting back with coal. Attar^[5] has found that ethylene can react with hydrogen sulfide at 370–430°C, and achieved a better desulfurization result by using pure ethylene as reactive gas for Illinois No.6 bituminous high sulfur coal in pressurized pyrolysis at low temperature. Liu et al also used ethanol as additives in coal pyrolysis desulfurization^[3]. In this paper, coal pyrolysis both in isothermal and non-isothermal manner was carried out by using nitrogen and a mixed gas of nitrogen and ethylene (MG) at atmospheric pressure to investigate the effect of ethylene on sulfur removal during pyrolysis.

Experimental

Huoligele lignite with a particle size -100 mesh was used in this study. The analysis results were listed in **Table 1**. The sulfur in the coal exists in 48% pyrite and 52% organic sulfur.

Table 1 Analysis of Huoligele lignite

Approximate analysis (wt%)			Ultimate analysis (wt%daf)				
M _{ad}	A _d	V _{daf}	C	H	N	O*	S
19.37	24.41	47.33	75.84	5.73	1.28	16.43	0.72

* by difference

Pyrolysis was performed in thermogravimetric analyzer (TGA/SDTA 851^c) at atmospheric pressure. The sample weight is

about 20 to 25mg. In non-isothermal experiment, coal was pyrolyzed from room temperature upto end temperature of 400°C, 450°C, 500°C, 550°C, 600°C, 650°C and 700°C, respectively, at heating rate of 5°C/min, then retained at that temperature for 20 min. while in isothermal experiment, the sample was heated from room temperature upto the required end temperature in about 1 to 2 minutes. The gas flow rate is 30ml/min when pure nitrogen was used, and 30ml/min nitrogen and 6ml/min ethylene when MG was used.

The sulfur removal (r_s) was calculated from the expression:

$$r_s(\%) = (S_{\text{char}} - S_{\text{coal}}) / S_{\text{coal}}$$

where S_{coal} : sulfur content in coal; S_{char} : sulfur content in char

Results and Discussion

Comparison of sulfur removal **Figure 1** shows the sulfur removal at different temperature with two gases in isothermal pyrolysis. It can be seen that the desulfurization result under MG is better than that under pure nitrogen at 400°C, while at the other temperatures there is nearly no difference under both atmosphere. The better sulfur removal at 400°C can be attributed to the reaction between ethylene and hydrogen sulfide released during the coal pyrolysis^[2], which can compete with the reactions between hydrogen sulfide and coal to hinder hydrogen sulfide from reacting back with coal and consequently gave rise to the removal of sulfur under MG. Since the reaction can only occur at 370–430°C, the trapping effect of ethylene for hydrogen sulfide can't work with the desulfurization at other temperatures.

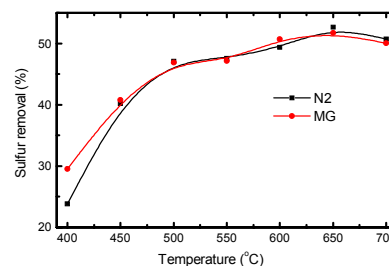


Figure 1 Sulfur removal in isothermal pyrolysis of coal

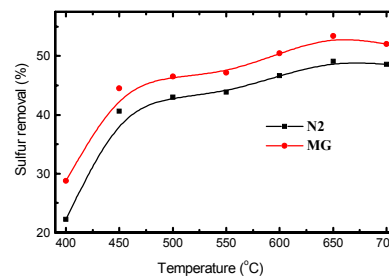


Figure 2 Sulfur removal in nonisothermal pyrolysis

The sulfur removal in nonisothermal pyrolysis was shown in **Figure 2**. Compared with the pure nitrogen pyrolysis, the sulfur removal under

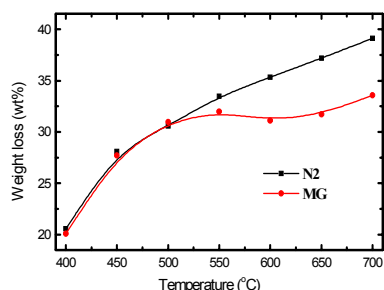


Figure 3 Final weight loss at different end temperature in isothermal pyrolysis

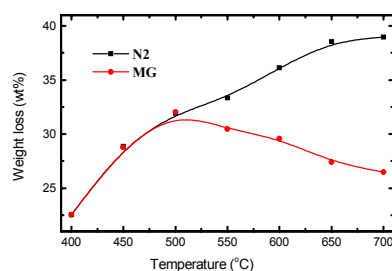


Figure 4 Final weight loss at different end temperature in non-isothermal pyrolysis

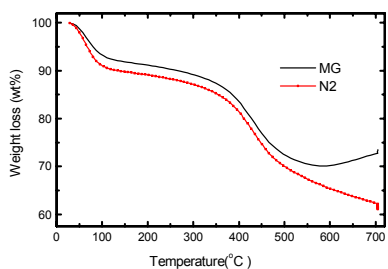


Figure 5 TG curve of Huolingele lignite pyrolysis in nitrogen and MG (25°C to 700°C at 5°C/min and with a 20min residence time at 700°C)

MG increased in the whole temperature range by 6.55% at 400°C and 4.00% or so at other temperatures. It may be explained that the nonisothermal pyrolysis at each final temperature can provide enough time for ethylene to trap hydrogen sulfide at proper temperature range (370-430°C) since the heating rate (5°C/min) is slow, and the additional 20 min residence time at proper temperature range (about 400°C) lead to the best sulfur removal in pyrolysis.

Comparison of weight loss **Figure 3** and **Figure 4** show the final weight loss of coal pyrolysis at different end temperature. It can be seen that before roughly 500°C the weight loss under two said gases is similar in both isothermal and nonisothermal pyrolysis, and after 500°C, MG made a lower weight loss than pure nitrogen. Combining with the TG curve shown in **Figure 5**, where the coal weight increased under MG instead of decreased under nitrogen with increase of temperature after about 500°C. This means that at high temperature ethylene may react with coal and/or pyrolysis to deposit heavy pyrolysis products on coal. The TGA of quartzite with MG under the same condition as that in **Figure 5** suggested that there is no increment in weight after 500°C at all, which means there was no deposition of ethylene pyrolysis products on quartzite. According to the property of the double bond of ethylene, it is possible that an extra reaction between ethylene and coal would occur, and this reaction made no effect on sulfur removal according to the results of **Figure 1** and **Figure 2**.

Correspondingly, the greater difference of weight loss between pure nitrogen and MG in nonisothermal pyrolysis (**Figure 4**) compared with the isothermal pyrolysis (**Figure 3**) may be attributed to the longer pyrolysis time which provide a longer reaction time between ethylene and coal.

Conclusion

A better sulfur removal in Huolingele lignite pyrolysis can be achieved by adding ethylene to nitrogen flow at low temperature (400°C or so). Ethylene can avoid the sulfur retained in coal pyrolysis at low temperature. The lower weight loss of coal pyrolysis under MG at high temperature compared to that under nitrogen may be attributed to the reaction of ethylene with coal.

Acknowledgment. The work was supported by fund of the National Key Fundamental Research and Development Project of China (G1999022101)

Reference

- [1] Liu, Shengyu; Zhao, Yulan; Xue, Yongqiang; Wang, Jian; Wu, Guoqing, *Coal Conversion*, 1997, 20(2), 20-22.
- [2] Wang, Na, Li, Wen; Li, Baoqing; *Journal of Fuel Chemistry and Technology*, 2001, 29(1), 29-32
- [3] Yu, Long; Yang, Jianli; Li, Yunmei, *ACS Fuel chemistry division preprints*, 2002, 47(1), 200
- [4] Attar, A., *Chemistry, Thermodynamics and Kinetics of Reactions of Sulphur in Coal-Gas Reactions: A Review*. *Fuel*, 1978, 57(4): 201-212
- [5] Attar, A., USP 4,465,493. August 14, 1984

DESULFURIZATION OF COAL THROUGH PYROLYSIS IN A FLUIDIZED-BED REACTOR

Yongqin Qi, Wen Li, Haokan Chen and Baoqing Li

State Key Lab of Coal Conversion, Institute of Coal Chemistry, Chinese Academy of Sciences, Taiyuan, Shanxi, 030001, China

Introduction

Sulfur in coal has greatly limited its utilization and much attention has been paid to the air pollution caused by combustion of coal in recent years. Sulfur removal is one of the most important problems in coal utilization. So far many methods have been developed to either remove sulfur from the coal, or from the flue gas. Among these methods, pyrolysis, an intermediate stage in various conversion processes such as liquefaction, gasification and combustion, is an important method of sulfur removal from coal prior to combustion because its cost is relatively low and can remove both inorganic and organic sulfur. The sulfur removal from coal through pyrolysis depends on many factors, such as coal rank, the quantity of sulfur and the sulfur forms distribution in the coal, the quantity and kind of mineral matter, the conditions in which the process is conducted. In this aspect, many important conclusions have been obtained, which are mainly based on studies in a fixed-bed reactor¹⁻⁴. In the present study, Yima (YM) and Datong(DT) coal were pyrolyzed in a fluidized-bed reactor in inert atmosphere to examine the sulfur removal efficiency.

Experimental

Coal samples

Raw coal with 0.15-0.25mm was washed by HCl / HF to remove minerals. Demineralized coals were further washed by CrCl₂ in order to remove pyrite. Table 1 and Table 2 show proximate, ultimate and sulfur form analysis of the samples.

Table 1 Proximate and ultimate analysis of samples w/%

Samples	M _{ad}	A _d	V _{daf}	C _{daf}	H _{daf}	N _{daf}	S _{daf}
YM	8.82	17.3	40.1	78.1	3.90	0.86	0.60
YM-ash	3.31	2.86	37.7	74.7	5.29	0.85	0.51
YM-p	2.38	1.45	37.6	73.6	5.18	0.81	0.61
DT	3.56	7.93	36.5	82.8	4.88	1.02	0.40
DT-ash	2.16	0.91	28.6	83.3	4.55	0.58	0.37
DT-p	2.51	0.65	28.4	83.4	4.59	0.69	0.38

Table 2 Analysis results of sulfur forms in samples w / %

Samples	S _{t,ad}	S _{s,ad}	S _{p,ad}	S _{o,ad}
YM	1.95	1.42	0.08	0.45
YM-ash	2.08	1.60	0.0	0.48
YM-p	0.59	0.0	0.0	0.59
DT	1.04	0.06	0.62	0.36
DT-ash	1.08	0.01	0.71	0.36
DT-p	0.37	0.0	0.0	0.37

YM-ash, DT-ash: demineralized coal

YM-p, DT-p: demineralized and de-pyrite coal

Pyrolysis

Pyrolysis was conducted in a quartz tube reactor (i.d 50mm) in nitrogen. There is a sintered quartz disk in the middle of tube to support coal, which can also be used as gas distributor. Pyrolytic temperature ranged from 500°C to 900°C and residence time was 30 minutes. The flow of fluidized-gas was from 0.15 to 0.21 m³/h. 20g of coal was fed into the reactor at 5g/min after the desired temperature was reached. The char was collected and weighed after temperature naturally dropped to ambient temperature. Sulfur removal (SR) was calculated according to the following equation:

$$SR\% = \frac{St, coal - St, char \times Yield}{St, coal} \times 100$$

Results and discussion

1. Effect of coal type on sulfur removal

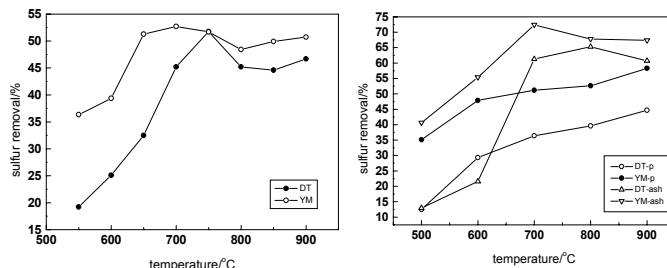


Figure 1 Sulfur removal as a function of temperature

Figure 1(a) shows the change of sulfur removal with temperature. YM is a lower rank coal compared with DT, hence YM is more active during pyrolysis than DT coal due to its low aromaticity. YM coal has a higher desulfurization than DT coal which reaches maximum desulfurization yield at relatively higher temperature. From demineralized and de-pyrite coal (**Figure 1(b)**), we can get the same conclusion. This proves that coal rank has effect on sulfur removal. At the earlier stage of pyrolysis, desulfurization has remarkable increase because decomposition of pyrite and thermally labile organic sulfur play an important role. The desulfurization decreases starting from 700°C for YM coal and 750°C for DT coal. According to a previous study⁵, sulfur fixation by alkaline-earth mineral begins at 700°C, which leads to increase of sulfur in char. On the other hand, high temperature leads to collapse of the pore structure, which inhibits further release of sulfur⁶. Moreover, the desulfurization tends to be constant between 800°C and 900°C because stable organic sulfur is difficult to be removed and sulfide sulfur can not further decompose. Hence there is an optimal temperature for maximum desulfurization and varies with coal rank.

2. Effect of mineral on sulfur removal

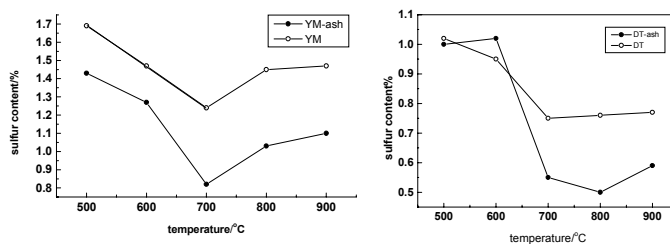


Figure 2 Sulfur content in char of demineralized coal vs temperature

Figure 2 indicates that sulfur content in char of demineralized coal first decreases to lowest value at 700°C, and then increases slightly for DT and evidently for YM. There is 10.42% and 1.69% CaO in the ash of YM and DT. The sulfur retention by CaO is contributed to the sulfur increase for raw coal. The transformation of inorganic sulfur to organic sulfur is responsible for the sulfur increase in the demineralized coal, mainly the transformation of pyrite to stable organic sulfur due to the influence of indigenous hydrogen and oxygen⁷. The Sulfation product by CaO will turn into sulphate during combustion and will not cause pollution.

3. Organic sulfur removal through pyrolysis

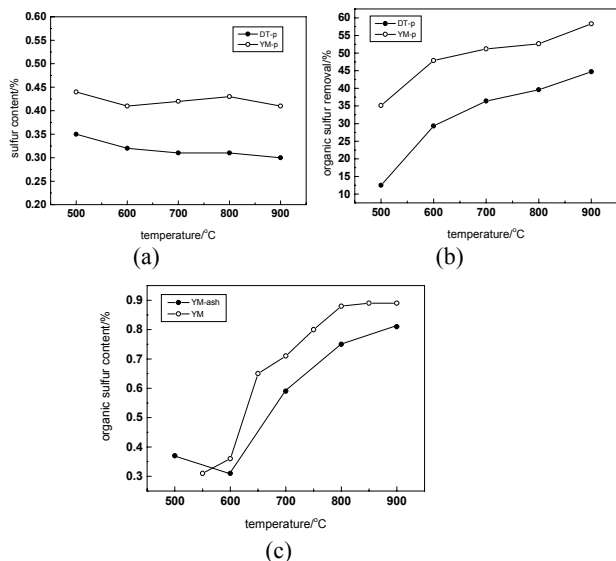


Figure 3 Organic sulfur removal vs temperature

Organic sulfur content in char has no apparent variation according to **Figure 3(a)**. However, yield of char decreases with increasing temperature, hence in fact part of organic sulfur is removed through pyrolysis as shown in **Figure 3(b)**. According to our AP-TPR study, there is more aliphatic sulfur in YM and more thiophenes in DT, which results in the high organic sulfur removal for YM. **Figure 3(c)** shows organic sulfur content in char through pyrolysis of YM raw and demineralized coal. It shows that organic sulfur tends to accumulate in char with increasing temperature. Attar⁸ believes that pyrolysis of sulfur compounds is the decomposition of C-S bond to free radicals R^{\bullet} and RS^{\bullet} . In pyrolysis, other hydrocarbon molecules supply the hydrogen to stabilize the radicals, but at high temperature there is no enough hydrogen and the radicals may transform into stable organic sulfur. In addition, lack of indigenous hydrogen may also leads to the transformation of pyritic sulfur into organic sulfur⁷. Cernic-Simic believes that sulfide contributes to increase of organic sulfur⁹. Therefore, alkaline-earth mineral leads to organic sulfur increase to some extent in raw YM. Organic sulfur in the char of YM-ash still accumulates with increasing temperature, clearly sulfide is not the main reason here. Contrasting **Figure 3(c)** with (a), we deduce that the interaction of pyrite with the organic matrix of coal plays an important role in organic sulfur accumulation in char.

4. Effect of residence time on sulfur removal

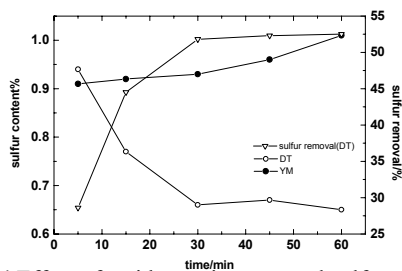


Figure 4 Effect of residence time on total sulfur content of char

The effect of residence time on desulfurization is examined at the temperature for maximum desulfurization. For YM coal the sulfur content in char varies little with time and yield of char is almost not changed at the same temperature. Hence longer residence time has no

enhancement effect on sulfur removal for YM coal. However, sulfur content in char of DT coal decreases with increasing time during the first 30 minutes, which leads to increase of sulfur removal. This indicates that DT coal is less active than YM coal to some extent. Therefore, sulfur is difficult to release rapidly in DT coal. However, when most of labile sulfur has released after a period of time, stable sulfur can not decompose and sulfur content in char has little change. Hence for different coal, there is also optimal residence time for maximum desulfurization.

Conclusions

- 1 There is optimal temperature and residence time for maximum desulfurization, varying with type of coal.
- 2 The alkaline-earth mineral in the raw coal plays an important role for the fixation of sulfur and makes desulfurization decrease.
- 3 The interaction of pyrite with the organic matrix of coal is the main reason that leads to organic sulfur accumulation in char.

Acknowledgment

Financial support for this work by the Special Funds for Major State Basic Research Projects (Contact NO. G1999022102) is gratefully acknowledged.

References

- 1 Sugawara, K., Tozuko, Y., Sugawara, T., Nishiyama, Y., Fuel Processing Technology. 1994, **37**, p. 73-85.
- 2 Ibarra, J., Bonet, A., Moliner, R., Fuel. 1994, **73** (6), p. 933-939.
- 3 Gryglewicz, G., Fuel Processing Technology. 1996, **46**, p. 216-226.
- 4 Gryglewicz, G., Fuel. 1995, **74** (3), p. 356-361.
- 5 Gryglewicz, G., Jasienko, S., Fuel. 1992, **71** (11), p. 1225-1229.
- 6 Lin, L., Khang, S. R., Keener, T. C., Fuel Processing Technology. 1997, **53**, p. 15-29.
- 7 Chen, H. K., Li, B. Q., Zhang, B. J., Fuel. 2000, **79**(13), p. 1627-1631.
- 8 Attar, A., Fuel. 1978, **57** (4), p. 201-213.
- 9 Cernic-Simic S., Fuel. 1962, **41** (2), p. 141-151.

ZINC FERRITE AND RELATED SORBENTS FOR HOT GAS DESULFURIZATION PROCESS

Michihiro Ishimori,* Takashi Inaba,** and Masafumi Katsuta**

*Advanced Research Institute for Science and Engineering
Waseda University

**Department of Mechanical Engineering
Waseda University
3-4-1 Okubo, Shinjuku-ku, Tokyo
169-8555 Japan

Introduction

Recently global environment issues have been raised worldwide. In relation with CO₂ emission which may lead to climate change, development of the highly efficient coal thermal technology is considered to be increasingly of importance. Integrated Coal Gasification Combined Cycle (IGCC) has been recognized as the most promising coal gasification power generation technology and large scale power plants are currently operated in the United States and in Europe, although thermal efficiencies are not yet so high. In Japan a national project of the 200t/d IGCC pilot plant was carried out at Nakoso from 1986 to 1996. The targets of this project were developments of the air-blown pressurized entrained-flow gasifier, hot-gas cleanup systems, and a gas turbine for low Btu coal gas, where 3 types of hot-gas desulfurization systems were tested by using iron oxide (Fe₂O₃/Fe₃O₄) sorbents.^{1,2}

In order to realize the highly effective coal gasification power plants, development of hot-gas cleanup system, especially highly efficient desulfurization technology for hot coal gas is required. We have studied zinc ferrite and related compounds as sorbents for hot reductive gas produced by an entrained-flow gasifier, with consideration of the results of desulfurization operations at Nakoso pilot plant. The characteristics of zinc ferrite and related systems were investigated in terms of sorbents for hot-gas desulfurization process using simple reductive gas involving reductive sulfur substance represented by H₂S, as described hereafter.

Experimental

Sorbents. Zinc ferrite and related sorbents were prepared as follows. A mixed solution of zinc nitrate (1.5 mol/l, 50 ml) and iron nitrate (III) (1.5 mol/l, 100 ml) was stirred in a flask in the presence of colloidal silica. Then ammonia aqueous solution was added to this solution. The precipitates obtained from the solution (pH 7-8) were washed with water after filtration, dried at 120 °C and calcined at 800°C for 5h. ZnFe₂O₄-SiO₂ sorbent thus obtained was confirmed by XRD analysis. ZnFe₂O₄-SiO₂-ZrO₂ or ZnFe₂O₄-SiO₂-TiO₂ sorbent was prepared by mixing ZnFe₂O₄-SiO₂ sorbent with ZrO₂ or with TiO₂ (anatase), and calcined at 500 °C for 1h. The composition of the sorbents was determined by the atomic ratio of component oxides using XRF (X-ray fluorescence system) and ICP (Inductively coupled plasma) methods.

Desulfurization. Sorbent performance test for desulfurization-regeneration (cycle of sulfidation and oxidation of sorbent) was carried out in a down flow fixed-bed reactor made of quartz under atmospheric pressure. The reductive gas for H₂S absorption test is composed of 20% of H₂, 1000 ppmv of H₂S, and N₂ (balance). The sorbent such as ZnFe₂O₄-SiO₂-ZrO₂ (or TiO₂) system was prepared by composition of 200 mg of ZnFe₂O₄-SiO₂ sorbent and 400 mg of ZrO₂ (or TiO₂). Analyses of the inlet gas and outlet gas from the reactor were carried out by gas chromatography using a thermal conductivity detector (TCD) and a flame photometric detector (FPD). The total gas flow rate was 100 ml/min (20°C, standard) by using mass flow controllers. Concentration of H₂S at the outlet of the

desulfurization reactor was determined by gas chromatography equipped with a flame photometric detector (FPD) with a sensitivity of 1 ppmv, where the outlet gas auto-sampling instrument was used. Regeneration of the sulfided sorbent was conducted by oxidation using 2% of oxygen and N₂ (balance) at 450°C.

The breakthrough curves were recorded with a closed measurement system, composed of a reactor equipped with Shimaden model DSM temperature control unit, Yanaco model GSH-263A gas auto-sampling instrument, Yanaco model G2800FPD gas chromatograph, and Simadzu model C-R8A Integrator.

Results and Discussion

ZnFe₂O₄-SiO₂-ZrO₂ sorbent. The following three sorbents systems of zinc ferrite and related mixed oxides were prepared: ZnFe₂O₄, ZnFe₂O₄-SiO₂, and ZnFe₂O₄-SiO₂-ZrO₂ sorbents.³ The desulfurization tests for the reductive gas by the above three sorbent systems were carried out at 450°C under atmospheric pressure, using a fixed-bed type reactor. The reductive gas for H₂S absorption test is a simplified simulation gas of the coal gas in composition assuming an air-blown entrained-flow gasification.

It was found that, as the results of desulfurization test of ZnFe₂O₄-SiO₂-ZrO₂ sorbent, concentration of H₂S involved in the reductive gas was decreased from 1000 ppmv to less than 1 ppmv. The activity of the sorbent was observed to be completely regenerated by oxidation, after sulfidation. Breakthrough curves of H₂S for ZnFe₂O₄-SiO₂-ZrO₂ system are shown in **Figure 1**. The feature of H₂S breakthrough curves is that all breakthrough profiles are almost identical, suggesting that deactivation of the sorbent during the absorption-regeneration cycles is negligible.

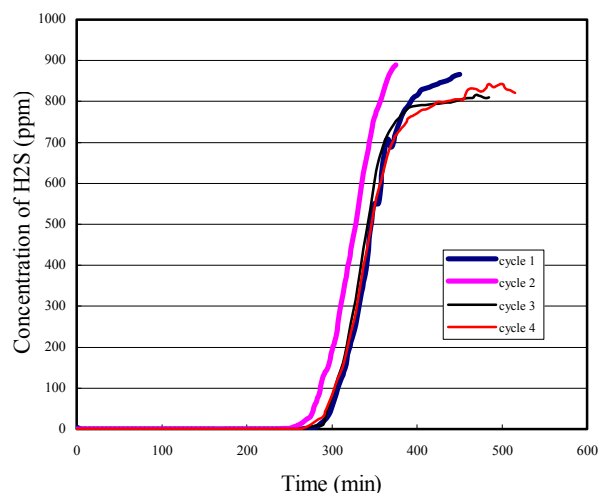


Figure 1. Breakthrough Curves of H₂S for ZnFe₂O₄-SiO₂-ZrO₂ system. (Concentration of H₂S: data at the outlet of the reactor).

On the other hand, desulfurization performance with ZnFe₂O₄ sorbent itself was found to be unfavorable; time length of high desulfurization (H₂S concentration of less than 1ppm) is very short, compared with ZnFe₂O₄-SiO₂-ZrO₂ sorbent. Another sorbent of ZnFe₂O₄-SiO₂ system showed high desulfurization performance similarly to ZnFe₂O₄-SiO₂-ZrO₂ sorbent at the first desulfurization test. However, performance of the regenerated sorbent obtained after the first desulfurization run, was extremely lowered. It might be thus indicated for the excellent performance of ZnFe₂O₄-SiO₂-ZrO₂ sorbent system that activity of ZnFe₂O₄ is promoted by SiO₂ and that activity of ZnFe₂O₄-SiO₂ species formed is structurally supported by

ZrO₂. In the course of studies, excess Fe₂O₃ present in the ZnFe₂O₄-SiO₂-ZrO₂ sorbent was not found to be unfavorable in desulfurization, whereas excess ZnO was observed to show deactivation effect on the sorbent performance.

ZnFe₂O₄-SiO₂-TiO₂ sorbent. Desulfurization tests for ZnFe₂O₄-SiO₂-TiO₂ system were carried out under similar reaction conditions described above. It was found that ZnFe₂O₄-SiO₂-TiO₂ sorbent is more favorable in comparison with ZnFe₂O₄-SiO₂-ZrO₂ sorbent from the aspect of time length of high desulfurization performance. Breakthrough curves of H₂S for ZnFe₂O₄-SiO₂-TiO₂ system are shown in **Figure 2**.

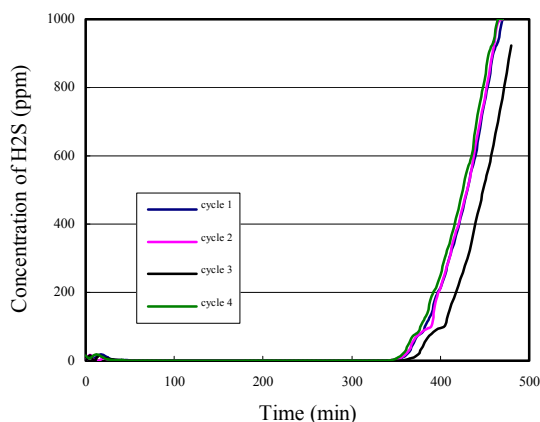


Figure 2. Breakthrough Curves of H₂S for ZnFe₂O₄-SiO₂-TiO₂ system. (Concentration of H₂S: data at the outlet of the reactor).

Amount of H₂S reacted with ZnFe₂O₄-SiO₂-TiO₂ sorbent was studied. The actual amount of reacted H₂S was experimentally determined by the integration using breakthrough curves of H₂S for ZnFe₂O₄-SiO₂-TiO₂ sorbent shown in **Figure 2**. Theoretical amount of H₂S reacted was calculated by the composition and quantity of sorbent used, assuming the equation (A); excess Fe₂O₃ (1 mol) was assumed to become FeS (2 mol) by reaction with H₂S.

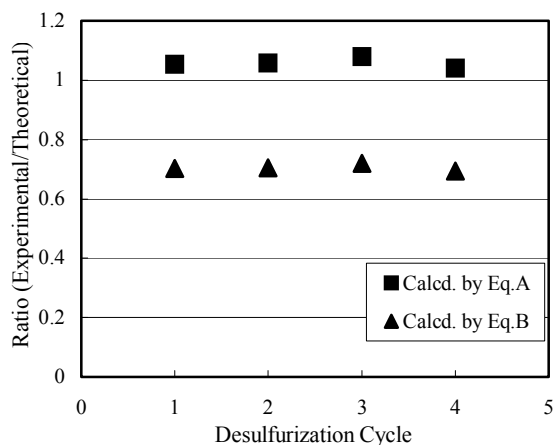
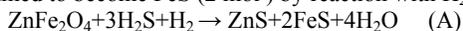


Figure 3. Temperature Effect on Breakthrough Curves of H₂S for ZnFe₂O₄-SiO₂-TiO₂ system.

The ratios of amount of H₂S reacted “Experimental/Theoretical” are shown in **Figure 3**. The desulfurization reaction is usually considered to proceed by equation (A). However, experimental value is higher than theoretical value, that is Experimental/Theoretical > 1. The results indicate that another type of reaction such as equation (B) also takes place; formation of Fe_{1-x}S and/or FeS₂ were confirmed by XRD analyses of sulfided sorbents, although quantitative data could not be obtained by this analytical method.

Desulfurization tests for ZnFe₂O₄-SiO₂-TiO₂ system were carried out at various temperatures. It was confirmed that highly effective desulfurization was observed in a broad range of temperatures at 600°C~250°C, as shown in **Figure 4**. The fact indicates the above system to be favorable sorbent for hot coal gas from gasifier, since temperature of such gas is variable with time due to deposition of coal ash on gas cooler (heat exchanger).

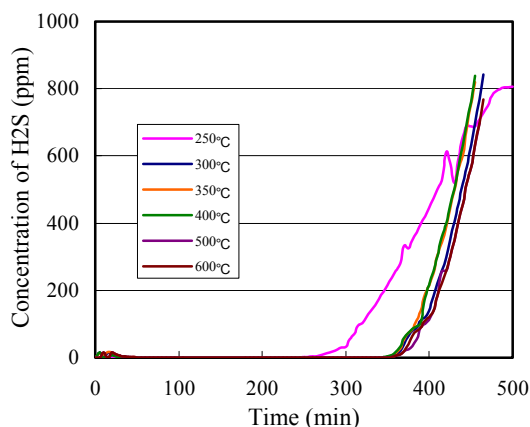


Figure 4. Temperature Effect on Breakthrough Curves of H₂S for ZnFe₂O₄-SiO₂-TiO₂ system. (Desulfurization: 250°C ~ 600°C).

Conclusion

The sorbents of ZnFe₂O₄-SiO₂-ZrO₂ and ZnFe₂O₄-SiO₂-TiO₂ systems prepared in this study were found to show excellent desulfurization performance; the sorbents are considered to be satisfactorily used for hot gas desulfurization process of advanced IGCC plant equipped with high temperature gas turbine, on the basis of the operation data of desulfurization processes of the hot gas cleanup system at Nakoso pilot plant. The sorbents will also be able to be adopted for the Integrated Coal Gasification Fuel Cell Combined Cycle (IGFC) having high temperature fuel cell technologies such as molten carbonate fuel cell (MCFC) to be developed in near future, where concentration of sulfur compounds of the fuel gas is required to be less than 1ppm.

Acknowledgment. This work was partially supported by the Ministry of education, Science, Japan, under contract of a grant-in-aid for priority areas.

References

1. Ishimori, M., Senshu, S., *Eighth Annual Conference on Coal Gasification*, Sponsored by EPRI (Electric Power Research Institute, U. S. A.), San Francisco, **1988**; *EPRI Proceedings GS-6485*, 15-1, **1989**.
2. Ishimori, M., *J. Japan Institute of Energy*, **1995**, 74, 673.
3. Ishimori, M., Katsuta, M., *The 18th Annual International Pittsburgh Coal Conference, Proceedings, Session33*, 39-03, Newcastle, Australia, **2001**

PREPARATION OF ZINC FERRITE IN THE PRESENCE OF CARBON MATERIAL AND ITS APPLICATION TO HOT-GAS CLEANING

Toshimitsu Suzuki, Na-oki Ikenaga, Hiro-aki Matsushima, and Yousuke Ohgaito

Department of Chemical Engineering, Kansai University
3-3-35 Yamate-cho, Suita, Osaka 564-8680, Japan

Introduction

Increasing attention is being paid to integrated gasification combined cycle (IGCC) process and gasification-molten carbonate fuel cell (MCFC) technology as one of the most promising technology to reduce CO₂ emission. For these technologies, several thousands ppm of hydrogen sulfide containing in an effluent gas from gasifier must be efficiently removed to several ppm for IGCC and <1 ppm for MCFC at a high temperature. Zinc ferrite (ZnFe₂O₄) is known to be one of the candidates for hydrogen sulfide removal^{1,2}. In addition to zinc ferrite, various sorbents, such as manganese oxides³ and zinc titanate⁴, have been investigated. We have recently found that activated carbon-supported ZnFe₂O₄ could be prepared at much lower calcination temperature required for dry process for ferrite synthesis and that its absorption capacity was much higher than that of dry process ferrite⁵.

In the present work, activated carbon-, activated carbon fiber-, and coal-supported zinc ferrite were prepared at a low temperature in order to obtain an effective absorbent for H₂S at a high temperature. Performance of absorption behavior of the prepared absorbent was evaluated using a fixed-bed flow type reactor. Regeneration of the used sorbent was investigated.

Experimental

Preparation of sorbent.

Homogeneous precipitation method. Into a mixed solution of Fe(NO₃)₃ and Zn(NO₃)₂ (150 mmol/L, 80 mL), 0.04 mmol of urea and 0.3 g of activated carbon (AC, Wako Pure Chemical Industries, Ltd., 100-mesh pass, 993 m²/g), activated carbon fiber (ACF, AD'ALL, Co., Ltd., 2000 m²/g), or Yallourn coal (YL, C 66.3; H 4.70; N 0.48; S 0.26 daf%; Ash 2.0 d%, 100-mesh pass) was added. The mixture was allowed to keep 90 °C for 2h. During this stage, Zn(OH)₂ and

Fe(OH)₃ were precipitated on AC, ACF, or YL coal. The mixture was dried at 70 °C in vacuo, and then it was calcined at 400 or 500 °C in air for 2h.

Coprecipitation method. A 0.3 g of AC or YL coal was added into a mixed solution of Fe(NO₃)₃ (20 mmol/L, 100 mL) and Zn(NO₃)₂ (10 mmol/L, 100 mL), and then into this suspension aqueous ammonia was added until pH of the suspending solution reaches 10. The combined precipitates were separated and dried in vacuo. The mixture was calcined at 300 or 500 °C in air for 2h.

Impregnation method. Zinc ferrite was prepared on AC or YL by the impregnation method described in the previous literature⁵.

Characterization of sorbents. The ferrite prepared here and the metal species obtained after the absorption of hydrogen sulfide were analyzed by powder X-ray diffraction using an X-ray diffractometer (Shimadzu XRD-6000) with monochromated CuKα radiation. The surface areas of activated carbon-loaded and unloaded ferrite were measured using a Micromeritics Gemini 2375, applying adsorption isotherms of nitrogen at -196 °C to the BET equation.

Breakthrough behavior of sorbents measured by a fixed-bed reactor. The breakthrough curves were obtained by using a fixed-bed flow type reactor according to the procedure that was described in the previous paper⁵.

Results and Discussion

Preparation and characterization of sorbents. Table 1 summarizes results of surface area and the content of oxides of various absorbents loaded on activated carbon, activated carbon fiber, and Yallourn coal char prepared by various methods. In the cases of ferrites loaded on organic support, oxide content in the total absorbent was evaluated based on the weight decreases of the samples, by burning the organic part by using a thermogravimetric balance in a flowing air. The surface areas of zinc ferrites prepared in the presence of ACF and AC (Samples D, F, and G) were higher than those zinc ferrites (Samples A, B, and C), which were prepared without carbon materials. The surface area of ZnFe₂O₄/ACF reached 1190 m²/g due to a large amount of remained high surface area ACF. Surface areas decreased to 50 m²/g with a decrease in the amount of carbon remaining (1-14 %). XRD analyses exhibited only diffraction peaks ascribed to ferrite phase after the calcinations in air at above 500 °C, with the exception of some cases. Samples E, F, and H showed very weak diffraction peaks ascribed to ZnO and Fe₂O₃, in addition to those of zinc ferrite.

Table 1 Surface area and oxide content of various sorbents

Sample	Sorbent	Method	Calcination temp. °C	Phase determined by XRD	S.A. m ² /g	Oxide content wt%	Absorption capacity % ^a
A	ZnFe ₂ O ₄	Dry process	1000	ZnFe ₂ O ₄	17	-	49
B	Fe ₂ O ₃	PPT	500	Fe ₂ O ₃	40	-	94
C	ZnFe ₂ O ₄	CoPPT	500	ZnFe ₂ O ₄	41	-	48
D	ZnFe ₂ O ₄	CoPPT	300	Amorphous	134	-	116
E	ZnFe ₂ O ₄ /ACF	HomoPPT	400	ZnFe ₂ O ₄ , ZnO, Fe ₂ O ₃	1190	10.7	145
F	ZnFe ₂ O ₄ /AC	HomoPPT	500	ZnFe ₂ O ₄ , ZnO, Fe ₂ O ₃	317	66.2	113
G	ZnFe ₂ O ₄ /AC	CoPPT	500	ZnFe ₂ O ₄	463	56.9	84
H	ZnFe ₂ O ₄ /AC	IMP	500	ZnFe ₂ O ₄ , ZnO, Fe ₂ O ₃	50	96.8	100
I	Fe ₂ O ₃ /AC	IMP	500	Fe ₂ O ₃	67	99.0	113
J	ZnFe ₂ O ₄ /YL	HomoPPT	500	ZnFe ₂ O ₄	51	93.1	98
K	ZnFe ₂ O ₄ /YL	CoPPT	500	ZnFe ₂ O ₄	58	95.5	97
L	ZnFe ₂ O ₄ /YL	IMP	500	ZnFe ₂ O ₄	50	86.0	90

a) Carried out using a fixed-bed reactor (N₂+H₂S(0.96 vol%) 5 mL/min, H₂ 2mL/min, Absorption temperature 500 °C)

PPT: Precipitation method, CoPPT: Coprecipitation method, HomoPPT: Homogeneous precipitation method, IMP: Impregnation method

Absorption behavior of hydrogen sulfide. Figure 1 shows examples of breakthrough behavior of H₂S using various sorbents measured at 500 °C. The horizontal axis of Figure 1 designates the absorption capacity, which was calculated assuming that all zinc and iron in the ferrite would be transformed into ZnS and FeS. The absorption capacity exceeded 100% because a part of the iron was transformed into FeS₂. The absorption capacity of each sorbent is shown in the last column of Table 1. The absorption capacities of hydrogen sulfide (48-49%) with unloaded zinc ferrite (Samples A and C) were lower than those (>85%) of loaded zinc ferrites. When Fe₂O₃ (Samples B and I) and ZnFe₂O₄ prepared by dry method (Sample A) were used for H₂S absorption, high concentrations of H₂S (<20 ppm) were observed until the breakthrough point. On the other hand, the absorption capacities of H₂S increased to nearly 100% or more with ZnFe₂O₄ prepared on AC, ACF, and YL coal (Samples E-L). These absorbents showed no H₂S leakage in the effluent gas (less than 1 ppm). Although the surface areas of Samples F and G were higher than those of Samples E and H-L, the absorption capacities did not change. This fact indicates that the surface area seems not to be an important factor for the high absorption capacity of H₂S.

To examine the effect of the absorption temperature on the absorption capacity of the sorbent, the absorption of H₂S was carried out with ZnFe₂O₄/YL at 400-700 °C. When hydrogen sulfide was absorbed at 400 °C and 450 °C, the absorption capacities were 116% and 120%, respectively, and then that slightly decreased to 103% with increasing the absorption temperature to 500 °C and 600 °C. An elevated absorption temperature (700 °C) decreased the absorption capacity to 63%, indicating that optimal temperature of H₂S removal with ZnFe₂O₄/YL is 400-600 °C.

In order to elucidate the effect of the calcination temperature of the sorbent on the absorption behavior of H₂S, the breakthrough curves of the YL coal-supported zinc ferrites were calcined at 500-800 °C were measured at absorption temperature of 500 °C. The absorption capacity of ZnFe₂O₄/YL gradually decreased with increasing the calcination temperature to 800 °C, indicating that crystallite size of ZnFe₂O₄ determined by XRD analyses increased. This result clearly indicates that a crystallite size of ZnFe₂O₄ seems to be important for the high absorption capacity of H₂S.

Regeneration and repeated use of sorbent. Regeneration and repeated use of sorbent for H₂S removal is crucial to practical use. In order to ascertain the possibility of regeneration of sorbent after the

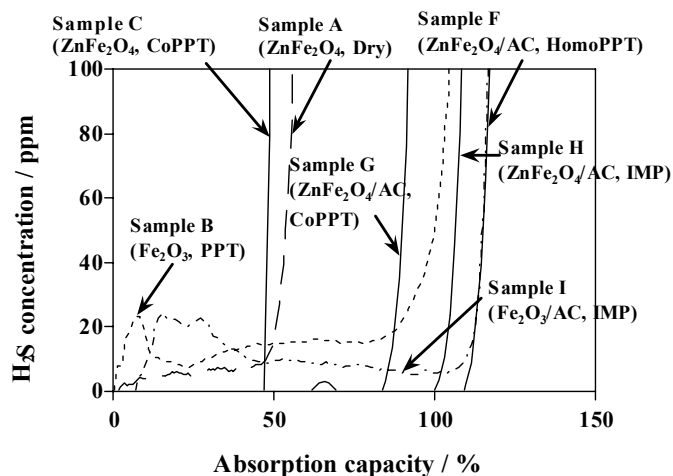


Figure 1 Breakthrough curves of H₂S absorption using various sorbents obtained at 500 °C. (Conditions: Ar 5 mL/min, N₂+H₂S 5 mL/min, H₂ 2 mL/min)

absorption reaction of H₂S, the temperature programmed oxidation of the H₂S absorbed ZnFe₂O₄/YL (ZnS, FeS₂, Fe_{1-x}S) was carried out using a mixed gas of Ar and O₂ (50vol%). The releases of SO₂ and SO₃ were confirmed with a mass spectroscopy from 350 to 530 °C. Regeneration of H₂S absorbed ZnFe₂O₄/YL was carried out at 450 °C for 30 min using the fixed-bed reactor in oxygen-argon gases (O₂: 50vol%, Ar: 50vol%). According to the XRD analyses of ZnFe₂O₄/YL before the H₂S absorption and after four sulfurization-regeneration cycles, ZnFe₂O₄/YL exhibited diffraction peaks ascribed to ZnFe₂O₄ and very weak diffraction peaks of ZnO and Fe₂O₃. YL coal or AC loaded ferrites could successfully be regenerated at 450 °C. YL coal was burned out during the regeneration at 450 °C in a flowing air and the amount of carbon material decreased to nearly nil. Figure 2 illustrates the breakthrough curves that were measured at 500 °C using regenerated zinc ferrite, after second (R-2), third (R-3), and fourth (R-4) regeneration cycles. The absorption capacity of hydrogen sulfide with the fresh sorbent was 90%, and repeated use of the sorbent slightly decreased the absorption capacity to 75%. However, H₂S concentration in the tail gas was kept very low values.

Conclusion

Zinc ferrites could be prepared on activated carbon, activated carbon fiber, and Yalourn coal. Performance of the zinc ferrite for H₂S absorption was evaluated using a fixed-bed flow type reactor. These absorbents efficiently remove H₂S at an absorption temperature of 500 °C. Coal-loaded zinc ferrite could be regenerated by air oxidation at 450 °C. The regenerated zinc ferrite can be used for repeated absorption of H₂S with a slight decrease in the absorption capacity.

Acknowledgment. This work was financially supported by a grant-in-aid for priority area (11218212) from the Ministry of Education, Science, Japan.

References

1. Pineda, M.; Palacios, J.M.; Alonso, L.; Garcia, E.; Moliner, R., *Fuel*, **2000**, 79, 885.
2. Alonso, L.; Palacios, J.M.; Garcia, E.; Moliner, R., *Fuel Process. Tech.* **2000**, 62, 31.
3. Slimane, R.B.; Abbasian, J., *Adv. Environ. Res.*, **2000**, 4, 147.
4. Ozdemir, S.; Bardakci, T., *Sep. Purif. Technol.*, **1999**, 16, 225.
5. Ikenaga, N.; Chiyoda, N.; Matsushima, H.; Suzuki, T., *Fuel*, **2002**, 81, 1569.

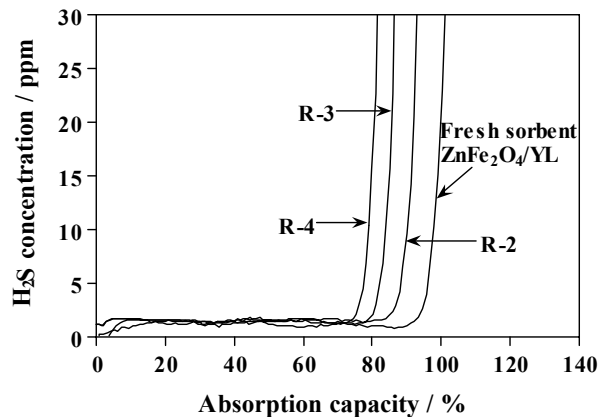


Figure 2 Breakthrough curves of H₂S absorption using ZnFe₂O₄/YL and regenerated

EXPERIMENTAL STUDY ON SO₂ REMOVAL IN O₂/CO₂ COAL COMBUSTION

Xiaoping ZHANG, Jianrong QIU, Xuwen DONG, Hong WANG,
Hao Liu

National Laboratory of Coal Combustion
Huazhong University of Science and Technology
Wuhan, Hubei 430074, P.R.China

Introduction

Coal combustion is the most main sources of CO₂, SO_x and NO_x emission. About 85% of CO₂, 90% of SO₂, 70% of NO_x in total pollutants are from coal combustion in China. SO₂ emission increased about 3 times over the past two decades in China. CO₂ and NO_x emission have also been increasing. Limestone desulfurization efficiency is very low although it is of low cost. O₂/CO₂ recycling combustion is a new coal combustion style developed in recent years¹⁻². This combustion style is expected to be one of promising systems on CO₂-recovery without the process of concentration from pulverized coal-fired power plants. In the system, pulverized coal is fired in a CO₂-based atmosphere. The combustion style use oxygen/recycled flue gas, CO₂ is used to institute the N₂ in combustion air. This style Increases the CO₂ concentration in the flue gas by eliminating N₂ in air. Up to 95% CO₂ in dry flue gas may be attained, therefore, nearly pure CO₂ for reuse or disposal. Meanwhile, a higher plant efficiency resulted from reducing of volume throughput (60-80%). Most importantly, this combustion style is possible to control CO₂, NO_x and SO₂ emission simultaneously³⁻⁴. However, the mechanism of SO₂ removal is not understood thus far.

The objective of this work is to demonstrate the feasibility of removal of SO₂ and NO_x in O₂/CO₂ coal combustion, to compare the emissions of SO₂ and NO_x under O₂/CO₂ and conventional combustion conditions with and without limestone injection, to explore the mechanism of SO₂ and NO_x removal under O₂/CO₂ conditions and finally find the relationship between the optimal SO₂ and NO_x removal efficiency and CO₂ concentration and temperature.

Experimental

Experimental Device. The experiments have been performed on a horizontal electric heating reactor and a drop tube furnace⁴.

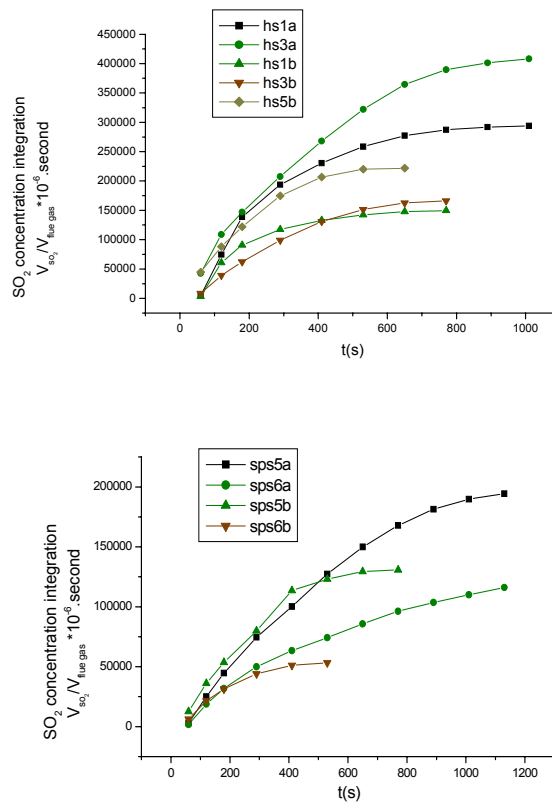
Coal Samples. In this experiment, two kinds of coal referred to as Hs and Sps with varying volatile matter and sulfur content were provided respectively. Proximate analysis was performed with a LECO MAC-500 by the standard procedure. Carbon, hydrogen and nitrogen were determined with a LECO CHN600 analyzer, and sulfur with a LECO SC-132 sulfur analyzer by the standard procedure. The fusion temperature at reducing atmosphere was measured by ash fusion temperature auto-analyzer (AF600) according to the GB219-74 standard. Chemical method was used to analyze the ash chemical composition. The analyses are shown in Table 1 and Table 2.

Table 1 Coal analysis data

Proximate analysis (%)					Ultimate analysis (%)			
Sample	W ^f	V ^f	A ^f	C ^f	C	H	N	S
Sps	2.5	10.60	18.0	68.8	72.0	2.12	0.90	2.56
Hs	4.8	18.23	41.7	35.2	36.6	2.22	0.76	5.51

Results and Discussions

The Effect of CO₂ on SO₂ Emission

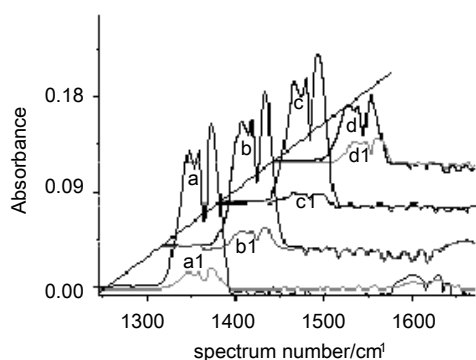


a: air; b: 21%O₂/79%CO₂
1: 700 °C, 3: 900 °C, 5: 1000 °C

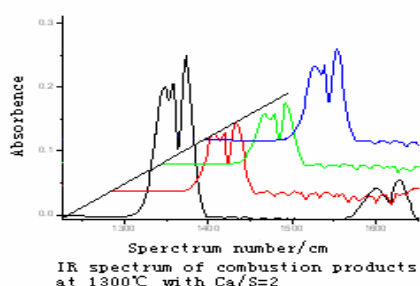
Figure 1. Total SO₂ emission as a function of time under different conditions

Figure 1 plots the SO₂ emission under air and O₂/CO₂ environment respectively at different temperature. Comparing with conventional air condition, the high CO₂ concentration significantly changed the SO₂ emission during coal combustion. For HS coal, the SO₂ emission in the exhausted gas in O₂/CO₂ condition is about 50% of that in O₂/N₂ condition at the temperature of 700 °C (hs1b compares with hs1a). As temperature increase, SO₂ emission increase, but the amplitude in O₂/CO₂ combustion style is lower than that in O₂/N₂ atmosphere. The SO₂ reduction is more notable in O₂/CO₂ combustion style at high temperature.

For SPS coal, the SO₂ emission in O₂/CO₂ condition is about 70% of that in O₂/N₂ condition at the temperature of 1000 °C. At the temperature of about 700~1100 °C, the SO₂ emission of all investigated coals under O₂/CO₂ are less than that under conventional air combustion.



(a) 800°C



(b) 1300°C

a: air; b: 20%O₂+15%CO₂+65%Ar;
c: 20%O₂+40%CO₂+40%Ar; d: 20%O₂+80%CO₂
1: Ca/s=2

Fig.2. FTIR spectrum of exhaust gas under different atmosphere

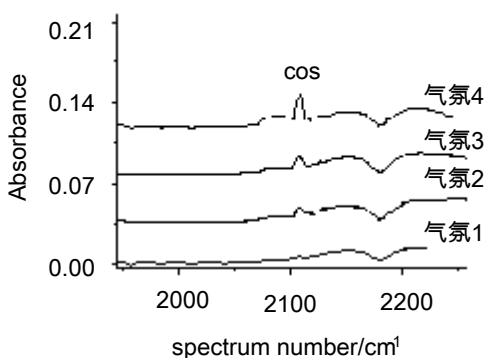


Fig.3 FTIR spectrum of COS in the flue gas under different atmospheres at 800°C

SO₂ emission spectrum under different atmosphere from 800--1300°C are shown in Figure 2. At low temperature, only high CO₂ concentration (curve d) can remove SO₂ emission effectively. However, at high temperature, the SO₂ emission has a remarkable reduction under CO₂ conditions.

The main reasons of SO₂ removal under high CO₂ condition are as follows: O₂/CO₂ environment lowers the overall combustion rate of coal char because thermal properties for gas mixtures of O₂/CO₂ and O₂/N₂ are different, which resulting in decrease of sulfur evolution. CO₂-C reaction which causing a reducing atmosphere and CO formation, which has a comparative contribution to decrease of SO₂ emission because of the part formation of H₂S and COS. Sulfur retention by coal ash is higher in O₂/CO₂ than in air environment because the presence of CO₂ changes the surface structure and increases the reactivity of alkaline matter. Furthermore, Presented CO₂ mitigates the sintering of CaO at high temperature and subsequent produce more reactive surface. The high limestone desulfurization efficiency is consequently resulted by high reactivity CaO reaction with SO₂ under CO₂ environment. Meanwhile, CO₂ inhibits the decomposition of CaSO₄ and improves the conversion ratio and consequently improved SO₂ removal efficiency.

Acknowledgment

This work is supported by the National Key Project for Fundamental Research, the Ministry of Science and Technology of China (G1999022204-07), and supported by the Teaching and Research Award Program of High Education Institution of China.

References

1. Wolsky A.M., A new method of CO₂ recovery. 79th Annual Meeting of the Air Pollution Control Association, Minneapolis, Minnesota, 1986, June 22-27, 1986.
2. Kimura N., Omata K., Kiga T., Takano S. and Shikisima S. The characteristics of pulverized coal combustion in O₂/CO₂ mixtures for CO₂ recovery. Energy Convers. Mgmt 1995, Vol.36, No.6, pp.805-808.
3. Yamada T, Kiga T., Okawa M., Omata K., Characteristics of Pulverized-Coal Combustion in CO₂-Recovery Power Plant Applied O₂/CO₂ Combustion, ICOPE-97, 1997, Vol.2, pp.285-290.
4. Jianrong Qiu, Bo Feng. SO_x Reduction Mechanism during O₂/CO₂ Recycling Combustion. Proceeding of the 2nd Korea-China Joint Workshop on Coal & Clean Energy Utilization Technology, 1998, pp. 71-82

Reactor Designed for Continuous Removal of SO₂ in Flue Gas over Pitch Based Activated Carbon Fibers

Kei Tada¹⁾, Takashi Enjoji¹⁾, Seoung-Ho Yoon¹⁾, Yozo Korai¹⁾,
Isao Mochida^{1)*}, Akinori Yasutake²⁾, and Masaki Yoshikawa³⁾

1) Institute of Advanced Material Study Kyushu University,
6-1 Kasuga-koen, Fukuoka 816-8580 JAPAN

*E-mail: mochida@cm.kyushu-u.ac.jp

2) Mitsubishi Heavy Industry Corporation
5-717-1 Fukahori-cho, Nagasaki 851-0392 JAPAN

E-mail: yasutake@ngsrdc.mhi.co.jp

3) Osaka Gas Company

Technology Coordination Office Research & Development Department
6-19-9 Torishima, Konoha-Ku, OSAKA 554-0051 JAPAN

E-mail: yoshikaw@osakagas.co.jp

Introduction

The present authors have proposed SO₂ removal over pitch based activated carbon fibers (ACFs) by recovering aq.H₂SO₄ at ambient temperatures according to the scheme¹⁻³⁾ illustrated in **Figure 1** with humidity of 5~10%. Heat-treatment of ACF at 1,100 °C was found to enhance its activity markedly by introducing more active sites. High concentration of H₂O and O₂ in the feed gas is favorable for SO_x fixation while NO inhibits the SO₂ removal.

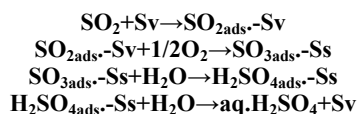


Figure 1. DeSO_x Scheme over ACF

In the present study, reactor for ACF packing was designed to enhance its activity by the same amount of the same ACF in order to reduce the reactor volume, ACF amount, H₂O and O₂ concentration necessary for the complete SO₂ removal at high temperature. The key concept for the reactor design is to recognize that the produced H₂SO₄ occupies the active site to reduce the activity of the ACF. Hence several types of reactors were designed to accelerate the elution of H₂SO₄ with its least contact to the ACF.

The reactors examined were

1. Reactor shape to change width vs length of ACF bed
2. Staged reactors for separation of produced H₂SO₄ at the stages

Experimental

An OG series active carbon fiber (OG-20A) was supplied by Osaka Gas Company. It was heat-treated in Ar gas at 1100°C for 1hr. OG20A-H1100 carried high surface area of 1500m²/g. SO₂ removal was carried out at 60°C. ACF was packed densely in the reactor tube. The flow rate was fixed at 100ml/min. Produced H₂SO₄ was trapped at the bottom of the reactor. Therefore, the concentrations of SO₂ in the inlet and outlet gases were analyzed continuously by a flame photometric detector (R268Y-Hamamatsu Photonics).

In **Figure 3** reactors were reference one (diameter 14mm) and wide one (diameter 16mm), respectively. Two reference reactors were arranged in parallel. The parallel reactor corresponded to the broaden one. H₂SO₄ produced in the first reactor was recovered before the second reactor located in sequence. Another type was staged reactors. Staged reactors had separated ACF bed and reduced the inhibition of H₂SO₄ by intermediate trap in **Figure 4**.

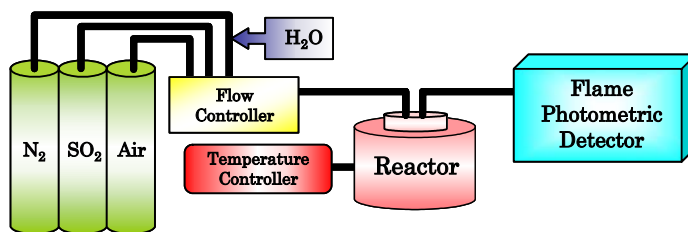


Figure 2. Experimental apparatus for oxidative fixation of SO₂

Results

Bold type reactor was certainly superior to the reference reactor as in **Figure 5**. The reactors of larger diameter showed better performance, confirming the influence of diameter/length ratio of ACF bed in the single reactor.

In figure 6, the performances of various reactor type were compared by using the same amount of ACF and same flow rate of gas feed. The heights of ACF were 50mm in the single reactor and 25mm in the parallel reactor respectively. The parallel reactor showed longer breakthrough time, suggesting the more efficient desulfurization with broad ACF bed. Staged type had better performances too, but not so good compared to parallel type. **Figure 7** compares the performances of the reference, parallel staged reactors against 750ppm SO₂. This result was the staged type. Staged Reactor completely removed SO₂ about 60hr. Parallel was same breakthrough time to reference but better removal ratio. **Figure 8** shows the activity of more amount of ACF (1.0g) achieved complete SO₂ removal by the parallel reactors and staged reactors whereas the reference reactor allowed still breakthrough by 34hr.

Discussion

The present study revealed that the reactor design was very influential on the performance for SO₂ removal of the ACF of the same amount. The up-flow is certainly better than the down flow. Broader reactor is better than thinner one. The intermediate reactors equipped with the respective device for H₂SO₄ recovery at every stages are certainly better than the single reactor at the same ACF amount. All these results indicate that the shorter path for aq.H₂SO₄ elution from the produced to the recovered locations allowed, better performance. Occupation of the active site by produced H₂SO₄ is minimized by the designed reactors to achieve lower SO₂ elution amount.

The reason why the intermediate recovery reactor is inferior to the parallel reactor is smaller supply of water to the upper reactor of the intermediate reactors, since most of water is trapped at H₂SO₄ trap located at the lower reactors. Small amount of water supply at the top of upper reactor solver the problems.

Staged type was the best in **Figure 7**, while parallel type was excellent in the others conditions. This different performance could be due to the different concentration of SO₂ feed gas and removal efficiency of formed H₂SO₄. the amount of H₂SO₄ was mainly related to H₂O and elution speed is the most important parameter.

References

1. I. Mochida, K. Kuroda, S. Kawano, Y. Matsumura, and M. Yoshikawa, *Fuel*, **76**, 533(1997).
2. I. Mochida, K. Kuroda, S. Kawano, Y. Matsumura, M. Yoshikawa, E. Grulke, and R. Andrews, *Fuel*, **76**, 537(1997).
3. I. Mochida, Y. Korai, M. Shirahama, S. Kawano, T. Hada, Y. Seo, M. Yoshikawa, and A. Yasutake, *Carbon*, **38**, 227(2000).

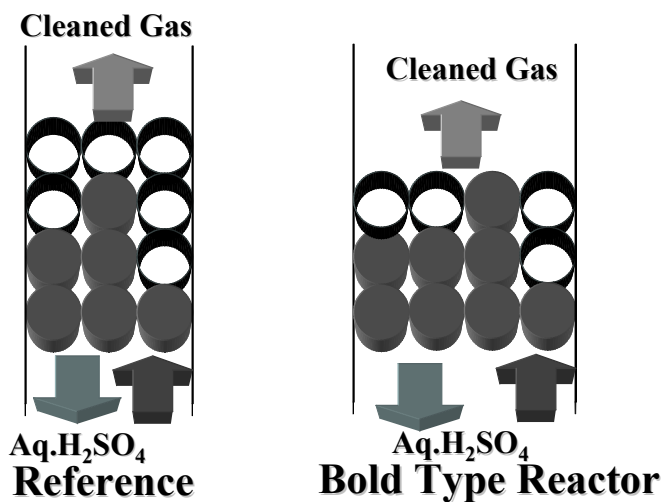


Figure 3. Concept of Designed Reactors (1)

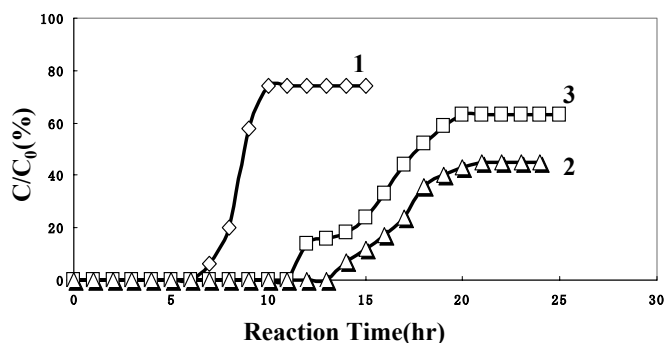


Figure 6. Breakthrough profiles of SO₂ in a reference, Parallel and Staged Reactors
 SO₂=1000ppm, O₂=5vol.% H₂O = 10 vol.%, N₂ balance
 W/F = 5.0×10⁻³g·min⁻¹·ml⁻¹ Reaction temperature 60°C
 1: Reference Reactor
 2: Parallel Reactors
 3: Staged Reactors

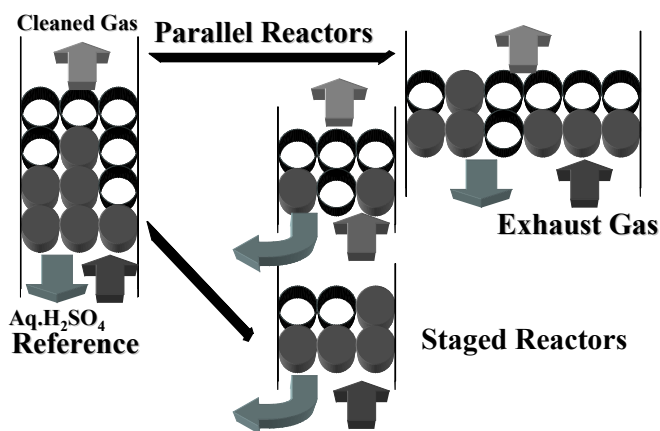


Figure 4. Concept of Designed Reactors (2)

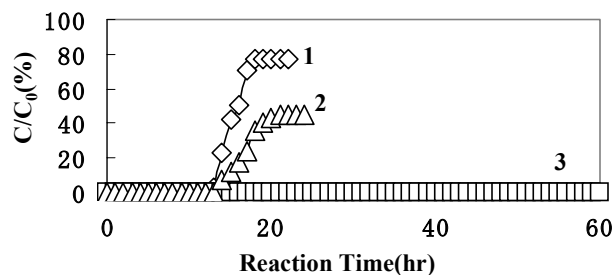


Figure 7. Breakthrough profiles of SO₂ in a reference, Parallel and Staged Reactors
 SO₂=750ppm, O₂=5vol.% H₂O = 10 vol.%, N₂ balance
 W/F = 5.0×10⁻³g·min⁻¹·ml⁻¹ Reaction temperature 60°C
 1: Reference Reactor
 2: Parallel Reactors
 3: Staged Reactors

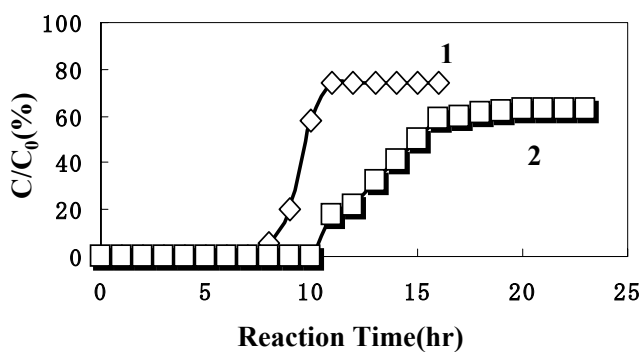


Figure 5. Breakthrough profiles of SO₂ in a reference and Bold Reactor
 SO₂=1000ppm, O₂=5vol.% H₂O = 10 vol.%, N₂ balance
 W/F = 5.0×10⁻³g·min⁻¹·ml⁻¹ Reaction temperature 60°C
 1: Reactor Diameter(14mm)
 2: Reactor Diameter(16mm)

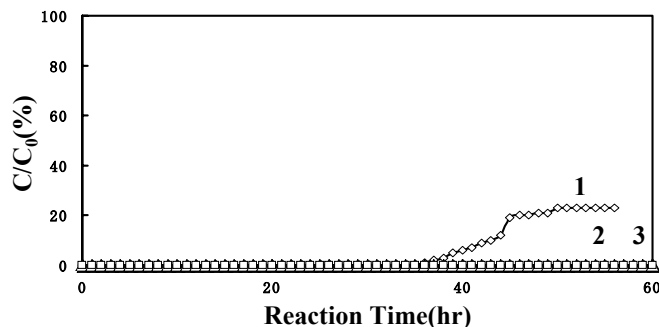


Figure 8. Breakthrough profiles of SO₂ in a reference, Parallel and Staged Reactors
 SO₂=1000ppm, O₂=5vol.% H₂O = 10 vol.%, N₂ balance
 W/F = 1.0×10⁻²g·min⁻¹·ml⁻¹ Reaction temperature 60°C
 1: Reference Reactor
 2: Parallel Reactors
 3: Staged Reactors

Ash Rejection Behavior on Continuous Column Flotation Process

Yasushi SEKINE, Daisuke YAMAGUCHI, Kiyohiro ISHIKAWA,
Eiichi KIKUCHI, Masahiko MATSUKATA

Department of Applied Chemistry
Faculty of Science and Engineering
WASEDA University
3-4-1 Ohkubo, Shinjyuku,
Tokyo, Japan 169-8555

Introduction

Column flotation is one of the promising processes for the low-cost next generation coal cleaning technologies. As for the column flotation system, many efforts have focused on optimization of apparatus and/or improvement of flotation results so far. However there have been few studies which tried to estimate the relation of flotation results and characteristics properties of coal. Then we investigated the characterization of demineralization in the column flotation system to estimate the flotation behavior by measuring the contents of inorganic elements in the cleaned coal and the tail refuse. Furthermore we investigated the distribution of coal minerals and their average particle size.

Experimental

Continuous Column Flotation. We employed the continuous column flotation system for the simple coal cleaning process. Samples which used in this study were; Adaro, Wallarah, Ermelo, Datong, Taiheiyu, and they were crushed into particles and sieved under 150 μm . The proximate analysis value and ultimate analysis value of these coal was shown in **Table 1** and the schematic diagram of experimental apparatus was shown in **Fig. 1**. At first, coal and ion-exchanged water were mixed for 30 min in slurry tank after adding Kerosene 1 mg / g-coal. Simultaneously column whose height was 2 m was filled with ion-exchanged water, and 4-methyl-2-pentanol(MIBC) 150 μL / L-water was added to it. Then coal-water mixture was supplied into the column continuously at the rate of 1 L / min from the upper of the column by using a static pump. MIBC was supplied into column continuously from the bottom of column by using a micro feeder. During the experiment, wash-water was supplied into the upper of the column. In upper and bottom of the column, coal-water mixture was obtained and dried. We regarded the upper part; cleaned coal, and the bottom part; ash rejection. Then average particle size of their particles was measured by laser particle size distribution measurement equipment. Inorganic elements of dissolved coal were measured by using ICP-AES after a microwave treatment.

Mineral analysis by CCSEM. The analysis of mineral part was conducted by CCSEM(Computer Controlled Scanning Electric Microscope). For the sample preparation, coal powder was mixed with Carnuba wax and cross-sectional polish of a sample was performed after heat-molding using the automatic grinder. Then, in order to enhance the conductivity of the sample section, carbon evaporation under vacuum condition was performed. The fixed quantity and the quality of the inorganic element contained in the particle on a section were measured. And the classification and the existence form of ash contents (included or excluded) were distinguished according to the mineral-form by using original conversion software.

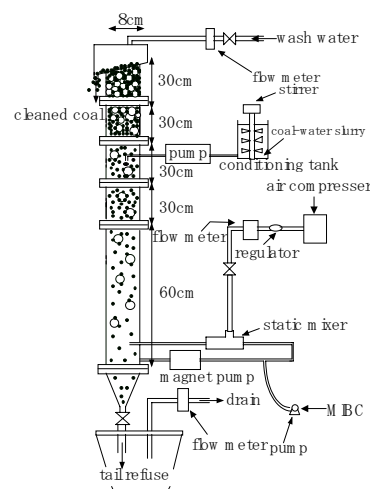


Fig. 1 Schematic diagram of experiment apparatus.

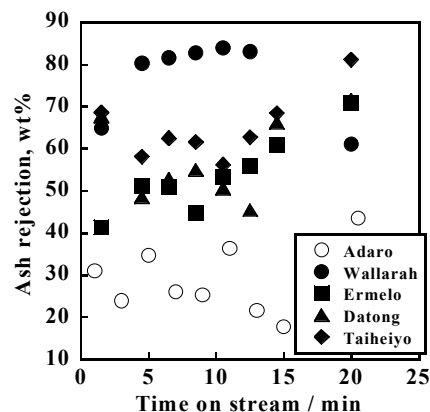


Fig. 2 Time on course of ash rejection.

Table 1 Proximate and ultimate analysis of coal employed in this study

Coal		Adaro	Walarah	Ermelo	Datong	Taiheiyu
Proximate Analysis value [a.d %]	Water Content	12.58	3.00	3.50	5.21	5.55
	Ash	1.58	13.7	12.90	10.24	11.35
	Volatiles	40.65	29.40	30.90	27.66	43.36
	Fixed carbon	45.19	53.90	52.70	56.89	39.74
Ultimate Analysis Value [db %]	Carbon	71.73	71.90	71.10	71.90	67.33
	Hydrogen	5.02	4.20	4.23	4.40	5.59
	Nitrogen	1.06	1.39	1.76	0.90	1.09
	Sulfur	0.00	0.30	0.65	0.61	0.08
	Oxygen	20.38	8.05	8.89	11.39	13.89
Ash Composition [db %]	SiO ₂	21.34	58.30	48.00	57.10	46.26
	Al ₂ O ₃	9.18	28.97	29.39	19.19	24.37
	Fe ₂ O ₃	10.53	4.24	5.00	11.88	8.27
	CaO	20.63	1.99	7.13	3.72	8.79
	MgO	6.84	0.92	2.60	0.82	2.65
	Na ₂ O	5.84	0.54	0.29	0.45	1.73
	K ₂ O	0.76	1.62	0.83	1.47	0.96
	SO ₃	23.08	0.56	3.74	3.87	3.67
	P ₂ O ₅	0.07	0.05	0.14	0.40	1.07
	TiO ₂	0.48	1.29	1.26	0.69	1.27
	V ₂ O ₅	0.04	0.03	0.04	0.03	0.06
	MnO	1.09	0.06	0.09	0.20	0.08

Results and Discussion

Continuous column flotation. Time on course of ash rejection was shown in Fig. 2. Ash rejection came to be steady state in 5~14 minutes, and that of Wallarah coal showed highest rejection level. So Wallarah coal was employed for subsequent experiments because of its high separation ability.

The average particle distribution of raw coal, cleaned coal and tail of Wallarah coal were shown in Fig. 3. In the raw coal, the distribution of particle size was high around the particle diameter about 100 μm , and the shoulder peak was observed near 10 μm . Although the particles in the tail rejection had the same distribution, the fraction around 100 μm became large. On the other hand in the cleaned coal, the particles near 100 μm were not contained, but the distribution has the peak around 80 μm and 10 μm . From these phenomena, we considered that many of mineral matter were contained in the particle near particle diameter 100 μm , and their particles were removed by the column flotation as the bottom rejection.

Distribution of inorganic elements. Inorganic elements distribution of the cleaned coal and the tail rejection that were obtained during steady state, was shown in Fig. 4. As a result, most of contained inorganic elements eluted into the column, or obtained as the tail rejection. In particular, most of Na, Al, and Mn were removed as the tail rejection.

Mineral analysis by CCSEM. The demineralization efficiency of each mineral in Wallarah coal was calculated and shown in Fig. 5. Demineralization efficiency means "the ratio of the actual amount of each mineral" by "the theoretical value". The theoretical value is the amount of minerals at the time of separating into cleaned coal and tail, without demineralization. Most of minerals in Wallarah coal were efficiently removed to tail. And Aluminosilicate and Si-Rich minerals were removed in particular.

Conclusion

Most of contained inorganic elements in Wallarah coal were eluted into the column, or obtained as the tail rejection. In particular, most of Na, Al, and Mn were removed as the tail rejection. Most of minerals in Wallarah coal were efficiently removed by the continuous column flotation process. And Aluminosilicate and Si-Rich minerals were removed in particular.

Acknowledgement

This work was partly supported by the fund of National Department of Science and Technology Japan (its group leader; Prof. K.Miura from Kyoto Univ.).

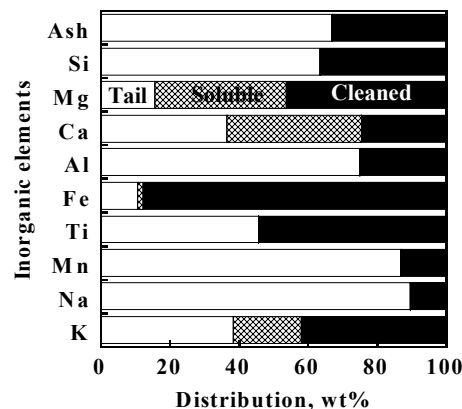


Fig. 3 Distribution of average particle (raw coal, cleaned coal, tail).

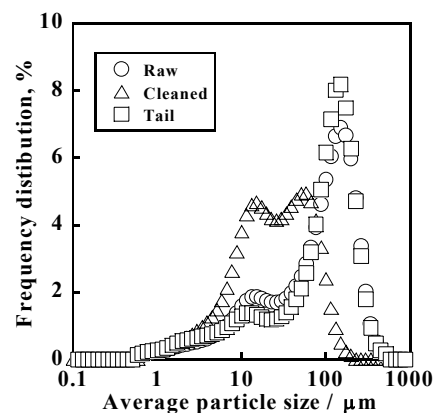


Fig. 4 Distribution of inorganic elements.

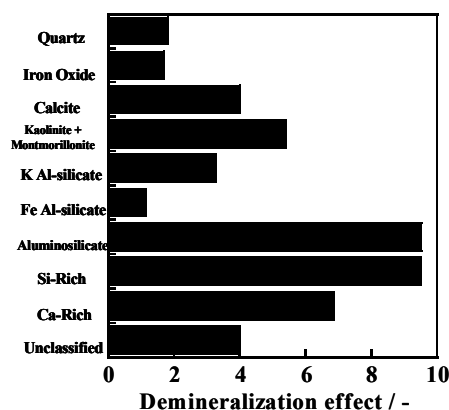


Fig. 5 Comparison of demineralization effect.

A novel coal cleaning with pretreatment in methanol

Takayuki Takarada, Kenji Goto, Megumi Ookawa, Jie Wang¹
and Kayoko Morishita

Department of Biological and Chemical Engineering,
Gunma University,
1-5-1 Tenjin-cho, Kiryu 376-8515 JAPAN

^{*1}Institute of Multidisciplinary Research for Advanced Materials,
Tohoku University

Introduction

Coal demineralization prior to use has received much attention because mineral matter in coal causes problems in many aspects of conventional and advanced coal utilization. Physical beneficiation has long been used to reject discrete mineral inclusions from coal. For efficient physical separation of mineral matter, it is necessary to liberate mineral-rich grains by the breakage of coal particles through coal grinding. In order to improve the liberation of mineral inclusions and the efficiency of grinding energy utilization, pretreatment of coal by swelling agents has been explored. In this paper, we use the relatively cheap and available methanol as a swelling agent to study its effect on the breakage of coal particles.

Experimental

Coal Sample. Eleven coals were used in this study. Their proximate analysis and carbon content are shown in Table 1. The coal particle was screened to 1~2 mm before pretreatment.

Table1 Analysis of coal samples

	Carbon [wt%d.a.f]	Mois.	V.M. [wt%]	F.C.	Ash
Pasil	72.0	2.1	47.4	48.5	2.0
Taiheiyo	78.7	3.8	43.9	40.2	12.1
Kitasyuku	78.7		36.4	50.8	12.8
Yangsong	80.5	3.3	40.3	48.3	8.1
Ebenezer	81.2	2.2	38.1	45.2	14.5
Hong-Yie	81.7	0.8	47.3	22.3	29.6
San-Zu-Pa	82.6	1.0	14.3	50.3	34.4
Datong	82.7	3.2	28.7	58.4	9.7
Miike	82.8	1.9	39.9	45.0	13.2
Newlands	85.9	2.5	26.3	56.2	15.0
I-Tem-Pou	86.9	0.8	15.0	64.8	19.4
Burton-st	89.8	1.5	16.6	70.6	11.3

Methanol Treatment. A 100 g sample of coal was treated with 200 mL methanol at room temperature for the desired time. After treatment, the sample was filtered and then dried at 107 °C for 2 h.

Compressive strength. The compressive strength of sample was measured with Kiya strength meter.

Grindability test. It was conducted in a cylindrical ball mill made of stainless steel (i.d., 85 mm; height, 90 mm) with 30 stainless balls. In each test, a 20 g sample of coal was ground at 110 rpm for the predetermined time.

SEM Analysis. SEM was utilized to observe the morphology of coal sample upon the methanol treatment. CCSEM was used to measure quantitatively the mineral inclusion distribution for the fine coal sample with or without methanol treatment, it was accomplished on a TOPCON, ABT-60 scanning electron microscope equipped with

an energy dispersive x-ray analyzer (EDAXPV9750) and a computer controlled program.

Results and Discussion

Compressive strength. The compressive strength of samples with and without the methanol pretreatment were shown in Fig. 1. The strength of the treated coal particles was reduced to about a half of that of parent coal.

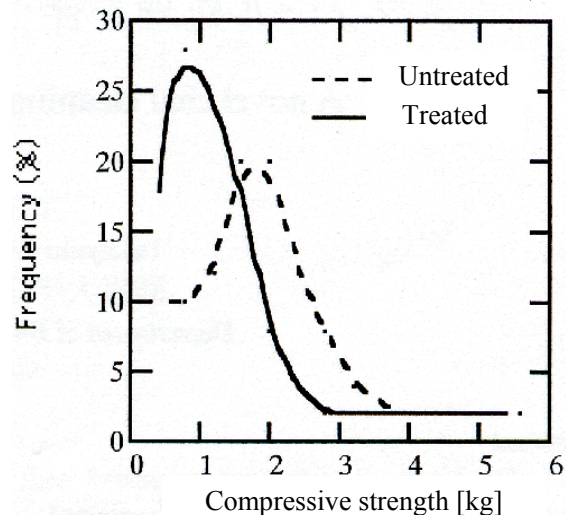


Fig.1 Compressive strength

Grindability. Fig.2 shows the particle size distributions by grinding Yangsong raw coal and the treated coal. The data are the weight percent of the size-graded particles. The grindability of the treated coal was quite higher than that of raw coal. Fig.2 shows the effect of treatment time on the grindability. Prolonged swelling from 2 to 120 h increased the cumulative weight percent of the particles under 150 μ m from 41.8 to 58%.

Similar experiments were conducted for eleven coals. After methanol treatment, all the coals tended to be easily ground. However, the effectiveness of the methanol pretreatment on the grindability depended on coal type. The effectiveness of the pretreatment evaluated as the ratio of the cumulative weight percent

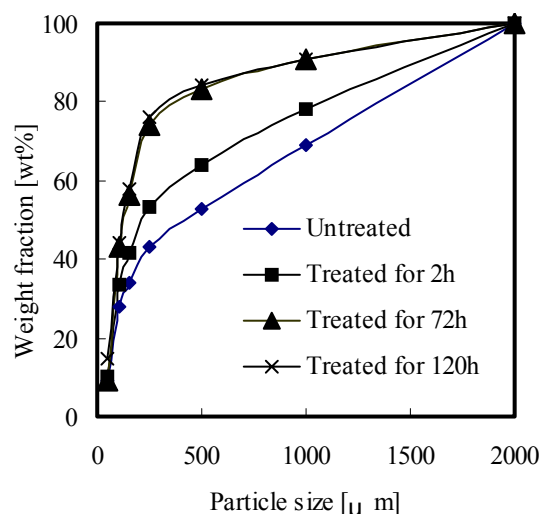


Fig.2 Grindability of Yangsong coal

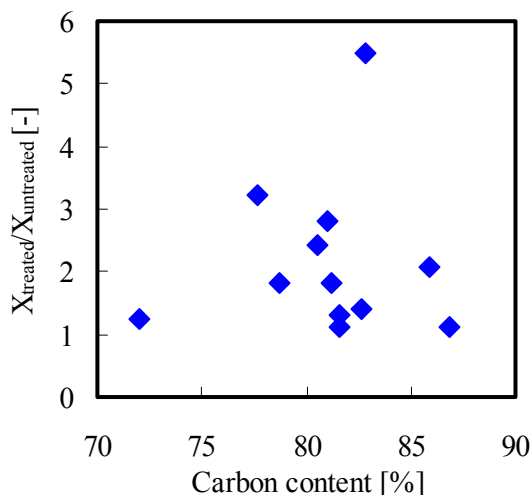


Fig.3 Effectiveness of treatment for various coals

of the particles under 150 μm for raw coal to that for the treated coal is shown in Fig.3. It appears that the effectiveness of the treatment has no correlation with coal rank. The effectiveness for coal with carbon content of around 82 wt% was quite large.

SEM Observation. Fig.4 displays the SEM images for the Yangsong raw coal and treated coal samples. There were many fractures formed after methanol treatment. Wang et al.¹⁾ found the preferential crack along the boundaries between mineral and coal matrix using some mixed agents. Tamai et al.²⁾ observed the crack along the boundaries between macerals by the pretreatment with liquid ammonia. The crack formed in the treated coal is one of the reasons for high grindability of treated coal.

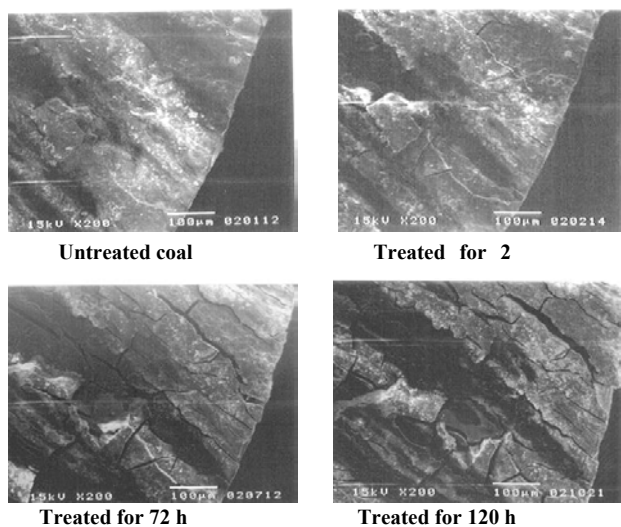


Fig.4 SEM images for Yangsong coal

CCSEM Analysis. To observe the liberation of mineral inclusions from coal matrix, we used CCSEM to quantitatively analyze two Yangsong coal samples with or without methanol treatment, which were subject to the same milling and then were both screened to the particles under 150 μm prior to analysis. Figs.5 and 6 show the particle number ratio of the particles having different mineral contents. The counted particle numbers were 2168 and 2412, respectively, for the raw coal sample and the treated sample. The mineral content is evaluated from cross sectional area of mineral in coal particle analyzed with CCSEM. Through treatment, the number

of the mineral-rich particle containing 90-100% mineral was increased and that of particle containing 50-80% mineral was decreased. From the results obtained, the selective mineral reduction may be achieved by using methanol pretreatment. Some iron-containing minerals appeared to decrease in the number. XRD showed that Yangsong coal mainly contained pyrite, kaolinite, gypsum, ferrous sulfate, and quartz (not shown). Gypsum and ferrous sulfate were significantly dissolved out upon the methanol treatment.

Conclusions

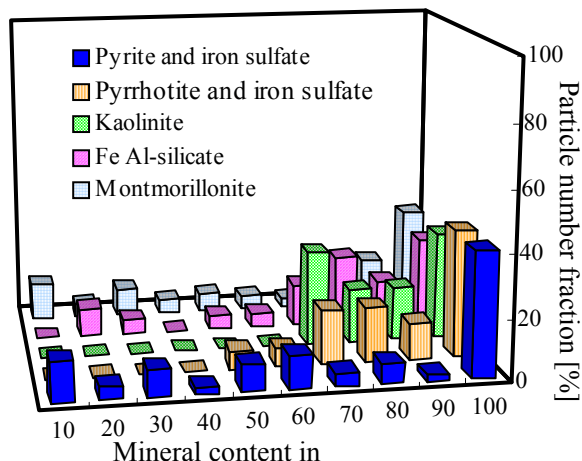


Fig.5 CCSEM analysis of untreated Yangsong coal

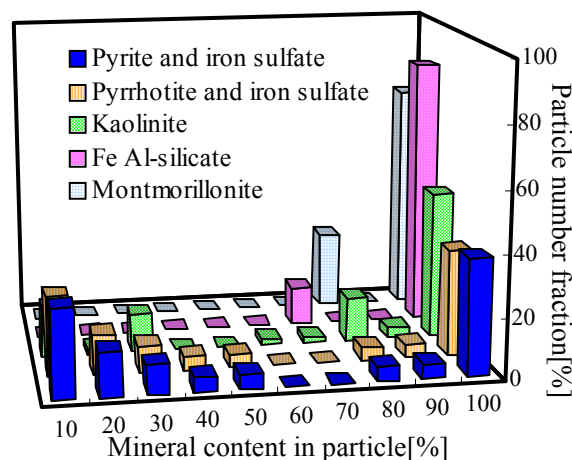


Fig.6 CCSEM analysis of treated Yangsong coal

The compressive strength of the treated coal particles was reduced to about a half of that of parent coal and the grindability of the treated coal was higher than that of raw coal. Many cracks were formed in coal particle by the treatment. CCSEM analysis revealed the possibility of selective mineral reduction by the beneficiation with pretreatment in methanol.

Acknowledgement. This work is under a Scientific Research of Priority Areas---"Development of Clean Coal Technology for Mitigating Global Warming".

References

- (1) Wang, X. H. et al. *Coal Prep.* **1996**, 17 (3-4), 185-198
- (2) Tamai, T.;Tomita, A.;Takarada, T. *J. Chem. Soc. Jpn.* **1980**, 951-958

PRODUCTION OF CLEAN FUELS BY SOLVENT SKIMMING OF COAL AT AROUND 350 °C

Kouichi Miura, Hiroyuki Nakagawa,
Ryuichi Ashida, and Takayuki Ihara

Department of Chemical Engineering, Kyoto University,
Kyoto 606-8501, Japan

Introduction

The authors have recently presented a new coal extraction method by which various kinds of coals ranging from brown coals to bituminous coals could be extracted up to 80 % in a flowing stream of tetralin or a coal derived oil, carbol oil, under 10 MPa at 350 °C^{1,2,3}. However, it doesn't seem cost-effective to use pure solvents from the viewpoint of practical application of the extraction method. In this study the effect of solvent recycling on the extraction behavior was investigated to make the method practically applicable.

It was also found in the previous papers that the extract was almost free from mineral matters^{1,2,3}. To examine the result in more detail, the distributions of inorganic elements through the extraction were measured and discussed.

Experimental Section

Coal Samples. The analyses of four coal samples used are given in Table 1.

Table 1. Ultimate Analyses of Coal Samples Used

Coal (Abbreviation)	Ultimate analysis [wt%, d.a.f.]				Ash [wt%, d.b.]
	C	H	N	O+S (diff.)	
South Banko (SB)	68.8	5.2	1.4	24.7	4.2
Prima (PR)	76.3	5.5	1.4	16.8	5.4
Miike (Mi)	80.8	6.2	1.3	11.7	19.8
Pittsburgh #8 (PITT)	83.2	5.3	1.6	9.9	9.3

Solvents Used. Tetralin was used as a model solvent, and a coal tar derived oil, so-called carbol oil, was used as a candidate solvent for practical application of the proposed extraction method. The carbol oil is a coal tar distillate whose boiling point ranges from 180 to 220 °C. Main components of the oil are phenolic derivatives.

Experimental Procedure for Extraction. Figure 1 shows a schematic diagram of the apparatus used for extraction. 100 to 1000 mg of coal samples were placed on a filter (11.2 mm OD and 0.5 µm opening) in a reactor made of Swagelok. The solvent was supplied continuously using a high-pressure pump at the flow rate of 1 to 5 ml/min. The pressure was regulated using a pressure-regulating valve (TESCOM) at 10 MPa. The reactor was heated at the rate of 10 K/min to 350 °C where it was kept for 90 min, and then it was cooled immediately by immersing into a sufficient amount of water. The coal fractions extracted at the reactor temperature, which are solubilized in the solvent, came out from the reactor with the flowing solvent, but a part of the solubilized components precipitated as solid when the solvent flow was cooled to room temperature. The solid thus precipitated, called deposit in this paper, was collected by 3 filters (20, 10, and 2 µm openings) placed in series just before the pressure-regulating valve. The deposit that passed these filters was collected in a separation trap with the soluble components at room temperature. The soluble components are called "soluble" here. Product gas was collected in a gasbag, and analyzed using a gas chromatograph for the components smaller than C6 hydrocarbons in molecular weight. The weights of the residue and the deposit were directly measured after drying them in vacuo at 150 °C for 5 hours. The weight of gaseous components was calculated from the analysis using the gas chromatograph. The rest of the product was regarded as the soluble.

Experiments recycling the solvent containing soluble fraction were also performed using tetralin as the solvent. For this purpose, 150 ml of tetralin was used and it was supplied to the extractor at the rate of 5 ml/min. The tetralin, recovered in the separation trap with the soluble fraction, was recycled to the extractor. The recycling solvent passed the coal layer 5 to 6 times during 90 min of experiment. The solvent recovered after the experiment was used again to the extraction of a fresh coal. This extraction cycle was repeated 10 times by using the fresh coal for each cycle.

Analyses of the products. The contents of main inorganic elements in the soluble and the deposit, Na, Mg, Al, Si, Ca, and Fe, were analyzed by the inductive coupled plasma spectrometry (Shimadzu, ICPS7500). The contents of trace elements, Co, Cr, Cu, Mn, Ni, Pb and Zn, in the deposit and the residue were also measured by ICP-AES and Hg, Se, As were analyzed by CVAAS, HGAAS, and GFAAS, respectively⁴.

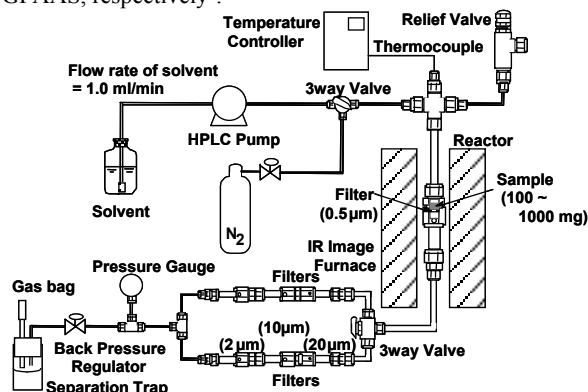


Figure 1. Schematic of experimental apparatus used for extraction in flowing solvent.

Results and Discussion

Effect of Solvent Recycling on the Extraction Behavior.

Experiments recycling the solvent were performed using PITT. Figure 2 shows the relationship between the yield of each component and the number of cycle. The yield of deposit increased with the number of cycle, while the yield of soluble stayed almost constant. The yield of deposit reached 41 % at a maximum, which was twice as large as that in the first extraction. The extraction yield of 80 % was achieved at its maximum. The soluble concentration in the recycling tetralin increased from 0.001 kg/kg-solvent of the 1st cycle to 0.012 kg/kg-solvent of the 10th cycle. These results suggest that the increase of the solubility of the coal with increasing extraction cycle was realized by the increase in the concentration of soluble in the tetralin. It could be concluded that solvent recycling was

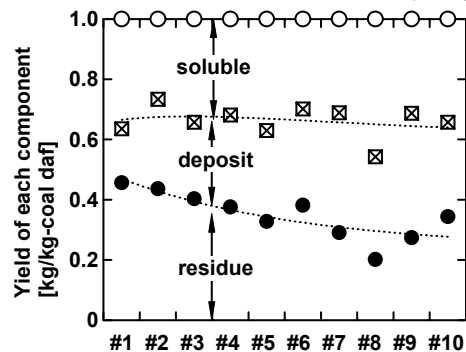


Figure 2. Relationship between the yield of each component and the number of cycle for PITT through the extraction in recycling tetralin at 350 °C.

effective to enhance the extraction yield, suggesting a possibility of the solvent recycling as a cost effective method.

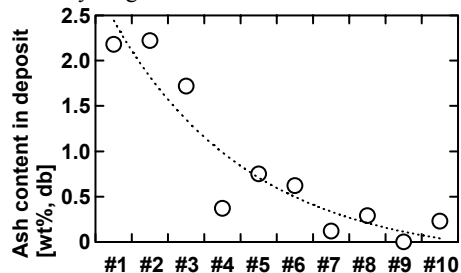


Figure 3. Relationship between the ash content in the deposit and the number of cycle for PITT through the extraction in recycling tetralin at 350 °C.

Figure 3 shows the relationship between the ash content in the deposit and the number of cycle. As presented in the previous papers, the deposit obtained by the extraction using one pass tetralin contained little mineral matters^{1,2,3}. The solvent recycling still further reduced the mineral matter content in the deposit. The content decreased dramatically from 2.2 % to 0.2 % with the number of cycle. Thus, it was found that the solvent recycling was effective not only to enhance the extraction yield but also to remove the mineral matters from coals.

Mineral Matters in the Extract. **Figure 4** shows the contents of main inorganic elements in the soluble and the deposit fractions for extractions using tetralin and those in the soluble fractions for extractions using the carbol oil. The figures in the brackets represent the contents of elements in the parent coals. The yields of these fractions through the extractions were also given in **Figure 4**. Only a small amount of Na and Si were detected in the soluble fractions obtained by the tetralin extraction, indicating that the soluble is very clean. On the other hand, the amounts of the elements in the deposit fractions obtained by the tetralin extraction and the soluble fractions obtained by the carbol oil extraction were relatively larger than those in the soluble fractions obtained by the tetralin extraction, especially for Fe. However, the contents of most elements in the extracts were less than several percents of those in the parent coals.

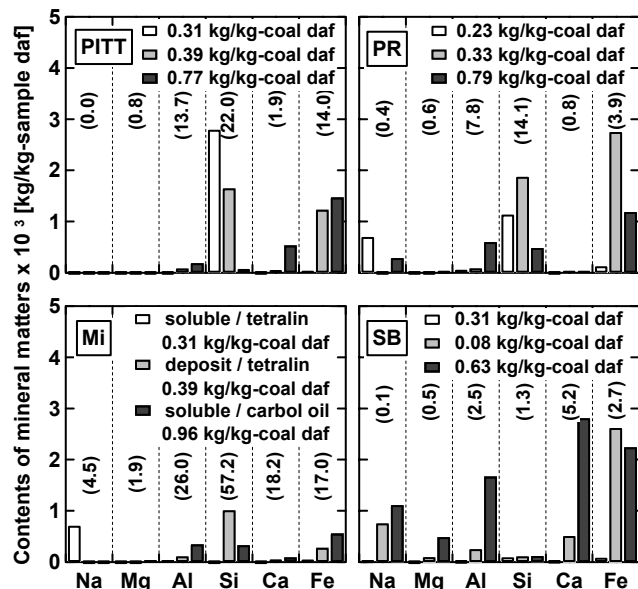


Figure 4. Contents of main inorganic elements in the extracts.

The contents of trace elements including hazardous heavy metals were analyzed as well⁴. **Figure 5** shows the contents of trace elements in the deposit fractions obtained by the first and fifth cycle of extractions of PR in recycling tetralin. The yields of deposits for the extraction cycles are also listed in **Figure 5**. The contents of Cr, Cu, Ni and Pb in the deposit fractions obtained by the first cycle were larger than those in the parent coal. The Ni content in the deposit fraction obtained by the fifth cycle was still larger than that in the parent coal. The contents of the other elements, Mn, Zn, As, Co, Hg and Se, in the deposit fractions, however, were much less than those in the parent coal, indicating that the proposed method is effective to remove some of the hazardous elements from coals. Furthermore, the contents of almost all the trace elements in the deposit fraction decreased with the number of cycle, which agreed with the results shown in **Figure 3**. The five cycles of extractions reduced the contents of Mn, Zn and Co in the deposit to 29 %, 19 % and 30 % of those in the parent coal, respectively. These results suggest that the solvent recycling enhances the degree of removal of hazardous trace elements.

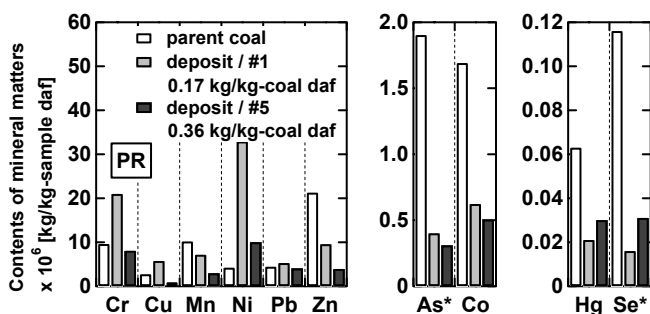


Figure 5. Contents of trace elements in the deposit and parent coal (* calculated from the contents in the parent coal and the residue).

Conclusion

The effect of solvent recycling on the extraction behavior was examined from the viewpoint of practical application of the proposed extraction method. It was found that the solvent recycling was effective not only to enhance the extraction yield but also to remove the mineral matters from coals, suggesting a possibility of the solvent recycling as a cost effective method.

To examine how mineral matters are removed by the extraction, the distributions of inorganic elements, including hazardous trace elements, through the extractions were investigated. It was clarified that the proposed method is effective to remove most of the inorganic elements from coals, although it depends on the kind of element.

Acknowledgement. This work was supported by the Ministry of Education and Science of Japan through the Scientific Research of Priority Area (B) "Development of Clean Coal Technology for Mitigating Global Warming"(Grant NO. 737). The authors express their sincere thanks to Prof. A. Ohki for measuring the contents of trace elements.

References

- Miura, K.; Shimada, M.; Mae, K. *15th Pitt. Coal Conf.*, **1998**, Paper No.30-1.
- Miura, K.; Shimada, M.; Mae, K.; Huan, Y. *Fuel*, **2001**, *80*, 1573.
- Miura, K.; Mae, K.; Shindo, H.; Ashida, R.; Ihara, T. *18th Pitt. Coal Conf.*, **2001**, Paper No.2.6-6.
- Xu, Y.; Nakajima, T.; Ohki, A. *Toxicol. Environ. Chem.*, **2001**, *81*, 55.

EFFECT OF ACID TREATMENT ON THERMAL EXTRACTION FOR "HYPERCOAL" PRODUCTION

Chunqi Li¹, Toshimasa Takanohashi¹, Takahiro Yoshida¹,
Ikuro Saito¹, Hideki Aoki², and Kiyoshi Mashimo²

¹ Institute for Energy Utilization,
National Institute of Advanced Industrial Science and Technology

² College of Science and Technology, Nihon University

Introduction

Thermal extraction using an organic solvent was carried out to produce ashless coal (HyperCoal).^{1,2} HyperCoal is expected to be fired directly in a gas turbine to achieve higher net power output and minimize CO₂ emission. The required extraction yield is higher than 60%, and ash content in the HyperCoal is less than 200 ppm, in addition to less than 0.5 ppm sodium and potassium. In our previous work,¹⁻³ the extraction yields of higher than 60% were obtained for several bituminous coals using a flow-type extractor at 360°C, with nonpolar solvents of 1-methylnaphthalene (1-MN) and Light Cycle Oil (LCO). While, in the case of polar solvents *N*-methyl-2-pyrrolidinone (NMP) and Crude Methylnaphthalene Oil (CMNO) the extraction yields of higher than 80% were attained. The high extraction yields were considered to be mainly due to the heat-induced relaxation of coal aggregates in the case of 1-MN, while in NMP, not only due to the heat-induced relaxation but also solvent-induced one.³ However, what kinds of coal aggregations were released during the thermal extraction was not clear yet. In addition, these solvents give relatively low extraction yields for some low-rank coals. In the present work, different ranks of coals were acid-treated in organic acids. Effects of acid treatment on the thermal extraction yields and the changes of coal structure were investigated. Furthermore, mechanisms for thermal extraction and acid treatment are discussed.

Experimental

Table 1. Ultimate Analysis and Ash Content of the Coals Used

coal sample	ultimate analysis (wt%, daf)					ash (wt%, db)
	C	H	N	S	O ^a	
Pocahontas No.3(POC)	89.7	4.5	1.1	0.7	4.0	4.8
POC acid-treated ^b	90.0	4.3	1.2	0.6	3.9	3.3
Upper Freeport(UF)	86.2	5.1	1.9	2.2	4.6	13.1
UF acid-treated ^b	86.7	5.0	1.7	2.3	4.3	12.2
Illinois No.6(IL)	76.9	5.5	1.9	5.6	10.1	15.1
IL acid-treated ^b	76.5	5.3	2.0	5.8	10.4	12.0
Wyodak(WY)	75.0	5.4	1.1	0.5	18.0	8.8
WY acid-treated ^b	74.5	5.6	1.2	0.6	18.1	3.9
Ardaro (AR)	73.0	5.1	1.1	0.0	20.8	1.8
AR acid-treated ^b	72.9	5.2	1.1	0.0	20.8	0.7
Pasir(PA)	73.5	5.3	1.9	0.2	19.1	4.9
PA acid-treated ^b	74.4	5.3	1.7	0.2	18.4	3.5
Beulah-Zap(BZ)	71.6	4.8	1.0	0.9	21.7	9.6
BZ acid-treated ^b	72.0	5.0	1.1	0.8	21.1	3.0
Banko 97(BA)	70.0	5.3	1.3	0.3	23.1	2.4
BA acid-treated ^b	70.4	5.4	1.2	0.4	22.6	0.8

^a By difference ^b 1.0 M methoxyethoxy acetic acid

Coal samples. Six Argonne Premium coals; Pocahontas No.3, Upper Freeport, Pittsburgh No.8, Illinois No.6, Wyodak, Beulah-Zap(<150 μm), and three Indonesia coals; Adaro, Pasir (<150 μm),

Banko 97 coal(<74 μm) were used. All coal samples were dried in vacuo at 80 °C for 12h. The ultimate analysis and ash content are shown in Table 1.

Acid treatment. Acid treatment of coal was carried out using aqueous methoxyethoxy acetic acid (MEAA) or acetic acid, which were reported to be effective agents to liberate cation-bridging cross-links through oxygen functional groups in low-rank coals.^{4,5} Approximately 4.0g dried coal sample was treated in 150 mL aqueous acid with 10% ethanol under nitrogen atmosphere at room temperature for 24 h. Then, the acid-treated coal was washed with deionized water until the pH of deionized water became near 6.0. Finally, the acid-treated coal was dried in vacuo at 80 °C for 12 h. The ultimate analysis and ash content for acid-treated coals are also listed in Table 1.

Thermal extraction. 1-MN and NMP were used as the thermal extraction solvent without further purification. Thermal extractions of coals were carried out using a flow-type extractor as described before.¹ The coal sample (0.2-0.5 g) was charged into a stainless cell (ca. 4cm³) that was fitted with stainless filters (0.5μm) on both sides and then set in an oven. The thermal extraction was carried out by supplying fresh solvent (flow rate: 0.1mL/min) under N₂ atmosphere (1Mpa) at extraction temperatures (200, 300, 360 °C) for 60 min. After the extraction, the extract was precipitated by adding *n*-hexane to the extract solution when 1-MN was used as the extraction solvent, or the solvent was evaporated from the extract solution and then the extract obtained was washed with water when NMP was used as the extraction solvent. The extraction yield was calculated on dry ash-free basis from the weight of residue.³

FT-IR measurement. FT-IR spectrum was recorded by a diffuse reflectance method using a spectrometer (Nicolet MAGNA-IR) at resolution of 4 cm⁻¹.

Results and Discussion

Effect of the acid treatment on the extraction yield. Figure 1 shows that the extraction yield in 1-MN for the acid-treated (1.0 M MEAA) WY coal did not change significantly. While, the yield in NMP for the acid-treated coal greatly increased to 82.9% from 58.4% for the raw coal. The acid treatment also increased the extraction yield in NMP for a subbituminous AR coal, and a lignite BZ coals. In contrast, for a subbituminous PA, and a lignite BA coal, the acid treatment gave a small effect on the extraction yields. The acid treatment also gave little effect on the extraction yields for high-rank IL, UF and POC coals.

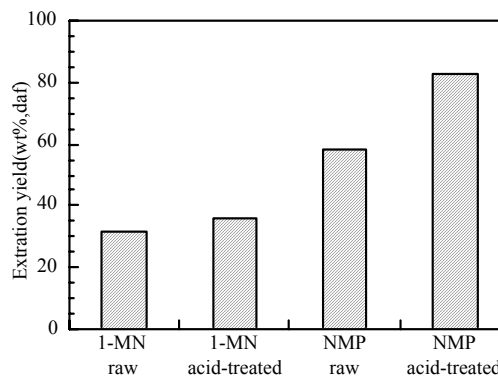


Figure 1. Extraction yields of acid-treated Wyodak coal extracted in 1-MN and NMP at 360°C for 1h.

Figure 2 shows the extraction yields for the acid-treated (1.0 M MEAA) and raw WY coals extracted in NMP at different temperatures. Similar as that of the raw coal, the extraction yields for acid-treated coal were increased with increasing the extraction temperature from 200 °C to 360°C, especially, a high extraction yield (81.3%) was obtained at 300 °C, similar to that at 360 °C.

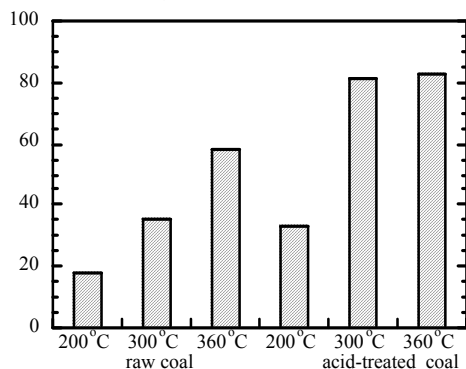


Figure 2. Extraction yields of the acid-treated Wyodak coal extracted in NMP at different temperatures, together with those of the raw coal.

Effect of acid treatment on coal structural changes. Figure 3 shows FT-IR spectra of WY coal acid-treated in 1.0 M MEAA (a), the raw coal (b), and the difference spectrum:(c), (a)-(b). Figure 3 (c) shows that the bands near 1,550 and 1,400 cm^{-1} decreased and the band near 1,720 cm^{-1} increased. The bands near 1,550 and 1,400 cm^{-1} are assigned to carboxylate groups, and that at 1,720 cm^{-1} is assigned to carboxylic acid group.⁶ The carboxylate groups were converted to the carboxylic acid groups by the acid treatment,^{6, 7} as a result, the cation-bridging cross-links formed through the carboxylate groups in the raw coal might be released, and hydrogen bonds form among the carboxylic acid groups.⁴ While, as shown in Figure 4, after the acid treatment for BA coal, there were no clear changes near 1,555 and 1,400 cm^{-1} , and near 1,720 cm^{-1} . Although the acid treatment for BA coal decreased the ash content from 2.4% to 0.8%, as shown in Table 1, there was a small effect on the extraction yield, as described above. BA coal has a high concentration of carboxyl groups,⁸ however, as shown in Figure 4, no peak corresponding to carboxylate groups was observed in the raw coal, therefore, most of these functional groups may be in carboxylic acid form.

The removal of cation-bridging cross-links in WY coal maybe allow more NMP to diffuse the inside of coal, and newly formed hydrogen bonds might be more easily broken by NMP, resulting in the higher extraction yield for the acid-treated WY coal. The high yield for BA raw coal with NMP can be also due to releasing weaker noncovalent bonds, such as hydrogen bonds in the coal.

Therefore, releasing some noncovalent bonds, such as hydrogen bonds for low-rank coals can be one reason of heat/solvent-induced relaxation of coal aggregates in NMP.³ While, for high-rank coals, the structure can be different from that for low-rank coals. The mechanism on the heat/solvent-induced relaxation of coal aggregates during the thermal extraction needs further investigations.

Conclusions

The acid-treatment greatly increased the thermal extraction yields for some low-rank coals, due to conversion of carboxylate groups to carboxylic acid groups. Releasing some noncovalent bonds, such as

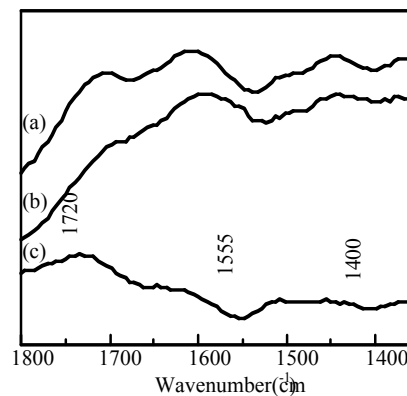


Figure 3. FT-IR spectra of acid-treated Wyodak (a), the raw coal (b), and the difference spectrum :(c), (a)-(b).

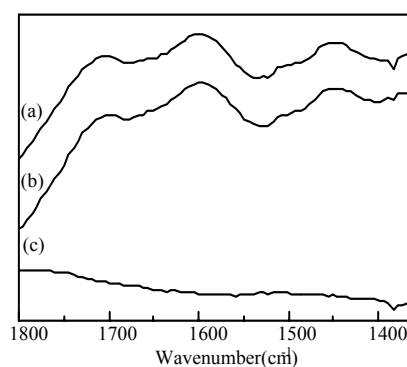


Figure 4. FT-IR spectra of acid-treated Banko 97 (a), the raw coal (b), and the difference spectrum:(c), (a)-(b).

hydrogen bonds, can be one reason for the relaxation of coal aggregates during the thermal extraction with NMP.

Acknowledgement. This work was financially supported by the New Energy and Industrial Technology Development Organization (NEDO).

References

- (1) Yoshida, T.; Takanohashi, T.; Sakanishi, K.; Saito, I.; Fujita, M. and Mashimo, K. *Energy Fuels*, **2002**, 16, 1006.
- (2) Yoshida, T.; Li, C.; Takanohashi, T.; Matsumura, A.; Sato, S. and Saito, I. *APCCChE/CHEMECA 2002*, submitted.
- (3) Li, C.; Yoshida, T.; Takanohashi, T.; Saito, I.; Iino, M. *Proceeding of the Japan Institute of Energy Conference*, **2002**, 42.
- (4) Shimohara, T.; Mochida, I. *J Fuel Soc Jpn* **1987**, 66, 134.
- (5) Sakanishi, K.; Watanabe, I.; Nonaka, T.; Kishino, M. and Mochida, I. *Fuel* **2001**, 80, 273.
- (6) Opaprakasit, P.; Scaroni, A. W. and Painter, P. C. *Energy Fuels* **2002**, 16, 543.
- (7) Aida, T., Yoshinaga, T., Yamanishi, I., Tsutsumi, Y., *Proc. Int. Conf. Coal Sci.* 1997, vol. 1, 179.
- (8) Murata, S.; Hosokawa, M.; Kidena, K.; Nomura, M. *Fuel Processing Technology*, **2000**, 67, 231.

ELUTION BEHAVIORS OF METAL COMPONENTS FROM COAL DURING PRETREATMENT AND SOLVENT EXTRACTION

Kinya Sakanishi*¹⁾, Eiko Akashi²⁾, Hiroyuki Kawashima¹⁾, Ikuo Saito¹⁾, and Takayuki Takarada²⁾

- 1) National Institute of Advanced Industrial Science and Technology (AIST), Tsukuba, Ibaraki 305-8569, Japan
- 2) Gunma University, Kiryu, Gunma 376-8515, Japan

Introduction

Pretreatments for removal of mineral matters and modification of coal have been reported. Recently, UCC (Ultra Clean Coal) project in Australia and HyperCoal(HPC) project in Japan have been demonstrated for the development of efficient demineralization process of coal by alkali solution and organic solvent extraction, respectively. In the former process, the product obtained still contains 0.3-0.7 % of ash, which can damage gas turbine, while the latter process can produce the extract(HPC) at high yields of ca. 60 % with much less ash content as low as 200 ppm under relatively mild conditions without any hydrogen consumption.¹ HPC is expected for the direct introduction to gas turbine power generation system for the higher efficiency and reduction of CO₂ emission.

Coal pretreatment with methanol has been reported for the improvement of selective grindability of organic substance and mineral matters in coal.² Coal pretreatments with dilute acid solutions have been also reported for the enhancement of coal depolymerization, liquefaction, and pyrolysis reactions.³

In the present study, the effects of pretreatments with methanol and dilute acid solutions on the production of HPC are investigated. Elution behaviors of metals and mineral matters during such pretreatments are also examined based on the characterization of the original coal and its derived HPC.

Experimental

Samples. A Chinese Enshu(EN) coal and an Australian Stratford(STF) coal, and their solvent-extracted coals(Hyper coal: HPC) were used in this study. Their ultimate and proximate analyses are summarized in Table 1.

Coal Pretreatments. Sequential treatment of coal with H₂O, 1 M CH₃COOH and 1N HCl/10%ethanol solution at room temperature was performed as follows;

- H₂O washing : about 4 g of coal was washed with 150 ml H₂O at room temperature for 24 h under N₂ flow, and filtered and dried in vacuo for 5 h at 60 °C.
- Acetic acid washing: Residue from H₂O washing was mixed with 150 ml acetic acid solution at room temperature for 24 h under N₂ flow, and filtered and dried in vacuo for 5 h at 60°C.
- HCl washing : Residue from acetic acid washing was mixed with 150 ml HCl at room temperature for 24 h under N₂ flow, and filtered and dried in vacuo for 5 h at 60 °C.

Analytical procedure . The filtrates after the pretreatment of coal were analyzed by ICP-AES(Shimadzu, ICPS7000) and cation chromatography(Nihon Dionex, IonPac CS15) for the measurement of eluted metals by the pretreatments. The residues obtained by pretreatments were also analyzed by X-ray fluorescence(XRF) and ICP-AES after the microwave irradiation acidic digestion treatment by a Maultiwave3000(Perkin-Elmer).

Solid-state ²⁹Si- and ²³Na-NMR spectra of the coals before and after acid treatments and solvent extraction were measured by a Chemagnetics CMX-300 spectrometer with SPE-MAS

method(Single-pulse excitation-magic angle spinning; pulse delay: 20 sec for ²⁹Si, 2 sec for ²³Na, MAS: 3-4 kHz for ²⁹Si, 15 kHz for ²³Na).

Results and Discussion

Properties of Coals and Their HPC

Enshu(EN) and Stratford(STF) coals contain 12.6 and 10.3 wt% of ash on dry basis, respectively. Although their coal rank and elemental composition were similar, the higher H and S contents and the lower ash in EN coal are noted. The extraction yields with 1-methylnaphthalene(1-MN) at 360 °C was above 60 % for both of the coals, the ash contents being as low as 200 ppm of the aimed levels as shown in Table 1.

Elution of Metals by Pretreatments.

Table 2 summarizes the eluted metals by the sequential treatment of the coals with H₂O, 1 M CH₃COOH and 1N HCl/10%ethanol solution. It is noted that some portions of Ca and Mg from the coals were eluted into water. Na and K were also detected in the water by cation chromatography. Elements associated with the organic part as ion-exchangeable cations present were easily removed from coal by CH₃COOH washing. Carbonates and oxides minerals were also removed by HCl washing according to the reference.¹ The minerals remaining in the coal after acid washing are indicated to principally consist of aluminosilicate and quartz identified by solid-state ²⁹Si-NMR and XRF measurements.

Table 1 Proximate and elemental analyses of coals and their HPC

Samples	Proximate analysis (wt %, dry)		Elemental analysis (wt %, daf)				
	Ash	VM	C	H	N	S	O ^a
Enshu(EN) coal	12.6	39.3	78.9	5.4	1.3	4.2	10.2
EN-HPC	0.02	51.8	83.4	5.6	1.4	1.8	7.7
Stratford(STF) coal	10.3	28.8	87.0	5.5	2.3	0.7	4.5
STF-HPC	0.02	38.8	87.7	5.3	2.1	0.7	4.2

^a by difference

Table 2 ICP analyses of metals removed from EN coal by sequential treatment with H₂O, CH₃COOH, and HCl aqueous solution

Coal-Treatment	Removed metals (wt% based on coal)				
	Ca	Fe	Mg	Si	Al
EN-H ₂ O	0.080	0.001	0.009	0.000	0.000
EN-CH ₃ COOH	0.152	0.034	0.035	0.000	0.018
EN-HCl	0.390	0.412	0.027	0.075	0.069
(Total sum:)	0.622	0.447	0.071	0.075	0.087)
STF-H ₂ O	0.009	0.000	0.006	0.000	0.000
STF-CH ₃ COOH	0.062	0.003	0.023	0.000	0.015
STF-HCl	0.195	0.020	0.054	0.098	0.077
(Total sum:)	0.266	0.023	0.083	0.098	0.092)

According to analyses of the pretreated filtrate with MeOH under the ultrasonic irradiation for 1 h by the cation chromatography, small

amounts of Na, Ca, Mg, and K were eluted during the pretreatment with MeOH or MeOH/H₂O solution. A small amount of Fe was also detected in the filtrate by ICP-AES. Although the accurate amounts of the metals eluted by the pretreatments were not determined due to their low concentration, such a simple impregnation pretreatment with MeOH/H₂O can be expected to remove some amounts of metals prior to solvent extraction as well as to modify the organic part in coal. In addition, since the pretreatment with MeOH has been reported to enhance the coal grindability and separation of organic substances from mineral matters,² a more practical coal preparation scheme can be designed by the combination of such pretreatment with coal grinding procedure. It was also reported that organically associated Ca and aluminosilicate species elute into HPC during solvent extraction at high temperature,¹ hence the pretreatment with dilute acidic solution is expected to remove such organically associated species beforehand, since dilute organic acids such as acetic acid have been recognized to reduce not only ion-exchangeable cations of alkali and alkali-earth metals,³ but also organically associated aluminosilicate species.¹

Na species in the coals and their HPC were detected by ²³Na-NMR to the levels of ppm, although the quantitative analysis of Na is very difficult because of the broadening of the peaks due to the quadrupole interactions of ²³Na.⁴ A preliminary result with ²³Na-NMR revealed that ion-exchangeable Na species may relatively remain in the solvent extracted fraction(HPC).⁵ Further detailed investigation is required for the more quantitative analyses.

By the combination with microwave acidic digestion with FI(flow injection)-ICP-AES, alkali metals in the coals before and after the pretreatments were quantified to a satisfactory level.⁶

Figure 1 shows the removal percent of metals by the pretreatments with MeOH, MeOH/H₂O(1:1), and 10% CH₃COOH aq. About 20% of alkali metals with 30-40 % of alkali-earth metals were removed even by MeOH and MeOH/H₂O. 10% CH₃COOH solution removed more amounts of alkali and alkali-earth metals, especially 90% of Ca was removed from EN coal. It is also noted that some of aluminum compounds were removed by such mild treatments, indicating that such Al species may be bonded to or associated with organic parts in the coal through oxygen functional groups.

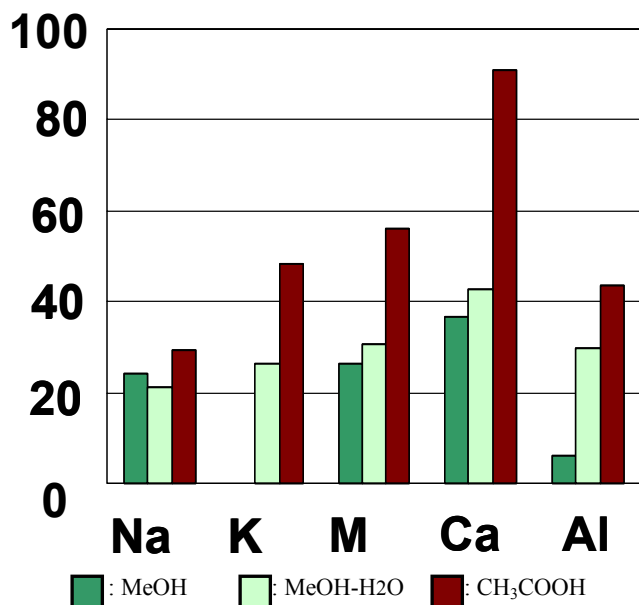


Figure 1 Removal percent of metals by pretreatments

Figure 2 illustrates the HPC yields from the pretreated coal (particle size: 32-60 mesh) under various conditions. The pretreatments with MeOH and MeOH/H₂O for 48 h gave a little higher extraction yield of 53.4 and 53.7 %, respectively, while the yield was 51.3 % from non-treated coal. The acid treatment with 1% HCl or CH₃COOH slightly increased the HPC yield to 52%.

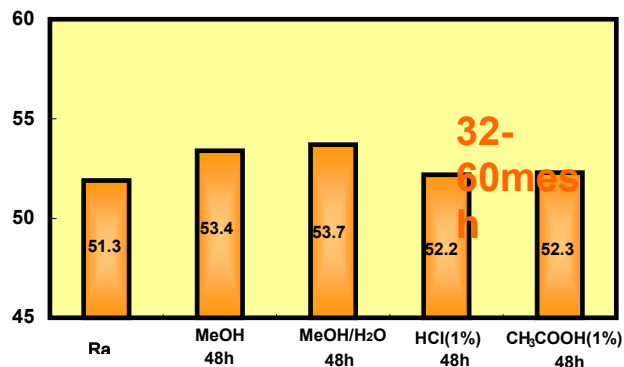


Figure 2 Effect of coal pretreatments on extraction yield(%)

Conclusions

Based on the present study, it is revealed that a mild pretreatment with MeOH, MeOH/H₂O, or dilute acetic acid solution can modify the organic parts of the coals to be more easily solvated with extraction solvent as well as remove some portions of alkali, alkali-earth, and other eluted metals prior to the solvent extraction procedure. A combination of such a mild pretreatment at room temperature with high temperature solvent extraction is expected to be one of the promising ways for the efficient production of HPC, because HPC is required to reduce its content of alkali and alkali-earth metals to the extremely low levels (Na+K < 0.5 ppm; Ca < 2 ppm) for the direct introduction to gas turbine power generation system. More extensive optimized procedures for the production of HPC should be designed in terms of its required strict quality and cost/performance.

Acknowledgment. The authors are grateful to Kobe Steel, Ltd. for providing the samples and useful discussion on the experiments. This work was supported by the New Energy and Industrial Technology Development Organization (NEDO) and Center for Coal Utilization Japan (CCUJ).

References

- Sakanishi, K., Saito, I., Ishom, F., Watanabe, I., Mochida, I., Okuyama, N., Deguchi, T., Shimazaki, K., *Fuel*, **2002**, 81, 1471.
- Takarada, T., Ohkawa, M., Wang, J., Goto, K., *Proc. 7th China-Japan Symp. Coal & CI Chem.*, **2001**, p.359.
- Sakanishi, K., Watanabe, I., Nonaka, T., Kishino, M., Mochida, I., *Fuel*, **2001**, 80, 273.
- Soma, M., Tanaka, A., Seyama, S., Hayashi, K., Hayamizu, K., *Clay Science*, **1990**, 8, 1.
- Sakanishi, K., Kawashima, H., Akashi, E., Saito, I., Takarada, T., *Proc. Japan Coal Science Meeting*, **2002**, No.57, p.131.
- Akashi, E., Sakanishi, K., Nakazato, T., Tao, H., Saito, I., Takarada, T., *Proc. Japan Coal Science Meeting*, **2002**, No.37, p.91.

CLEAN COAL CONVERSION OPTIONS USING FISCHER-TROPSCH TECHNOLOGY

André P Steynberg and Herman G Nel

Research & Development Division
Sasol Technology
1 Klasie Havenga
Sasolburg
1947
South Africa

Introduction

Any meaningful utilization of the vast coal resources in places like China, India, Australia, South Africa and the USA will involve conversion into some other form of energy. Coal, as a solid, has a high energy density and is therefore reasonably convenient as a heating fuel. The problem is that the associated pollutants negate any advantages compared to other cleaner burning fuels. Coal is rather converted into other cleaner forms of energy such as liquid hydrocarbons, synthetic natural gas (SNG) and electric power. Initially these conversion plants simply concentrated the pollutants in one large scale conversion site while enabling the end user of energy to experience a cleaner fuel. With time, more and more success has been achieved in cleaning up the emissions from large scale coal conversion facilities.

One fact that cannot be avoided is that every ton of carbon in mined coal will sooner or later end up as 3.67 tons of carbon dioxide in the atmosphere. Although some attention has been paid to the possibility of carbon dioxide sequestration this is not currently, and may never be a viable option. Certainly the cost of sequestration seems likely to favour the use of other fossil fuel alternatives such as crude oil and natural gas while these are still readily available.

The increased production of carbon dioxide per unit of useful energy for coal relative to other fuels is inevitable. Assuming this is acceptable, it becomes important to ensure that, when coal is used, it is used as efficiently as possible.

Combined production of hydrocarbon liquid and electrical power

The coal fired power stations in South Africa and elsewhere produce some of the world's lowest cost electrical power but this large scale coal combustion has an environmental penalty. An alternative approach is to gasify the coal in order to produce a low heating value synthesis gas which may be cleaned prior to combustion in a combined cycle power plant using both steam and gas turbines. There are alternative uses for this synthesis gas that may offer opportunities that are both economically more attractive and result in more efficient use of the coal. Where a region's economy is dependant on coal utilization, there is a strong case to be made to switch to more efficient and less polluting coal conversion technologies as these become available.

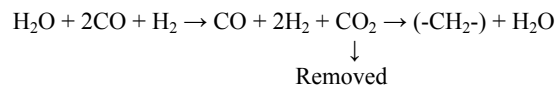
Synthesis gas can also be made from natural gas and the following comparison has been published previously by Shell¹:

	Syngas Manufacture	Fischer- Tropsch	Thermal* Efficiency	Relative Capital Cost
Coal:				
	$2(-\text{CH}-) + \text{O}_2 \rightarrow 2\text{CO} + \text{H}_2 \rightarrow (-\text{CH}_2-) + \text{CO}_2$		60%	200
Natural Gas:				
	$\text{CH}_4 + \frac{1}{2}\text{O}_2 \rightarrow \text{CO} + 2\text{H}_2 \rightarrow (-\text{CH}_2-) + \text{H}_2\text{O}$		80%	100

* Theoretical Maximum

This appears to paint a bleak picture for coal utilization but it ignores two factors. Firstly the high energy density of coal allows the feed to be delivered to the conversion plant at a lower cost. Secondly the lower energy efficiency ignores the opportunity to convert the byproduct heat into electrical power.

Another potential use for some of the byproduct heat is to generate steam for the use in the water gas shift reaction to modify the above coal conversion reaction as follows:



This then becomes equivalent to the natural gas route for the synthesis gas conversion step but twice as much oxygen has been used to prepare the synthesis gas and the cost of generating steam and removing carbon dioxide provides a further cost penalty.

The above equations also ignore the reality that coal is gasified with both steam and oxygen together. This leads to a lower oxygen consumption for gasification than is indicated by the above equations. For the coal conversion options considered, the oxygen consumption per unit of synthesis gas is actually not double that for the partial oxidation of natural gas.

The cost penalty is somewhat negated by the fact that steam generation is required anyway to remove the heat generated by the Fischer-Tropsch reaction and to cool the hot synthesis gas exiting the gasifier. Synthesis gas cleanup to remove acid gases is also required anyway for use in gas turbines.

The concept of producing Fischer-Tropsch liquid hydrocarbons and electrical power from coal derived synthesis gas has been around for quite a long time. A 1978 patent from Chevron pointed out the advantages of using this concept to cope effectively with power demand variations². The US Department of Energy (DOE) supported by contracted studies by MITRE Corporation^{3,4} and companies such as Texaco⁵, Air Products^{6,7} and Rentech^{8,9} showed that LTFT reactor technology can be used together with coal or petroleum coke gasifiers for the co-production of hydrocarbon liquids and electrical power. Fluor Daniel¹⁰ have proposed the use of HTFT for this purpose.

It is possible that the combined production of hydrocarbon liquids and electricity can compete with natural gas conversion to only the hydrocarbon liquids. This option has been studied for two

Fischer-Tropsch conversion options i.e. Low Temperature Fischer-Tropsch (LTFT) and High Temperature Fischer-Tropsch (HTFT) both using Iron based catalysts.

Cases Studied

For both cases the use of a Texaco Gasifier was assumed to make a synthesis gas with the following composition (mol%):

H ₂	37.36
CO	29.26
CO ₂	13.30
CH ₄	0.16
H ₂ O	19.43
Inert	0.49

For the LTFT case this gas is fed to a two stage reactor system to form liquid hydrocarbon products. The tailgas is sent to a gas turbine to produce power. Other sources of power are the steam generated in the process of cooling the synthesis gas from the gasifier and in removing the heat generated in the Fischer-Tropsch reactors.

For the HTFT case, a similar quantity of hydrocarbon product can be produced with a single stage reactor. For this case the synthesis gas is subjected to a sour gas shift prior to acid gas removal in order to increase the hydrogen to carbon monoxide ratio in the synthesis gas. This was also found to significantly increase the utility requirements for the acid gas removal step.

The mass and energy balances for the two cases are shown below. These are not necessarily fully optimized but are considered realistic to provide a fair basis for comparison.

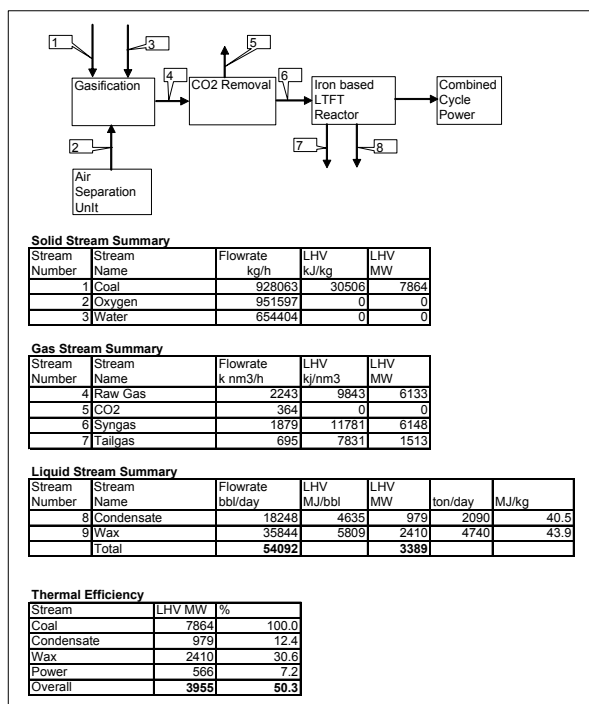


Figure 1. LTFT Based.

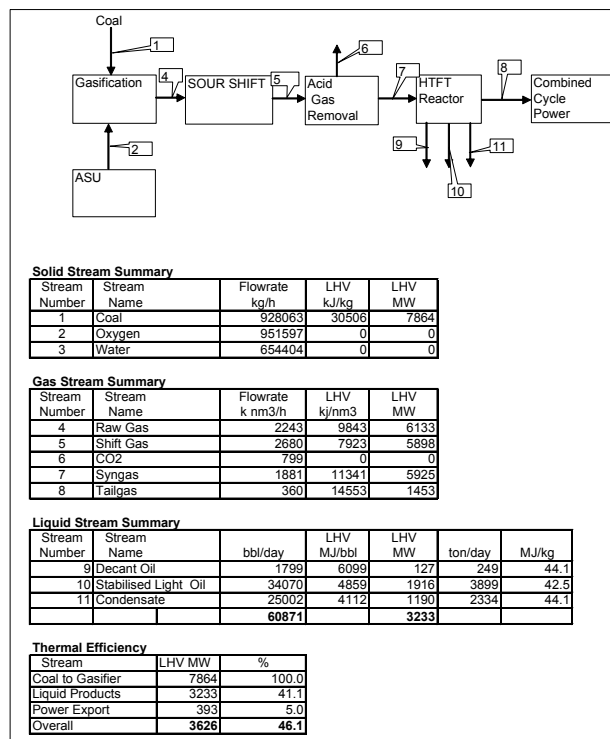


Figure 2. HTFT Based

Discussion of the results

Natural gas conversion processes can be expected to have thermal efficiencies in the range of 60 to 66%. For the current state of the technology, cost effective facilities will have thermal efficiencies closer to 60%. Coal conversion is clearly less efficient. It seems 50% efficiency is achievable. The cost of feedstock per unit of energy must therefore be less in order to compensate for this efficiency deficit. However, this is not unrealistic. Existing coal conversion plants operating with thermal efficiencies closer to 40% are cash positive.

Compared to natural gas conversion, the capital cost based on similar quantities of energy product are higher for a number of reasons. Firstly there is the need for acid gas removal from the synthesis gas. This step is not required for a sweet natural gas feed. The capital cost of synthesis gas generation is also significantly higher mainly due to the higher oxygen requirement (by a factor of nearly 1.7). The Fischer-Tropsch conversion step is marginally more expensive for the HTFT technology and nearly double the cost for the LTFT route when compared to natural gas conversion. This is the result of the coal derived synthesis gas being unsuitable for use with modern supported cobalt Fischer-Tropsch catalysts. Another factor that negatively impacts the coal conversion plant is that it is more utility intensive than a natural gas conversion plant. This is an inevitable consequence of the lower thermal efficiency.

Considering the comparison between the HTFT and LTFT options, it is clear that the LTFT route is more efficient. The main reason for the lower efficiency of the HTFT option is that the acid gas removal step becomes more utility intensive. As mentioned previously though, the capital cost for the Fischer-Tropsch section is higher. Only a detailed study beyond the scope of this paper will be able to determine whether the higher efficiency of the LTFT route

can compensate for the higher capital cost. The preferred solution may be different for different potential application sites and may be influenced by whether gasoline or diesel is the desired primary product.

The economic success of the coal conversion plant will inevitably depend on the price received for the products. It seems unlikely that the price for liquid hydrocarbons will be sufficient to provide a suitable return on the capital invested while the energy resources of crude oil and natural gas are still readily available. However, if some assistance is provided for the initial capital costs, coal conversion to liquid hydrocarbons together with electrical power is an efficient option relative to other coal conversion options. It may be important to reduce dependence on imported energy for countries with abundant coal resources. The coal conversion efficiencies are higher when liquid hydrocarbons are produced than for facilities producing only electricity.

Production of liquid hydrocarbons from coal as described above has two further advantages. Firstly the market is huge and the facilities can take advantage of economics of scale for very large facilities producing hydrocarbon fuels steam together with electricity. However, the huge capital investment involved is another reason why state assistance will probably be necessary to fund such a coal conversion facility. The other benefit is that the final liquid hydrocarbon fuels will be ultra clean and will not contain sulfur or nitrogen. This will lead to local environmental benefits where these fuels are used.

Conclusions

Certainly coal conversion to hydrocarbon liquids and electricity is economically attractive from an income/ cash cost viewpoint. However large capital investments are required to reap the benefits from economics of scale and the return on capital invested is not particularly attractive. It is therefore expected that these coal conversion plants will only become a reality if there is some form of state assistance with the initial capital investment, such as low interest loans. This would be motivated by the independence from imported energy and the more efficient and cleaner utilization of the local energy resource. The Chinese government has accepted this approach and China is likely to be the pioneer for this technology option. Places that have abundant coal are likely to use this resource. It is the duty of technology providers to ensure that technology is made available to allow the coal to be used as efficiently as possible.

References

- (1) Van den Burgt, M., Van Klinken, J. and Sie, S.T. 'The Shell Middle Distillate Synthesis Process', paper presented at the 5th Synfuels Worldwide Symposium, Washington, D.C., USA, November 11-13, 1985.
- (2) Egan, C.J., U.S. Pat., No. 4,092,826, **1978**
- (3) Gray, D., and Thomlinson, G.C., Contractor Report DE91-004668, **1990**.
- (4) Gray, D. and Thomlinson, G.C.; In *Natural Gas Conversion IV, Studies in Surface Science and Catalysis Vol 107*; de Pontes, M., Espinoza, R.L., Nicolaidis, C.P., Sholtz, J.H. and Scurrill, Ed.; Elsevier: Amsterdam, 1997; pp. 145-150.
- (5) Schrader, C and Shah L, "Gasification Technologies I: Applications, Texaco Gasification and Fischer-Tropsch Process", (September 2000)
- (6) Sorrensen et al, U.S. Pat., No. 5,865,023, **1999**.
- (7) Sorrensen et al, U.S. Pat., No. 5,666,800, **1997**.
- (8) Botha, MS and Benham, CB, "Coal-to-Liquids via Fischer-Tropsch Synthesis", 244 International Technical Conference on Coal Utilisation and Fuel Systems, (March 1999)
- (9) Bohn et al, U.S. Pat., 6,306,917, **2001**.

- (10) Stupin, W.; Ruvikumar, R.; and Hook, B.; "Liquid products from Petroleum Coke via Gasification and Fischer-Tropsch Synthesis", NPRA 2000 Annual Meeting, San Antonio, Texas, AM-0010 (March 2000).

Conversion of Coal to Hydrogen by Integrating the Exothermic and Endothermic, Gas Production and Separation Reactions in Gasifier

Shiying LIN, Michiaki HARADA, Yoshizo SUZUKI* and Hiroyuki HATANO*

Center for Coal Utilization, Japan
24, Daikyocho, Shinjuku-ku, Tokyo 160-0014

*National Institute of Advanced Industrial Science and Technology
E-mail: sy-lin@aist.go.jp

Abstract:

Addition CaO in gasifier can absorb CO₂ and release heat during coal gasification. This method was used for producing high concentration hydrogen from one reactor (HyPr-RING method). Previous experimental studies¹⁻⁵⁾ have confirmed that high concentration H₂ (above 80%) with a few CH₄ can be made, and no carbon oxides are detected in the product gas phase. In this study, we will discuss the general problems with using calcium base sorbents in high temperature absorption, and our solutions in HyPr-RING method for H₂ production. A H₂ production process was designed in consideration of these solutions, and higher as 75% H₂ production efficiency was expected.

Introduction:

It is necessary to solve the problem between the utilization of fossil fuel and the protection of environment. One of solution is to transform the fossil fuel energy to hydrogen, which is a most clean energy, generates only water without any pollutants.

In previous study¹⁻⁵⁾, we proposed to use a solid sorbent (CaO/Ca(OH)₂) to remove CO₂ at comparative high temperature which the coal gasification can occur with suitable rate. Namely, absorbing CO₂ in gasifier and releasing the heat of CO₂ absorption to the endothermic coal gasification simultaneously (Fig.1). For keeping CaO reactivity, it is better to like CaO first reacts with H₂O in the gasifier to form Ca(OH)₂, and then Ca(OH)₂ absorbs CO₂ to form CaCO₃. The flowing four reactions should be integrated in gasifier.

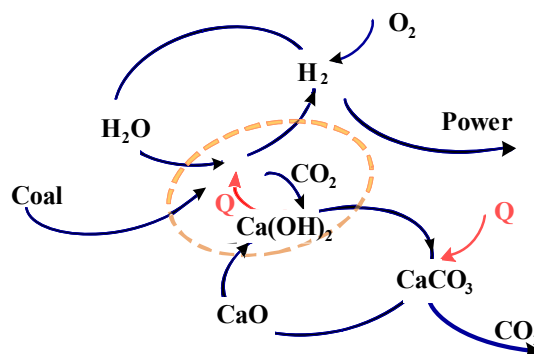


Fig. 1 Concept of HyPr-RING process

In this study, we will discuss in detail in the problems and their solutions in the CaO using process.

Discussion:

Fig. 2 shows problems and solutions in HyPr-RING method. CaO losing reactivity during sorbent recycle is an original problem for using Ca base sorbents. We considered recovering CaO reactivity by calcium hydration in gasifier. Theoretical and experimental results have confirmed that, at high temperature as 873-973 K, CaO can react with steam under higher pressure as 0.3-1.3 Mpa.

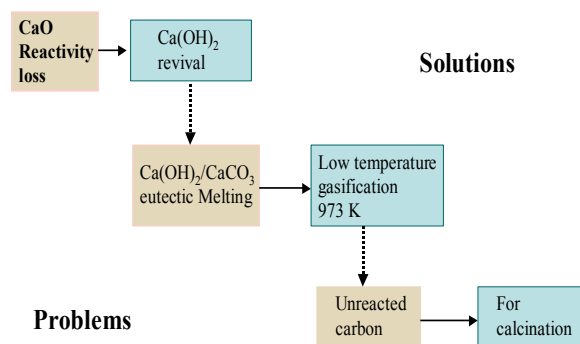


Fig.2 Problems for using CaO and their solution.

The next problem is Ca(OH)₂/CaCO₃ eutectic melting. Lower operation temperature must be chosen for the gasifier, such as our confirmations in experiment⁵⁾. We are considering using the unreacted carbon after gasification to be an energy source for CaCO₃ calcination (sorbent regeneration).

Fig.3 shows mass flow comparison of HyPr-RING with a conventional H₂ production.

Fig. 4 show an analysis of HyPr-RING process in consideration of above solutions. Since most of calcination energy become chemical energy of CaO, and can be released in the gasifier, higher as 75% hydrogen production efficiency was expected.

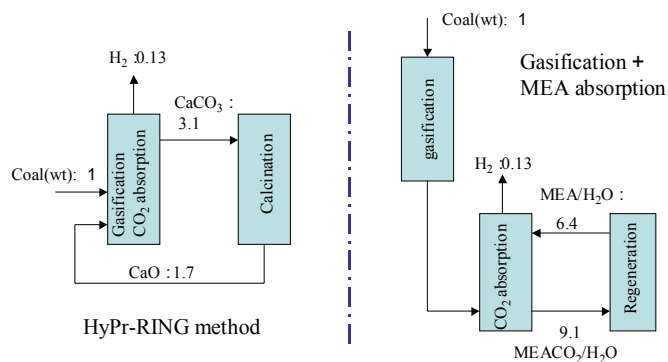


Fig. 3 Mass flow comparison of HyPr-RING with conventional processes.

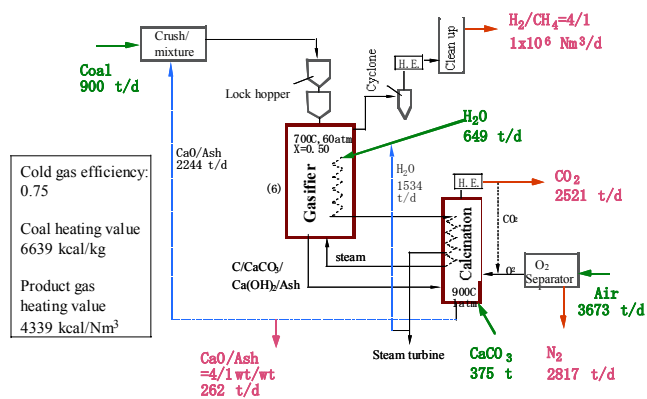


Fig. 4 An analysis of HyPr-RING process

Reference:

- (1) Lin et al., Kagaku Kogaku Ronbunshu 25(3), 498-500 (1999)
- (2) Lin et al., Energy & Fuel, 15(2), 339-343 (2001)
- (3) Lin et al., Journal of the South African Institute of Mining and Metallurgy, 101, 53-60 (2001)
- (4) Lin et al., J. of Energy Conversion & Management, 43, 1283-1290 (2002)
- (5) Lin et al., Fuel, 81, 2079-2085, 2002

TREATMENT OF WASTEWATERS FROM DEWATERING PROCESS OF BROWN COAL BY USE OF A NOVEL Ni-SUPPORTED CARBON CATALYST

Hiroyuki NAKAGAWA, Akio NANBA, Marc Boehlmann, and Kouichi MIURA

Department of Chemical Engineering
Kyoto University, Kyoto 606-8501, JAPAN

Introduction

Brown coals are important energy resources in the near future because of their abundant deposits. But dewatering (drying) process is necessary prior to use for power generation because their water content are very large, and reach as high as 60% by weight for some coals. Current technology for power generation from low rank coals removes most of water by evaporative drying, resulting in a direct loss of the heat of evaporation (~2.3MJ/kg). Therefore, development of an efficient dewatering process is desired for more utilization of brown coals.

Non-evaporating drying process is preferable for this purpose, since the water is separated in liquid form. Fleissner process¹⁾ has been applied commercially to brown coal since 1920's, and several processes utilizing non-evaporative dewatering have been proposed²⁾. In these processes, brown coals are treated under hydrothermal conditions at 200 ~ 300 °C, where upgrading as well as dewatering of brown coals are realized through the decomposition of oxygen functional groups. Simultaneously, a large amount of wastewater containing organic compounds derived from brown coal is discharged from the dewatering process. Wastewater treatment is a serious concern from the viewpoint of environmental preservation.

Recently the authors have developed a novel Ni-supported carbon catalyst³⁾ and showed that the catalyst is effective to gasify small molecular weight organic compounds to convert them to CH₄ and H₂⁴⁾. In this paper a brown coal was treated under the hydrothermal conditions for dewatering and the catalyst was applied to gasify the wastewater emitted during the dewatering. Organic compounds such as phenol were also gasified for comparison purpose.

Experimental

Catalyst preparation A metacrylic acid type resin (Mitsubishi Chemical, WK-11) was used as a starting material. The resin was treated in an ammonium complex ion aqueous solution of Ni(SO₄)₂ at room temperature. It was then heated at the rate of 10 K/min to 500 °C in a nitrogen stream to prepare the Ni-supported carbon catalyst. BET surface area of this catalyst was 170 m²/g. The amount of Ni supported surprisingly reached as high as 47wt% and Ni was found to be highly dispersed in the porous carbon from X-ray diffraction pattern. This catalyst was subjected to the experiment without any further treatments such as reduction by hydrogen.

Sample preparation A Victorian brown coal, Morwell, was used in this study. Water content of the coal was 1.31 kg/kg-dry coal. Hydrothermal treatment was conducted in a 20 ml autoclave. About 6 g of coal water mixture (1:1 on weight) was loaded in a reactor. The reactor was purged by 1 MPa of nitrogen several times to remove oxygen in the reactor before heating. The autoclave was heated to 300 °C at which the temperature was maintained for 60 min. The wastewater was obtained by filtering the coal/water mixture after the treatment. The total organic carbon in the wastewater was ca. 2000 ppm. Another type of wastewater derived from the mechanical/thermal dewatering process (MTE)⁵⁾ was also used.

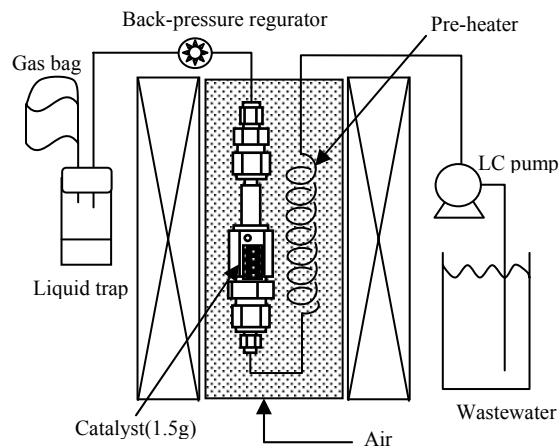


Fig.1 Apparatus for catalytic hydrothermal gasification.

Apparatus and procedure Figure 1 shows the experimental setup for the catalytic hydrothermal gasification. 1.5 g of catalyst was embedded in a reactor made of Swagelok. The wastewater or aqueous solution of containing one of organic compounds (2000 ppm) was supplied to the reactor at the rate of 0.2 to 1 ml/min under the pressure of 20 MPa to maintain liquid phase at the reaction temperature. The LHSV was changed from 10 to 50 h⁻¹. The reactor was heated in a fluidized sand bath where the temperature was maintained at 200 ~ 350 °C. The product gas and treated water was analyzed by gas chromatographs (GC) and a total organic carbon analyzer (TOC), respectively.

Results and Discussions

Catalytic hydrothermal treatment of wastewater Figure 2 shows the carbon conversion and the product gas yields when the wastewater was gasified at 200 ~ 350 °C. The LHSV was 50 h⁻¹. The product yields were all represented on the basis of 1 mol of carbon in the wastewater. The carbon conversion increased with the increase of reaction temperature and reached eventually at 350 °C.

The gaseous products detected were only CH₄, CO₂, and H₂.

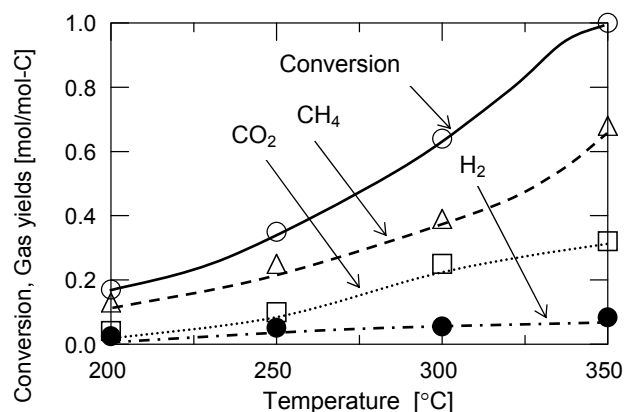


Fig.2 Catalytic hydrothermal gasification of wastewater at 20 MPa (LHSV = 50 h⁻¹).

CO was little produced under these conditions. The total yield of CH₄ and CO₂ was almost the same with the carbon conversion

estimated from the concentration of organic carbon in the wastewater before and after treatments. The gas yields all increased with the increase of reaction temperature. The yield of CH₄ was 0.68 at 350 °C. On the other hand, the yield of H₂ was much smaller than the yields of other gases and less than 0.1 even at 350 °C, indicating that CH₄ rich gas could be obtained through the catalytic hydrothermal treatment of wastewater. Above results clearly show that the hydrothermal gasification process using new catalyst is effective not only to treat the wastewater but to recover gaseous energy resources from the wastewater.

Molecular weight distributions of organics in wastewater before and after treatments To examine which components are gasified easily, molecular weight distributions of organics in the wastewater before and after treatments were analyzed by GPC. Figure 3 shows the elution curves of the organics in the wastewater before and after treatment. Corresponding molecular weight, which was calibrated using polyethyleneglycol (PEG), is shown above the figure. The wastewater before treatment contains a fairly large amount of small molecular weight components less than 200 g/mol. About a half of these components were gasified at 200 °C where the carbon conversion was 0.17. This result clearly indicates that the small molecular weight components are more reactive for hydrothermal gasification than high molecular weight components. However, even high molecular weight components more than 100,000 g/mol were completely gasified when the reaction temperature was raised up to 350 °C.

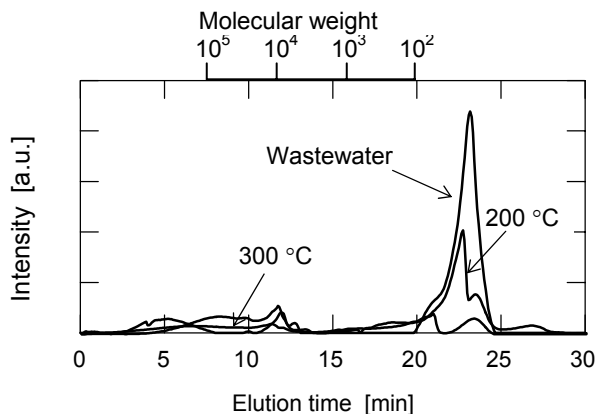


Fig.3 Elution curves of organics in the wastewater before and after treatment.

Treatment of various water-soluble compounds A water-soluble lignin, phenol, *m*-cresol, the wastewater of the MTE process were also gasified at 350 °C with the TOC of 2000 ppm. Figure 4 shows the product gas yields. The sum of the yields of CO₂ and CH₄ corresponds to the carbon conversion, because the formation of other gases containing carbon was negligible. The carbon conversions of lignin, phenol, and *m*-cresol were 0.52, 0.68, and 0.87, respectively when LHSV was 50 h⁻¹. These results indicate that these compounds are less reactive than the wastewater. As for product gas yields, the yields of CH₄ and CO₂ were almost the same for the phenol and cresol. The yields of hydrogen for lignin, phenol, and *m*-cresol were clearly larger than the H₂ yield for wastewater. When the LHSV was lowered to 10 h⁻¹, phenol, cresol, and the wastewater of the MTE process were almost completely gasified at 350 °C. The carbon conversion of lignin was also increased up to 0.77. The product gas composition was, however, not affected by the value of LHSV.

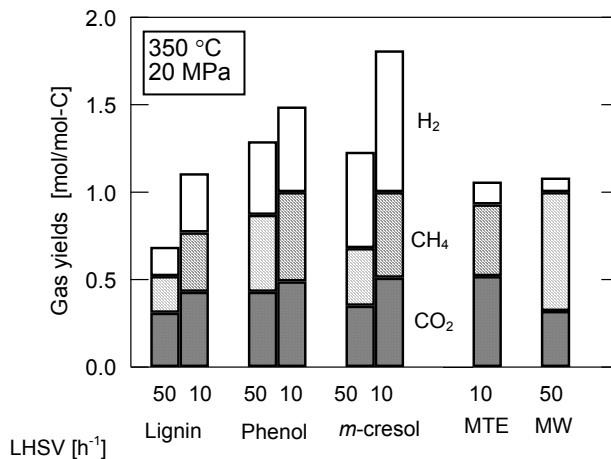


Fig.4 Product gas yields from the catalytic hydrothermal gasification of lignin, phenol, *m*-cresol, and wastewaters from dewatering. (350 °C, 20 MPa)

Conclusions

Wastewaters from the dewatering process of brown coals were gasified under hydrothermal conditions by use of a novel Ni/carbon catalyst developed by us. Organics in the wastewater were completely gasified under the hydrothermal conditions of 350 °C and 20 MPa, producing H₂, CH₄, and CO₂. This result indicates that this catalytic hydrothermal gasification can recover energy resources from organics in wastewater effectively. It was also found that small molecular weight components were more reactive for the catalytic hydrothermal gasification than large molecular weight components in the wastewater.

A water-soluble lignin, phenol, and *m*-cresol in water were also gasified under the same conditions. They were all less reactive than the organics in the wastewater coming from the brown coal dewatering process. It was found that the carbon conversion increased with the decrease of LHSV value whereas the product gas composition was not affected by the LHSV value.

Acknowledgement. This work was financially supported by Special Coordination Funds of the Ministry of Education, Culture, Sports, Science and Technology, Japan. (Grant No. 11218206)

References

- (1) Fleissner H., *Sonderdruck Sparte Wirtschaft Nos. 10 and 11*, 1927.
- (2) Allardice D.J. In *The Science of Victorian Brown Coal: Structure, Properties and Consequences for Utilization*; Durie R.A. Ed.; Butterworth-Heinemann: Oxford, 1991; pp. 104-150.
- (3) Miura K., Nakagawa H., Kitaura R., Satoh T., *Chem. Eng. Sci.* **2001**, *56*, 1623.
- (4) Miura K., Nakagawa H., Miwa M., Tamura T., *Int. Sym. on Chem. Reaction Eng.*, 2002, No. 169(Hong Kong).
- (5) Bergins C., Berger S., Strauss K., *Chem. Eng. Tech.* **1999**, *22*, 923